STUDY ON SOLUTE TRANSPORT THROUGH RO/NF MEMBRANES

ZHOU WENWEN

NATIONAL UNIVERSITY OF SINGAPORE

2004

STUDY ON SOLUTE TRANSPORT THROUGH RO/NF MEMBRANES

ZHOU WENWEN

(MPhil, HKUST)

A THESIS SUBMITTED

FOR THE DEGREE OF DOCTOR OF PHILOSOPHY

DEPARTMENT OF CIVIL ENGINEERING

NATIONAL UNIVERSITY OF SINGAPORE

2004

ACKNOWLEWDGEMENTS

"To love and be loved is to feel the sun from both sides." - David Viscott

First of all, I would like to express my sincere gratitude to my academic supervisor Associate Professor Lianfa SONG for his intellectual guidance, competent advice and support throughout this research. My sincere thank also goes to my co-supervisor Professor Say Leong ONG for his valuable comments and pertinent suggestions for this work. I have learned a great deal from both of them during the past three years at NUS.

Special thanks are extended to the other members of my Ph.D. committee, Dr. Jiangyong HU and Associate Professor Wen-Tso LIU and all the colleagues in Environmental Laboratory in Centre for Water Research.

Finally and foremost, I would like to express my deepest gratitude and love from the bottom of my heart to my parents Mr. Yiyu ZHOU and Ms. Lianhong WANG, and my boyfriend Mr. Douglas Man Tak WONG. Without their love, encouragement and understanding, this work could not have been completed. This thesis is especially dedicated to my parents.

To My Parents

TABLE OF CONTENTS

SUMMARY

Ion transport across membranes is of fundamental importance to many biological processes and industrial applications. Naturally, almost all membranes in a living body have electric charge with them; while synthetic membranes like reverse osmosis (RO) and nanofiltration (NF) membranes tend to acquire surface charge when they are in contact with an aqueous medium. With the recent development in membrane manufacturing industry, RO and NF membranes have been widely used in desalination, water purification and industrial wastewater treatment. Hence to understand ion transport across RO/NF membranes from the fundamental standing point is of practical significance. The overall purpose of this research work was to investigate the mechanisms and behaviors of the solute transport through RO/NF membranes and the role of electrical interactions on the transport. This research was mainly focused on developing a comprehensive ion transport theory and formulation for RO/NF membranes from the fundamental electrostatic and electrodiffusion principles.

In this work, the Nernst-Planck-Donnan model incorporated with Freundlich isotherm model has been developed and used to simulate the solute rejection through loose RO and NF membranes. This model seems to be practically feasible to describe the ion transport behaviors for loose membranes. It is mainly because that the large values of hindrance factor for convection obtained in Donnan model reflect the preponderant contribution of convection to ionic flux for loose membranes, where electromigrative effects are of no consequence. The inherent inadequacies and limitations of the commonly used Nernst-Planck-Donnan model have also been discussed from a more fundamental point of view.

Based on the fundamental principles of Brownian diffusion, electrostatic interaction, and electro-migration, a new formulation has been developed for a better description of ion transport through dense RO membranes. The new formulated mathematical model consists of the extended Nernst-Planck equation and Poisson equation. The well-defined boundary conditions at both membrane-solution interfaces at unsteady state make it possible to avoid using the invalid assumption of local electroneutrality. Simulation results show that net electrical charge or potential develops across the membrane as a result of transport of ions with different mobility. An electric field is noted to be induced by the imbalanced charges across the membrane and acts as a "flux regulator". Although the local electroneutrality is fault, the "no electrical current" at steady state remains valid for all situations, even for the cases in which the mobility of anions and cations are significantly different. The transports of different ions are then coupled and regulated by "the regulation medium" electro-migration in the induced electric field within the membrane.

Transport mechanisms have also been investigated in terms of diffusion, electromigration and convection. For membranes with no fixed charge density, the electric field can be induced by the unbalanced charge due to different ion diffusivities. Diffusion is likely to be the primary mechanism in ion transport, where electro-migration makes up the difference in diffusive fluxes of cations and anions. For the case of membrane with fixed charge density, the increase in fixed membrane charge density and co-ion (i.e., ions with the same charge of the membrane) valence will increase the electrostatic interaction between membrane and ions that in turn will increase the contribution of electro-migration. Electro-migration appears to be the primary mechanism at high membrane charge density.

Finally, simulations for mixed solutions show that the addition of a second salt can increase the permeability of more permeable ion and increase the rejection of less permeable ion. The higher selectivity is obtained in mixed solutions due to the change in induced electric field, which is dependent on ionic diffusion coefficients, feed salt concentration, mole fraction, membrane charge density and water flux. The effects of these parameters on ion transport can also be quantified by the analytical method derived in this study, which provide a much easier and more direct way to estimate the transport phenomenon in both single and mixed solutions.

NOMENCLATURE

c	Concentration within the membrane, mol/m^3
C	Concentration in solution, mol/m^3
D	Diffusivity in membrane, m^2/s
E	Electric field strength, volt/m
F	Faraday's constant = 96500 coul /mol
I	Electric current, A
J_i	Flux of ionic component i in membrane pore, m/s
J_v	Permeate flux, m/s
$k_{,c}$	Convective factor of component i
L	Membrane thickness, m
L_P, L_{PD}, L_{DP}, L_D	Phenomenological coefficients in I.T. models
ΔP	Applied pressure, kPa
q_1, q_2	Point charges, coulomb
q_s	Charge density, coul/m^2
Q	Charge density, coul/m^2
r	Distance between two point charges, m
R_j	Rejection rate, %
R	Universal gas constant = 8.314 J K^{-1}mole^{-1}
t	Time, sec
T	Absolute temperature, K
V	Volume, m^3
x	Transverse direction from the membrane surface, m

X	Fixed membrane charge density, mol/m^3
z_i	Valence of component *i*

Greek

ψ	Electrical potential, volt
$\Delta\psi$	Potential difference, volt
λ_i	Hindrance coefficient = ratio of radius of component *i* to pore radius
ε_0	Permittivity of free space, F/m
ε	Membrane electrical permittivity, F/m
ε_α	Dielectric constant
λ_0	Debye length on the feed side of the membrane, m
λ_L	Debye length on the permeate side of the membrane, m
σ	Reflection coefficient
$\Delta\pi$	Osmotic pressure, kPa
μ_i	Chemical potential of species *i*, J/mol
$\tilde{\mu}_i$	Electrochemical potential of species *i*, J/mol

Subscript

i	Component *i* of multi-component mixture
m	Membrane
0	Feed
p	Permeate

LIST OF TABLES

LIST OF FIGURES

Chapter 1

INTRODUCTION

1.1 Background

Membrane separation processes are being widely used for many applications such as water desalination, industrial and municipal waste treatment, gas separation, and biomedical engineering. Among different membrane processes, reverse osmosis (RO) and nanofiltration (NF) have had significant development in the past decade. RO processes have been used for separation and concentration of solutes in many fields, such as chemical and biomedical industry, food and beverage processing, and water and wastewater treatment (Hajeeh and Chaudhuri 2000; Song 2000); whereas as one of the important advances in membrane technology, NF membranes have been developed and are particularly well suited for removal of multivalent ions and dissolved organics from water and waste water treatment processes (Mulder 1991; Raman *et al*. 1994; Bhattacharjee *et al*. 2001). With the shortage of raw water sources and the more stringent standards for water quality, it is anticipated that the application of RO/NF membranes in water reclamation and water supply will further increase.

For all membrane processes, the design of membrane system, the optimization of operating conditions and the widening of the range of application would be greatly enhanced when quantitative methods for predicting process performance are readily available. Thus, an accurate model of RO/NF performance in process design and optimization is needed to meet the increased and extensive usages of RO/NF processes. In other words, the mechanisms of membrane separation process should be adequately understood and mathematical methods should be established and used for predicting the transport behaviors of solutes through RO/NF membranes.

For a RO or NF membrane, the permeate flux is well predicted (Slater and Brooks 1992; Song 2000). The transport of solutes through a membrane, however, is much less understood. In literature, many physical and mathematical models (Kedem and Katchalsky 1958; Reid and Breton 1959; Lonsdale *et al.* 1965; Meter 1966; Spiegler and Kedem 1966; Sherwood *et al.* 1967; Sourirajan 1970; Jonsson 1980; Soltanieh and Gill 1981; Mason and Lonsdale 1990; Wijmans and Baker 1995; Yaroshchuk 1995) and experimental studies (Rosenbaum and Skeins 1968; Pusch 1977; Schirg and Widmer 1992; Lipp *et al.* 1994) have been reported. The most popular mechanisms are summarized as follows:

(1) sieving mechanism

(2) the hydrogen bonding theory or wetted surface theory

(3) preferential sorption-capillary flow mechanism

(4) solution-diffusion mechanism

(5) finely-porous theory

Although the above theories have been put forward to describe the phenomena of salt transport through membranes, its mechanism and physicochemical criteria for salt rejection are still a matter of controversy (Jonsson 1980; Soltanieh and Gill 1981; Mason and Lonsdale 1990; Chaudry 1995).

1.2 Problem Statement

The above popular solute transport mechanisms are mainly focused on uncharged particles and are inadequate to describe the phenomena of ion transport. For instance, the solution-diffusion theory treats diffusion as the only mechanism for ion transport (Lonsdale *et al.* 1965; Meter 1966; Lonsdale *et al.* 1975; Wijmans and Baker 1995). RO and NF membranes are usually made of polymeric materials. A polymeric membrane acquires surface charge when being in contact with an aqueous medium (Shaw 1969; Jacobasch and Schurtz 1988; Childress and Elimelech 1996), where dissolved salts can be ionized and usually transport in pairs of cations and anions. Salt transport through RO/NF membranes is thus affected by the electrostatic interaction between ions and membrane, in addition to the common transport mechanisms in the membrane, such as diffusion and convection.

Although the three major mechanisms namely diffusion, convection and electro-migration of ion transport can be mathematically described by the extended Nernst-Planck equation (Schlögl 1966; Dresner 1972), the electrostatic interactions between ions and membrane are usually inadequately considered in the published studies in literature. Instead, this rather important interaction has been commonly studied by simply incorporating the existing models with the Donnan equilibrium (1924), which

describes the partitioning of ion concentration at the interface between the membrane and the external solution (Donnan 1995). The Donnan equation has been added into the friction model (Hoffer and Kedem 1967; Jitsuhara and Kimura 1983), solution-diffusion theory (Lonsdale *et al.* 1965; Meter 1966; Wijmans and Baker 1995), and most popularly, combined with the extended Nernst-Planck equation (Dresner 1972; Tsuru *et al.* 1991a; Bowen and Mohammad 1998b). Tsuru *et al.* (1991a) first calculated salt rejection by solving the Nernst-Planck-Donnan (NPD) model numerically. Since then NPD model has been widely used to describe ion transport behaviors through RO/NF membranes (Bowen and Mukhtar 1996; Hall *et al*. 1997; Bowen and Mohammad 1998a, b; Bhattacharjee *et al.* 2001; Ong *et al*. 2002).

However, this approach causes a physical paradox: a spatial electric field arises even in cases when the local electroneutrality is initially assumed (Hickman 1970; Jackson 1974; Martuzans and Skryl 1998). From electrostatic viewpoints, it is the net charge that gives rise to the electric fields. If the charge is neutral at each point along the membrane length, there should be no electric field across the membrane, i.e., no electric forces would assert on ions to cause electromigration through the membrane. The local electroneutrality assumption, which is made in NPD model in order to study the effect of electrostatic interaction on ion transport, ironically eliminates all the possibilities to study the electrostatic interaction. This is one of the lethal flaws in the NPD model that greatly reduces the value of the model. Furthermore, NPD model cannot be used without the local electroneutrality assumption associated with the Donnan equilibrium. Otherwise, the boundary condition on the membrane surface would become unspecified. In other words, current models or theories are not adequate to describe the ion transport process through RO/NF membranes. Thus, a more

fundamentally sound theory and a more comprehensive model is needed for predicting ion transport through RO/NF membranes.

1.3 Research Objectives

The overall objective of this study is to investigate the mechanisms and behaviors of the ion transport through RO/NF membranes from the fundamental principles. The specific objectives include:

1. To develop a sound theory and formulation for ion transport through RO/NF membranes from fundamental electrostatic and electrodiffusion principles;
2. To investigate ion transport mechanisms and the role of electrostatic interaction in RO/ NF membranes;
3. To investigate the ion/salt transport behaviors in single- and mixed-electrolyte solutions and the effects of operating parameters on solute rejections.

1.4 Organization of Thesis

Chapter 2 provides a comprehensive review on membrane process, transport models and their limitations reported in literature. Basic electrostatic and electrodiffusion theories, which are relevant to this study, are also introduced.

In Chapter 3, the Nernst-Planck-Donnan model incorporated with Freundlich isotherm model is presented. The behaviors of ion transport through loose RO and NF membranes have been simulated by using this model. Limitations and problems from Donnan model have been discussed.

Chapter 4 presents a new formulation based on Nernst-Planck-Possion model with the appropriate boundary conditions. The numerical solution for problems of ion transport through dense RO membrane has also been addressed.

Chapter 5 and Chapter 6 investigate the ion transport mechanisms and discuss the transport behaviors in both single and mixed electrolyte solutions under different operating conditions.

Chapter 2

LITERATURE REVIEW

2.1 Membrane and Membrane Processes

2.1.1 Definition of a Membrane

According to International Union of Pure and Applied Chemistry (IUPAC), membrane is termed as "a structure, having lateral dimensions much greater than its thickness, through which mass transfer may occur under a variety of driving forces" (IUPAC 1996). More specifically, membrane can be defined as a semi-permeable thin film, which acts as a selective barrier between two phases. The definition says nothing about membrane materials, structures or its functions; however, it implies its separation mechanism and hence the application. To obtain a more informative understanding, membranes can be classified from different points of view. The first distinctive classification is by its nature, i.e., biological or synthetic membranes, for these two types of membranes differ completely in structure and functionality. Based on the membranes materials, synthetic membranes can be subdivided into organic (polymer or liquid) and inorganic (ceramic, metal) membranes (Mulder 1996). This study focuses only on the polymeric membranes. With its pore size ranging from atomic

dimensions (< 10 angstroms) to 100+ microns, polymeric membranes can be used for a number of chemical separations.

2.1.2 Membrane Process and its Classifications

Membrane process is defined as a mass transfer process that occurs under a variety of driving forces between two phases. Membrane processes can be classified by the driving force and the nature of the membrane. The driving forces in membrane technology can be gradients of concentration, pressure, temperature, electrical potential, centrifugal force, and magnetic force. Some membrane processes and their driving forces are summarized in Table 2.1.

Other than the driving forces, the membrane itself is the principal factor determining the process performances. The nature of membranes, that is, its structure and material, determines the type of application, ranging from the separation of microscopic particles to the separation of molecules of an identical size or shape. For instance, Table 2.2 shows the pore size characteristics of commonly-used pressure-driven processes in water and wastewater treatment such as microfiltration (MF), ultrafiltraton (UF), nanofiltration (NF) and hyperfiltration or reverse osmosis (RO) and their applications.

Table 2.1 Some Membrane Processes and Their Driving Forces

Membrane Process	Phase 1	Phase 2	Driving Forces
Microfiltration (MF)	L	L	ΔP
Nanofiltration (NF)	L	L	ΔP
Reverse Osmosis (RO)	L	L	ΔP
Ultrafiltration (UF)	L	L	ΔP
Gas Separation	G	G	ΔP
Pervaporation	L	G	ΔP
Osmosis	L	L	Δc
Dialysis	L	L	Δc
Electrodialysis	L	L	ΔE
Theromo-osmosis	L	L	$\Delta T/\Delta P$
Membrane Distillation	L	L	$\Delta T/\Delta P$

Table 2.2 Pressure-driven Membrane Processes

Process	Operating Pressure	Pore Size	Material Retained
MF	~ 10 psi	0.05 – 1.0 μm	Suspended solids
UF	~ 10 – 100 psi	0.002 – 0.1μm	Bio-organisms, colloids, and macromolecules; suspended solids
NF	~ 10 – 100 psi	0.001– 0.01 μm	Multivalent salts; macromolecules & suspended solids
RO	~ 100 – 800 psi	1.0 – 15 Å*	Polysaccharides & salts; macromolecules & suspended solids

* 10 Å = 1 nm = 0.001 μm

All membrane processes are designed to achieve a separation purpose. Owing to the semi-permeability of the membrane, one component in solution could be transported more readily than the other. The stream containing penetrants that passes through the membrane is called "permeate"; while the stream that has been depleted of penetrants that leaves the membrane modules without passing through the membrane to the downstream is called "retentate" (or the concentrate) (IUPAC 1996). Generally, there are two configurations of membrane processes as shown in Figure 2.1. In dead-end filtration, retained components have no exit to leave the membrane module but accumulate inside the module with time. Therefore, the dead-end membrane process has to be stopped from time to time to remove the retained components. This means dead end filtration cannot be operated continuously. In contrast, the retained components in cross-flow filtration are carried away from the membrane module by a concentrate stream. For large scale industrial applications, a cross-flow operation is preferred because it can be operated in a continuous mode.

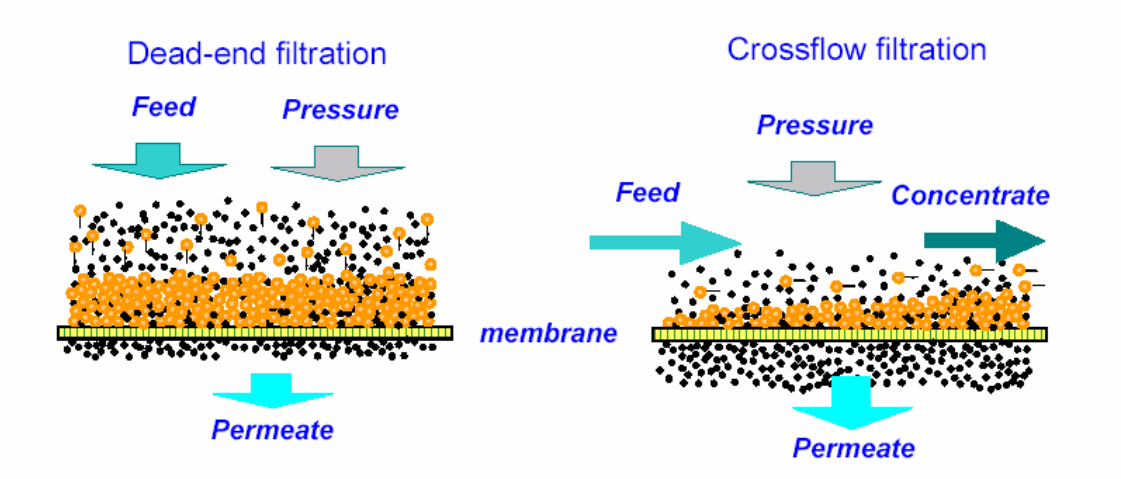

Figure 2.1 Configuration of Membrane Processes: (a) Dead-end Filtration and (b) Cross-flow Filtration

Membrane process performance is characterized by the process parameters, namely the water flux and retention or rejection rate, which represents the permeate rate and selectivity, respectively. The water flux or permeate production, J_v, is defined as the volume flowing through the membrane per unit area per unit time; while the retention or rejection rate, R_j, which expresses the degree to which a solute is retained by the membrane, is defined as:

$$R_j = 1 - \frac{C_p}{C_f} \tag{2.1}$$

where C_p is the permeate concentration and C_f is the feed concentration.

2.1.3 Reverse Osmosis and Nanofiltration

Reverse osmosis (RO), also known as hyperfiltration, is the finest filtration known. As shown in Figure 2.2, this process will allow the removal of particles as small as ions (particle size of around 1.0 nm) from a solution. Based on IUPAC's definition, reverse osmosis is a "pressure-driven process in which applied transmembrane pressure causes selective movement of solvent against its osmotic pressure difference" (IUPAC 1996). Reverse osmosis is used to purify water and remove salts and other impurities in order to improve the color, taste or properties of the fluid. Since its first major breakthrough in commercial application in 1975 (when Dow Chemical, Du Pont and Fluid Systems developed large-scale modules for the Office of Water Research and Technology, USA), RO processes have been widely used for separation and concentration of solutes in many fields, such as chemical and biomedical industry, food and beverage processing, and water and wastewater treatment (Hajeeh and Chaudhuri 2000; Song 2000). With the shortage of drinking water sources and the more stringent standards for drinking water quality, it is anticipated that the application of RO membrane in water reclamation and seawater desalination will further increase.

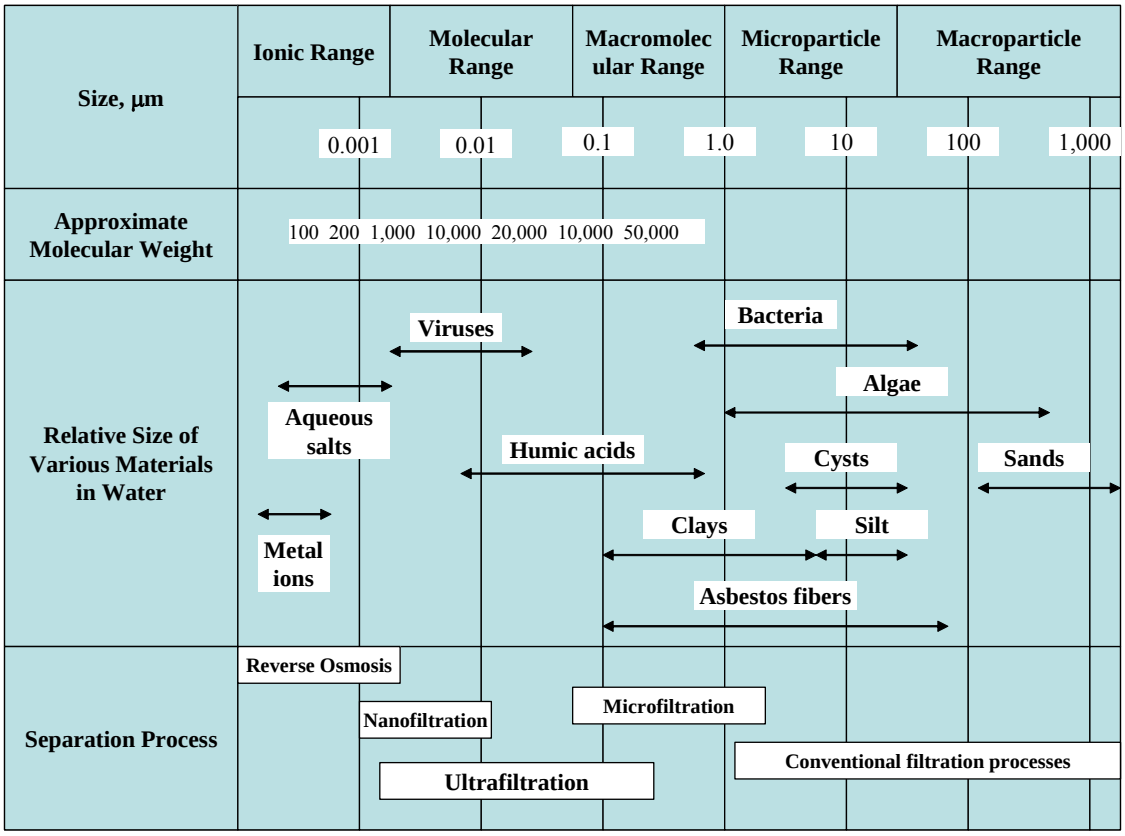

Figure 2.2 Common Membrane Operations in Water Treatment

As one of the most important advances in membrane technology, nanofiltration (NF) membranes have been developed and widely used in removal of salts in water treatment and the fractionation of salts and small molecules in a number of industries, such as drinking water production, dairy industry and the paper industry. According to International Union of Pure and Applied Chemistry, nanofiltration is defined as a "pressure-driven membrane-based separation process in which particles and dissolved molecules smaller than about 2 nm are rejected" (IUPAC 1996). These membranes have received their name as they have a molecular weight cut-off for uncharged molecules corresponding to pores of about one nanometer in diameter (Eriksson 1988a). NF membranes have properties between ultrafiltration (UF) and reverse

osmosis membranes, the solute separation mechanisms of which have been studied intensively (Bowen and Mukhtar 1996; Peeters *et al.* 1998; Bhattacharjee *et al.* 2001).

Nanofiltration is not as fine a filtration process as reverse osmosis, but it also does not require the same energy to perform the separation. Nanofiltration also uses a membrane that is partially permeable to perform the separation, but the membrane's pores are typically much larger than those used in reverse osmosis. Nanofiltration is capable of concentrating sugars, divalent salts, bacteria, proteins, particles, dyes, and other constituents that have a molecular weight greater than 1000 daltons. Nanofiltration, like reverse osmosis, is affected by the charge of the particles being rejected. Thus, particles with larger charges are more likely to be rejected than others. Nanofiltration is not effective on small molecular weight organics, such as methanol.

2.2 Solute Rejection

2.2.1 Membrane Transport Behaviors

The net driving force for water transport across the membrane is the pressure difference between the applied pressure and osmotic pressure, while the driving force for solute passage is the concentration difference between the feed and permeate sides (Kedem and Katchalsky 1958; Lonsdale *et al.* 1965; Rosenbaum and Skeins 1968; Sourirajan 1970; Pusch 1977a; Jonsson 1980; Soltanieh and Gill 1981; Mason and Lonsdale 1990; Mulder 1996). In addition, membrane properties, solution chemistry, as well as operating conditions are also important parameters that affect both water flux and solute rejection strongly (Gauwbergen and Baeyens 1999).

In literatures, many researchers showed that water flux increased linearly with operating pressure (Eriksson 1988b; Wijmans and Baker 1995; Levenstein *et al.* 1996; Gaubergen *et al.* 1997; Gauwbergen and Baeyens 1997). As shown in Figure 2.3 (a), a straight line passes through the origin when the distilled water is filtrated. When the concentration increases in the feed solution, the slope of line is decreasing and the obtained straight lines between the water flux and applied pressure intersect with the x-axis. The pressure at the intersection point is called "initial osmotic pressure", which is a characteristic of the feed solution. Water can be permeated only when the applied pressure is higher than the osmotic pressure. In addition, as illustrated in Figure 2.3 (b), it was also found that a nonlinear relation between the water flux and pressure could be developed when the applied pressure was below the initial osmotic pressure, especially for the high salt concentration (Rosenbaum and Skeins 1968; Pusch 1977b). Song (2000) first pointed out theoretically such nonlinearity and explained this phenomenon with a new model.

Solute flux was usually assumed to be linearly dependent on its driving forces (i.e., concentration differences) (Lonsdale *et al.* 1965; Metern 1966; Wijmans and Baker 1995). Levenstein *et al*. (1996), however, stated that a power relationship between solute flux and concentration was correlated well with their experimental data. It was also found that salt rejection increased with pressure but decreased with feed salt concentration nonlinearly (Soltanieh and Gill 1981; Peeters *et al.* 1998; Ong *et al.* 2002). However, current transport theories and models have failed to address the non-linear relationships between (a) water flux and operating pressure, and (b) solute flux and feed salt concentration as reflected from the respective transport equations.

Therefore, a comprehensive review on solute transport mechanisms and transport model is a necessity in this study.

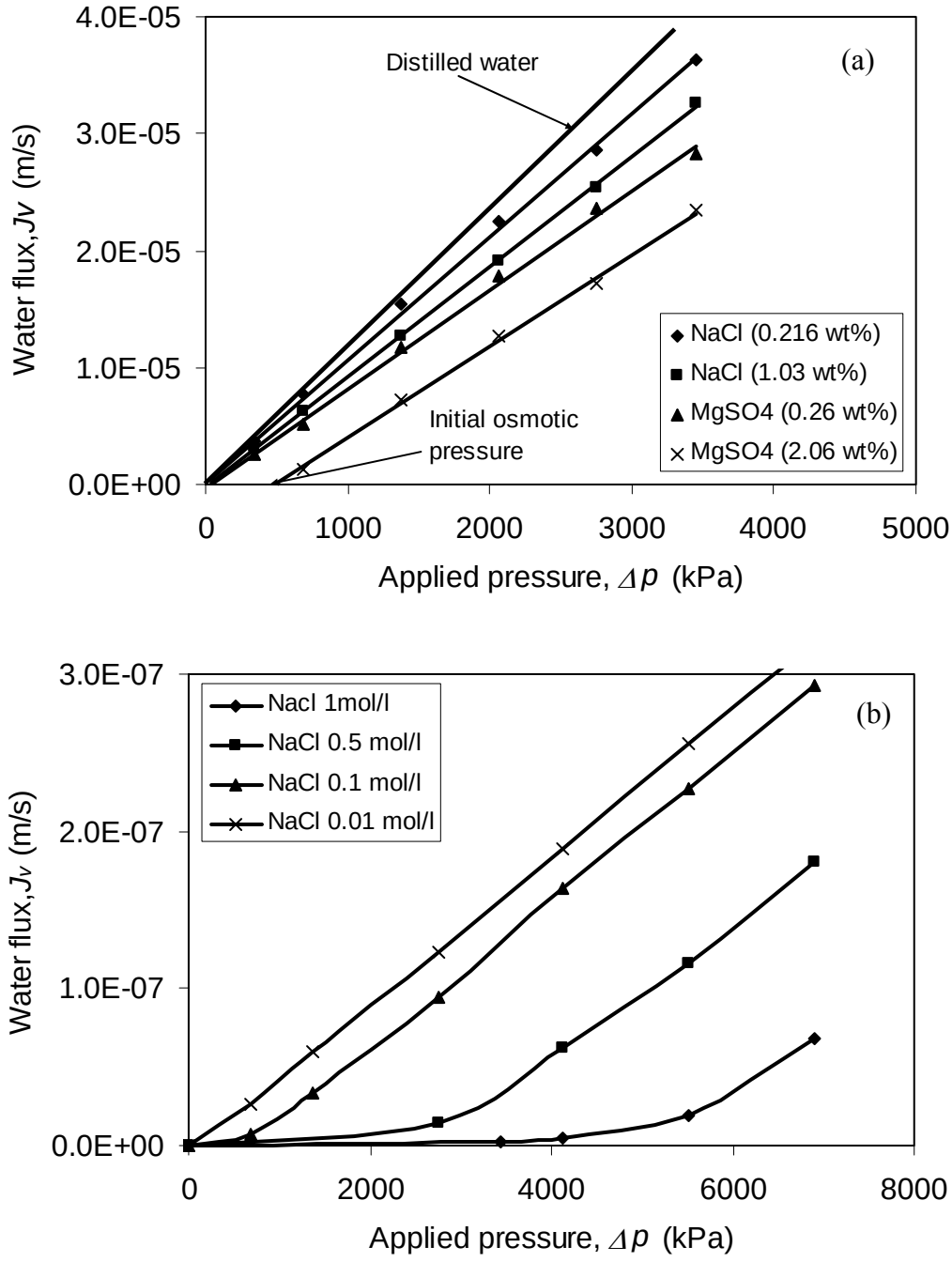

Figure 2.3 Plots of Water Flux versus Applied Pressure: (a) Data from Eriksson (1988) and (b) Data from Rosenbaum and Skeins (1968)

2.2.2 Possible Solute Transport Mechanisms

Figure 2.4 shows the general description of a membrane separation process. Solute transport through membrane from the feed solution region *a* to the permeate solution region *h*. In region *a*, solute concentration is uniform and no concentration gradient in the direction normal to the membrane surface. However, in the boundary layer *b*, retained solute builds up and causes a concentration polarization layer, which reduces the efficiency of solute rejection. Right at the surface of the membrane (i.e., region *c*), solute diffuses and is adsorbed into the membrane. The solute is then transported in the membrane, mainly rejected in the skin layer *d*. The penetrated solute is desorbed out of the membrane in surface region *f*. Concentration gradient is also built in region *g* before entering the permeate solution *h*, where solute concentration becomes uniform.

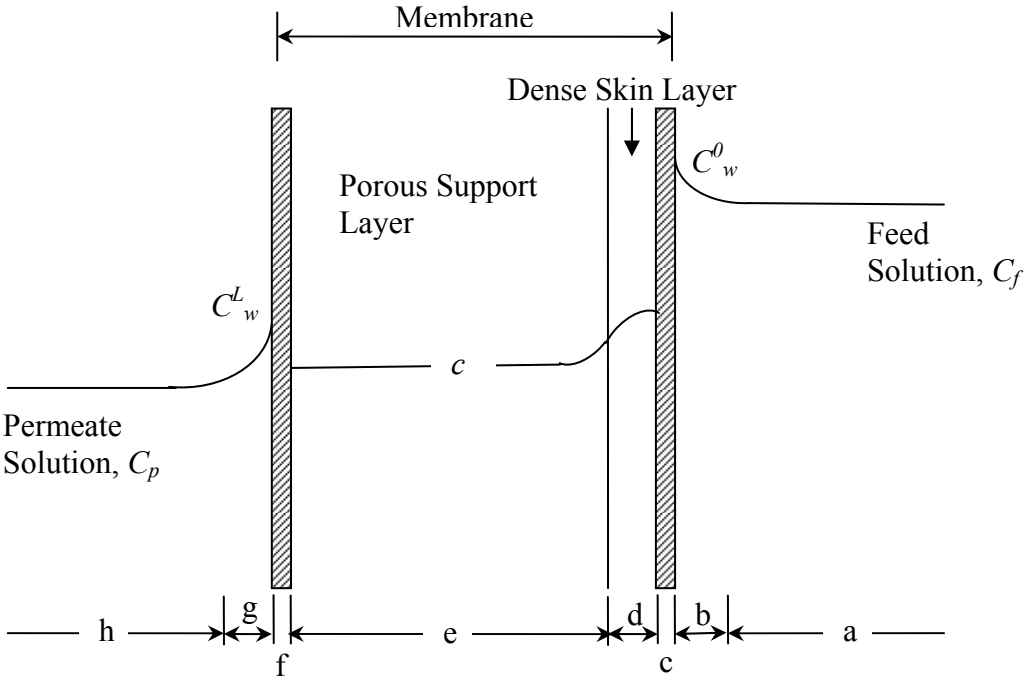

Figure 2.4 Schematic representation of transport through as asymmetric membrane

As shown from the above description, the solute rejection is mainly affected by the adsorption/desorption of solute and membrane properties. Several mechanisms of water and solute transport through RO/NF membranes are discussed in the literature (Kedem and Katchalsky 1958; Spiegler and Kedem 1966; Jonsson 1980; Soltanieh and Gill 1981; Mason and Lonsdale 1990; Tsuru *et al.* 1991a; Bowen and Muktar 1996; Peeters *et al.* 1998; Van Gauwbergen and Baeyens 1998; Kargol 2000; Bhattacharjee *et al.* 2001). Although many researchers have studied the solute transport through RO/NF membranes, its mechanisms of separation and physicochemical criteria for salt rejection is still a matter of controversy. However, there are several possible mechanisms proposed by previous researchers as summarized below.

Sieving Mechanism. Sieving mechanism is based on the difference of molecular size between the solute and solvent. It assumes that the membrane has its pore size larger than the molecular size of solvent but smaller than that of solute. As a result, the solute can be rejected at the membrane-solution interface, while solvent water penetrates the membrane. This mechanism is ruled out in reverse osmosis and nanofiltration, for the solution such as sodium chloride, the sizes of NaCl and that of H_2O are almost the same. However, H_2O can be permeated, but most of the NaCl is rejected by RO membranes. This implies that there should be some other mechanisms dominate the solute transport through RO/NF membranes. In addition, although sieving mechanism does not play an important role in RO/NF membrane transport, the pore size still has a significant effect on solute behaviors.

Solution-diffusion Mechanism. Solution-diffusion mechanism is one of the most popular theories used in design and optimization of membrane processes. It is assumed

that both solvent and solute dissolve in the homogenous nonporous surface layer of the membrane and then they are transported by a diffusion mechanism in an uncoupled manner (Lonsdale *et al.* 1965). Such a membrane is termed as 'perfect' membrane. According to Banks and Sharples (1966), the transport mechanism in reverse osmosis was one of diffusive flow through the pore – free layer in the membrane. However, the transport of water and solute cannot be independent; instead, the water flow would couple the passage of solute in one way or another.

Michaels *et al.* (1965) stated that water transport was by molecular diffusion through polymer matrix, and ion transport was by three parallel flow mechanisms: (1) by sorption and activated diffusion within the polymer matrix governed solely by the ion-concentration gradient across the membrane; (2) by pressure-biased activated diffusion of ions in near – molecular – sized pores in the membrane, governed by both the hydraulic gradient and the ion-concentration gradient; and (3) by hydrodynamic flow of saline solution through larger pores. Sherwood *et al.* (1967) introduced the solution-diffusion-imperfection model, which accounted for some imperfections on the membrane surface and thus allowed pore flow of solute and solvent in an undiluted form; i.e., the pore size was large enough to allow bulk flow. In this case, water flux is mainly transported by diffusion mechanism, but convection in membrane pores contributes to the salt flux significantly (Sourirajan 1970). However, when the pore size is small, this assumption is no longer valid and the concentration gradient within the membrane must be taken into account, which leads to the finely-porous model.

Water Clustering Mechanism. It was noted that the adsorption of the solute into the membrane was very important in understanding the separation mechanism (Soltanieh

and Gill 1981). Hence, another group of mechanisms were proposed based on the interaction between solute and membrane. One of such mechanisms is water-clustering mechanism. This mechanism, also called wetted surface mechanism, was proposed by Reid and Breton (1959) and further developed by Orofino *et al.* (1969). It recognized that membrane material was quite wettable and that solvent tended to cling to it by means of hydrogen bonding as an absorbed film. This film could obstruct the pores in the membrane and thereby prevented solute ions from entering. The solvent progressed through the membrane by passing from one wetted site to another within the membrane structure.

Preferential Sorption-capillary Flow Mechanism. In contrast to the solution-diffusion mechanism, the preferential sorption-capillary flow mechanism combines the effects of membrane pore sizes and the chemical properties of membrane surface (Sourirajan 1970). It assumes that the membrane skin layer has a preferential sorption or preferential repulsion for one of the constituents in solution. If the chemical nature of the skin layer is in contact with the solution, a preferential absorbed fluid layer forms at the interface, which is enriched by one of the constituents of the bulk solution. Polymeric membranes with low dielectric constant, such as cellulose acetate, repel ions in the close vicinity of the surface, resulting in preferential sorption of water. This layer of water is forced through the membrane capillary under pressure. For a given membrane and under certain operating conditions, there is a critical pore size that yields optimum solute separation and fluid permeability. This critical pore size, according to Sourirajan (1970), should be twice the thickness of the absorbed water layer.

The preferential sorption might be major mechanism in organic transports through NF membranes. Kiso *et al.* (2001) recently showed that hydrophobic compounds were adsorbed on the membranes and hydrophobicity was an important factor affecting organic rejection. In 1998, Hydranautics (Oceanside, CA) used the same concept to manufacture a so called low fouling membrane (LFM). As identified by Wilf and Klinko (1999), the hydrophilic character of LFM surface reduced the rate of adsorption of organic matter present in the feed water.

Donnan Exclusion Mechanism. Another important interaction between the solute and membrane is the charge effects. Reverse osmosis and nanofiltration membranes are made of polymeric materials. A polymeric membrane acquires surface charge when being in contact with an aqueous medium (Shaw 1969; Jacobasch and Schurz 1988; Childress and Elimelech 1996). Childress and Elimelech (1996) investigated the zeta potentials of some RO/NF membranes under different pH values. It was found that when pH value was higher than 5.0, all measured RO/NF membranes were negatively charged. This charge will affect the distribution of ions at the membrane-solution interface: co-ions (i.e., ions of same charge of the membrane) will be repelled while counter-ions (i.e., ions with the opposite charge) will be attracted by the charged membrane. The electrostatic repulsion of co-ions is termed as "Donnan exclusion". Thus, the salt separation is based not only on the other mechanisms mentioned above, but also on the Donnan exclusion, which exerts an electrostatic force on an electrolyte solution (Tsuru *et al*. 1991a; Peeters *et al.* 1998).

When a charged membrane is in contact with an electrolyte solution, the concentration of co-ions in the membrane will be lower than that in solution, while the counter-ions

have a higher concentration in the membrane than in the solution. Owing to this concentration difference of the ions, a potential difference is generated at the interface between the membrane and the solution to maintain electrochemical equilibrium between solution and membrane. This potential is called 'Donnan potential'. By Donnan potential, co-ions are repelled by the membrane while counter-ions are attracted. Since membranes can be easily charged, Donnan exclusion is another possible mechanism to reject salt through membranes.

Donnan exclusion of co-ions due to their interactions with fixed electric charges presents one well established non-sieving rejection mechanism. Counter-ions in binary electrolytes are transferred stoichiometrically owing to the zero electric current condition. Therefore, a salt as a whole is rejected. Studies show that Donnan exclusion might be the main mechanisms in ion transport for RO membranes (Bowen and Mukhtar 1996; Hall *et al.* 1997; Peeters *et al.* 1998; Bhattacharjee *et al.* 2001; Ong *et al.* 2002; Pievet *et al.* 2002; Szymczyk *et al.* 2003). The Donnan exclusion is dependent on the salt concentration, valence of ions, and fixed charge concentration in the membrane (Donnan 1995; Higa *et al.* 1998; Peeters *et al.* 1998).

2.2.3 Solute Transport Models

There are two types of membrane transport models. One is based on the irreversible thermodynamics (I.T.) whereby the membrane is treated as a black box (that is, no transport mechanism is assumed). The separation process through the membrane is slow and is taking place near equilibrium condition. Theories of irreversible thermodynamics can be found in literatures such as DeGroot and Masur (1962), Katchalsky and Curran (1975), and Kondepudi and Prigogine (1999). The other types of models are based on their assumed transport mechanism, such as the solution-diffusion models discussed earlier.

2.2.3.1 Irreversible Thermodynamics

Transport equations based on non-equilibrium irreversible thermodynamics were given by several researchers (Kedem and Katchalsky 1958, 1963; Spiegler and Kedem 1966; Johnson *et al*. 1966). Kedem and Katchalsky (1958, 1963) pointed out that the volume flux (J_v) and the solute flux (J_s) through a membrane were governed by three coefficients representing solute-solvent, solute-membrane, and solvent-membrane interactions. In their approach, coupling of solute and solvent flow was included as an independent parameter.

Kedem-Katchalsky Model. The model can be written as:

$$J_v = L_p\left(\Delta P - \sigma\Delta\Pi\right) \tag{2.2}$$

$$J_s = \left(c_s\right)_{\ln}\left(1-\sigma\right)J_v + \varpi\Delta\pi \tag{2.3}$$

where

$$\sigma = -L_{PD} / L_p \tag{2.4}$$

$$\varpi = (c_s)_{\ln}\left(L_D L_P - L^2{}_{PD}\right)/ L_P \tag{2.5}$$

L_P, L_{PD}, L_{DP}, and L_D are the phenomenological coefficients and

$$(c_s)_{\ln} = \frac{c_s{}^0 - c_s{}^{\Delta x}}{\ln \dfrac{c_s{}^0}{c_s{}^{\Delta x}}} \tag{2.6}$$

is the logarithmic average concentration.

Salt rejection is defined as the percentage of dissolved material that does not pass through the membrane, which can be expressed as follows:

$$R_j = 1 - \frac{C_P}{C_f} = 1 - \frac{J_s}{C_f J_V} \tag{2.7}$$

C_p and C_f are the concentration of permeate and feed, respectively. By using experimental data with different membranes, Pusch (1977) derived the rejection-volume flux relationship from Kedem-Katchalsky model. Based on Eqs. (2.2) and (2.3) and substituting for $\varpi = (c_s)_{\ln}\left(L_D L_P - L^2{}_{PD}\right)/ L_P$, rejection rate can be calculated by:

$$1/R_j = 1/R_\infty + \left(L_D / L_P - R^2{}_\infty\right) L_P \pi_R / R_\infty J_v \tag{2.8}$$

where $R_\infty = 1-(1-\sigma)(c_{s\infty})_{\ln}/C_R$, and $(c_{s\infty})_{ln}$ is the mean salt concentration at infinite J_v. Hence, a plot of $1/R_j$ versus $1/J_v$ should give a straight line with the slope of $(L_D/L_P - R_\infty{}^2)L_p\pi_R/R_\infty$ and the intercept of $1/R_\infty$. The data of Lui (1978) were used to verify Pusch's model (1977). It was found that not only $1/R_j$ vs. $1/J_v$ was linear for each concentration, but the lines for different concentrations were almost coincident.

Spiegler-Kedem Model. Based on the constancy of three coefficients, namely reflection coefficient (σ), solute permeability (P) and pure water permeability (L_p), for the cases of high concentration difference between the retentate and permeate, Spiegler

and Kedem (1966) expressed this relation in a differential form and calculated salt rejection by the well-known Spiegler-Kedem equation:

$$J = P\Delta x\left(\frac{dc}{dx}\right) + (1-\sigma)J_v\bar{c} \tag{2.9}$$

where $\bar{c} = \frac{c_b - c_p}{\ln\frac{c_b}{c_p}}$. The salt rejection rate can be calculated by the following equations:

$$R_j = \frac{\sigma(1-F)}{1-\sigma F} \tag{2.10}$$

$$F = \exp\left(-\frac{1-\sigma}{P}J_v\right) \tag{2.11}$$

As an extension of the Kedem-Katchalsky model, the parameters in this model are less sensitive to concentration (Soltanieh and Gill 1981). The nonlinear Spiegler-Kedem model was verified by Pusch's data (1977). It was found that the rejection rate decreased with the increase in permeate flux and feed concentration. However, the concentration effects have not been thoroughly investigated.

Irreversible thermodynamic models permit a simplified description of the retention of a single non-electrolyte or electrolyte by the membrane, but it cannot be extended to mixed solutions (Soltanieh and Gill 1981; Mason and Lonsdale 1990; Tsuru *et al.* 1991a; Hafiane *et al*. 2000). Moreover, these models are dependent on three parameters, which are found to be highly related to the feed concentration. Thus, effect of the salt concentration on membrane transport cannot be studied by these irreversible thermodynamic models.

2.2.3.2 Solution-Diffusion Model

Solution-diffusion model is commonly used for studying membrane transport and system design. As mentioned in Section 2.2.2, this model treats the membranes as non-porous and homogenous. Both solvent and solute are dissolved in the membrane and transported by diffusion mechanism under chemical potential gradient in an uncoupled manner. The volume flux and solute flux can be expressed as:

$$J_w = \frac{D_w c_w \overline{V}_w}{RT\Delta x}\left(\Delta p - \Delta\pi\right) \equiv A\left(\Delta p - \Delta\pi\right) \tag{2.12}$$

$$J_s = -D_s k_s \frac{C_P - C_R}{\Delta x} = k_2\left(C_R - C_P\right) \tag{2.13}$$

The volume flux is proportional to the applied pressure, while the solute flux is proportional to the concentration difference between the downstream and upstream of the membrane. The solute rejection is then calculated by:

$$R_j = 1 - \frac{C_P}{C_R} = 1 - \frac{D_s k_s RT}{D_w c_w \overline{V}_w} \cdot \frac{C_P - C_R}{C_R} \cdot \frac{1}{\left(\Delta p - \Delta\pi\right)} \tag{2.14}$$

Although solution-diffusion model is simple and easy to use, previous researchers found that for some membranes, the volume flux was not linearly proportional to the applied pressure; rather it increased exponentially with pressure (Paul 1976). Furthermore, the effect of pore flow in the membrane was large and was significant for solute transport (Lonsdale *et al.* 1965).

In solution-diffusion-imperfection model, the convection terms were added due to the pore flow in membrane (Sherwood *et al.* 1967). The total water flux, $N_{w,}$ and the total solute flux, N_s, are given by:

$$N_w = J_w + K_3 \Delta p C_w = A\left(\Delta p - \Delta\pi\right) + K_3 \Delta p C_w \tag{2.15}$$

$$N_s = J_s + K_3 \Delta p C_R = K_2\left(C_R - C_P\right) + K_s \Delta p C_R \tag{2.16}$$

The solution-diffusion-imperfection model can fit the experimental data well; however, the corresponding coefficients K_1, K_2, and K_3 vary with the feed concentration and applied pressure, which makes it difficult to use for design application. Therefore, a model with constant coefficients, i.e., not being function of the independent variables c and Δp, is highly desirable.

2.2.4 Unsolved Problems

Although in literature, significant progress has been made in manufacturing more efficient membranes with high water flux and salt rejection as well as in understanding the mechanisms of membrane separation process (Soltanieh and Gill 1980), the review on membrane transport model presented above clearly indicated that there are many problems that still need to be resolved. These include:

(1) Solution-diffusion mechanism is not adequate in describing the solute transport behaviors, especially the nonlinear effect of concentration on solute flux.

(2) Modifications in solute-diffusion theory assumed that convective flow due to membrane pore played a significant role in solute flux. However, this assumption is only applicable to loose RO or NF membrane. This is because dense RO membranes are considered to be non-porous.

(3) Irreversible thermodynamic models demonstrate a simple way for describing water and solute flux. However, there are several limitations: (a) no ideas about the transport mechanisms could be indicated in models; (b) I.T. models could not be extended to the mixed-electrolyte solution, while ion transport is the main concern in this study; and (c) the models are dependent on three phenomenological coefficients which are highly related to the concentration.

(4) Besides solution-diffusion, other mechanisms might be involved in solute transport and the interaction between membrane and solute components might play an important role in solute flux. Unfortunately, both of which could not be clearly demonstrated with the above theories and models.

As the current models or theories are not adequate to describe the solute transport process through RO/NF membranes, one hypothesis could be proposed from the discussion presented in the previous sections. That is, there should be some mechanism which could contribute to the solute transport by coupling the transport of different components in solute. Synthetic membranes tend to acquire surface charge when they are in contact with an aqueous medium (Shaw 1969; Jacobasch and Schurz 1988; Childress and Elimelech 2000). Even for the membranes initially uncharged, charge can be developed later as a result of imbalanced ion transport owing to mobility difference among various ions. Hence, for ion transport through RO/NF membranes, it can be expected that the electric field within the membranes might be another driving force for solute transport and the electrostatic interaction between charged membrane and ions might play an important role in transport process. However, the above theories and models could not reflect the effect of electrostatic interaction on ion transport, the issue of which is to be resolved in this research work.

2.3. Basic Electrostatic Theory

This section introduces basic concepts of electrostatics and provides a framework for understanding and quantitatively assessing electrostatic relations occurred in ion

transport. Good reference books can be found from Harnwell (1949), Page and Adams (1949) as well as Griffiths (1989).

2.3.1 Basic Concept

Electrostatics is associated with insulating materials and electrically isolated conductors. “Insulation” and “isolation” prevent easy migration of charge. So charges stay in place (i.e. “static”). The effects the charges produce are then important. It is charge which gives rise to the electric fields generating forces that attract thin films and particles to surfaces and charge which gives rise to high voltages in low capacitance systems.

Static Charge. Static electricity arises as the separation of positive and negative charges at the interface between two dissimilar surfaces. If one or other of the surfaces prevent easy migration of charge, or the conductor on which they reside is isolated, then this charge is “static” (on the surface) and remains available to influence the surroundings. Static electricity can also arise on surfaces as trapped ions from the air. Static charges may be electrons, or positive, or negative ions - but they are in the basic units of electronic charge 1.602×10^{-19} coulomb. On a surface there are some 10^{19} atomic sites per m^2 - so if the charge of even quite a small fraction of the surface atoms is changed then quite large quantities of charge are easily involved.

Electric Forces and Electric Field. Around a charged body there is a force of attraction or repulsion for any other charges. The force between two point charges is proportional to the product of their magnitudes and inversely proportional to the square of the distance between them, which is expressed in Coulomb’s law:

$$F = -\frac{q_1 q_2}{4\pi\varepsilon_0 r^2} \tag{2.17}$$

The force F is in Newtons, the quantities of charge q_1 and q_2 are in Coulombs and the separation distance d is in meters. The constant ε_0 is called the 'permittivity of free space' and has a value 8.854×10^{-12} (discussed in this section later). Charges of the same polarity repel each other and of opposite polarity attract.

A region in which electric forces are acting is called an *electric field*. The force experienced by the test charge when at rest relative to the observer at any point in the field is known as the *electric filed strength E*. The direction of the field at any point depends on the direction of force on a positive charge there - and is hence a vector parameter. Evidently the force F on a charge q placed at a point where the electric field strength is E is

$$F = qE \tag{2.18}$$

From Coulombs Law the electric field strength E at a distance d from a charge q_1 will be:

$$E = \frac{q_1}{4\pi\varepsilon_0 r^2} \tag{2.19}$$

Electric Potential. The *potential* ψ at a point is defined as the amount of work needed to bring a unit charge from infinity to that point. The potential difference between two points is then the work done to move a unit charge between these two points. The work done does not depend on the route followed so the potential is a scalar quantity. The potential at a radial distance d from a single point charge q is:

$$\psi = \frac{q}{4\pi\varepsilon_0 r} \tag{2.20}$$

The relation between electric field strength and potential is:

$$E = -\nabla \psi \tag{2.21}$$

Gauss' Law. Gauss' Law states that the surface integral of electric field strength over any closed surface is equal to the algebraic sum of all the charges enclosed by the surface divided by the permittivity constant ε_0:

$$\oint_s E \cdot ds = \frac{q}{\varepsilon_0} \tag{2.22}$$

where q is the total charge contained in the volume bounded by the closed surface s. For a surface charge, if q_s is the surface charge density, the total charge enclosed by the surface ds is $q_s\, ds$. According to Gauss' law, Eq. (2.22) becomes:

$$E_n = \frac{q_s}{\varepsilon_0} \tag{2.23}$$

Consider an isolated point charge q uniformly distributed over its surface, the flow or flux of electric field across any spherical surface enclosing a point charge q will then be q/ε_0. Hence, the electric field strength is:

$$E_r = \frac{q}{4\pi r^2 \varepsilon_0} \tag{2.24}$$

Electric Current. Current is the rate of flow of charge. In other words, current is a measure of the net charge that passes through a point in a circuit in a given time interval. The symbol for current is I. The unit of current is the ampere (A), or amp for short.

$$I = dQ / dt \tag{2.25}$$

$$\Delta Q = \int I dt \tag{2.26}$$

Although current in most cases consists of flowing electrons, the direction of the current on a circuit diagram is shown as the flow of positive charges, and in most cases positive charges flowing one direction is equivalent to negative charges flowing in the opposite direction.

Dielectric Constant and Permittivity. A dielectric material is a substance that is a poor conductor of electricity, but an efficient supporter of electric fields. If the flow of current between opposite electric charge poles is kept to a minimum while the electrostatic lines of flux are not impeded or interrupted, an electrostatic field can store energy. The charges in an insulator will respond to an applied field in such a way as to partially cancel an applied electric field. This property is useful in capacitors, especially at radio frequencies. Dielectric materials are also used in the construction of radio-frequency transmission lines. In practice, most dielectric materials are solid. Examples include porcelain (ceramic), mica, glass, plastics, and the oxides of various metals. Some liquids and gases can serve as good dielectric materials. Dry air is an excellent dielectric, and is used in variable capacitors and some types of transmission lines. Distilled water is a fair dielectric, while a vacuum environment is an exceptionally efficient dielectric.

The *dielectric constant* is a characteristic quantity of a given dielectric substance, sometimes called the relative permittivity (Bekefi and Barrett 1977). It acts as a factor that relates the polarization of an insulator to an applied electric field. The dielectric constant is the ratio of the permittivity of a substance to the permittivity of free space. It is an expression of the extent to which a material concentrates electric flux, and is the electrical equivalent of relative magnetic permeability.

Permittivity, also called electric permittivity, is a constant of proportionality that exists between electric displacement and electric field intensity. This constant is equal to approximately 8.85 x 10^{-12} farad per meter (F/m) in free space (a vacuum). In other materials it can be much different, often substantially greater than the free-space value, which is symbolized ε_o. In engineering applications, permittivity is often expressed in relative, rather than in absolute terms. If ε_o represents the permittivity of free space (that is, 8.85 x 10^{-12} F/m) and ε represents the permittivity of the substance in question (also specified in farads per meter), then the dielectric constant ε_a, is given by:

$$\varepsilon_a = \varepsilon / \varepsilon_0 = 1.13 \times 10^{11} \varepsilon \tag{2.27}$$

Table 2.3 shows the dielectric constants for different materials.

Table 2.3 Dielectric Constant Values of Different Materials

Material	Dielectric Constant, ε_a	Material	Dielectric Constant, ε_a
Air	1	Cell membrane	~ 9
Celluloid	4	Cellulose acetate	3.3 to 3.9
Dry soil	5 to 15	Glass	7.6 to 8
Paper	3.0	Polyethylene	2.5
Polyimide	3.4 to 3.5	Polystyrene	3.8
Rubber	2.8	Porcelain	5.1 to 5.9
Teflon	2.1	Water	78 to 80

In a membrane system, when membrane material has a sufficiently low dielectric constant (below 10), ions which are inside the membrane would be paired and the degree of distribution of solute from bulk solution to membrane inside would be

decreased. As a result, solute rejection would be increased. Such an effect is called "dielectric exclusion" (Yaroshchuk 2001). Some researchers pointed out that dielectric constant is a very important factor for solute separation (Glueckauf 1976; Min and Im 1992; Yaroshchuk 2001). However, due to its weak electric properties and complicity of the membrane system, it is very hard to determine the actual value of dielectric constant of membrane experimentally. Van der Bruggen *et al.* (2002) estimated the dielectric constant with theoretical equations and found its value ranged from 5 to 35 for nanofiltration membrane NF70. Lee *et al.* (1998) used impedance method to measure the electric properties of thin film composite RO membranes. The estimation obtained from their experimental data indicated that the dielectric constant for the tested polyamide (PA) RO membranes varied from 3.38 to 5.29; while the total value for the whole membrane system ranged from 30.09 to 48.70. As membrane acts as an insulator, the existence of membrane in the membrane-solution system makes the dielectric constant lowered by order of magnitude. It was also concluded by Lee *et al.* (1998) that the dielectric constant value used in RO process should be lower than the theoretically predicted value and that it should not exceed 3.0.

2.3.2 Poisson Equation

Since the charged particles would generate an electric field, understanding of ion transport through charged membranes requires a specification of how changes in ion concentration affect changes under a given electric potential. The following equation can be obtained by applying the Gauss' law to a very small differential volume, $dV = dxdydz$ with surface areas $dA_x = \pm dydz$, $dA_y = \pm dxdz$ and $dA_z = \pm dxdy$, and dividing the expression by dV:

$$\frac{\partial E_x}{\partial x}+\frac{\partial E_y}{\partial y}+\frac{\partial E_z}{\partial z}=\frac{\rho}{\varepsilon} \tag{2.28}$$

or $$\vec{\nabla}\cdot\vec{E}=\frac{\rho}{\varepsilon} \tag{2.29}$$

which is the vector differential way to write Gauss's Law. The quantity on the left-hand-side is called the divergence of the electric (vector) field. It can be seen that the divergence of the field at each point in space is directly proportional to the charge (density) at that point. Recalling that $E=-\nabla\psi$, the above equation can be written in terms of the scalar potential as:

$$\nabla^2\psi=-\frac{\rho}{\varepsilon} \tag{2.30}$$

This equation is known as Poisson equation, which describes how changes in the electric field correspond to the changes in the charge density. In a region where no free charges are present $(\rho=0)$, Poisson equation becomes Laplace's equation:

$$\nabla^2\psi=0 \tag{2.31}$$

There are a number of geometric forms for which the above equations can be solved analytically. Two and three dimensional finite element and finite difference computer modeling programs are available to find potential and electric field distributions within practical geometric arrangements.

2.3.3 Interaction of Charged Surface and Particles

Membrane materials play a critical role in membrane transport. Surface charge, as one of the predominant physio-chemical properties of membrane, determines the distribution of ionic concentrations on membrane-solution interfaces. In this section, the electrostatic interaction between charged surface and particles is reviewed.

Acquisition of Surface Charge. The electric field from each side of a sheet of uniform charge density, Q (coul/m^2), is $E = Q/(2\varepsilon_0)$. There can be no electric fields inside a conductor and the electric field outside is $E = Q/\varepsilon_0$. Thus a conducting body placed in an electric field will have charge induced on it with the density of charge proportional to the electric field. The charge induced on a conductor is of opposite polarity to that of the charge source. As opposite charges attract, there is an attraction between a charge and a conducting surface. For a plane conducting surface this image charge is an equal distance behind the surface so calculation of the force involves a distance equal to twice the separation distance from the conducting surface.

When brought into contact with an aqueous electrolyte solution, membrane acquires an electric charge. The possible mechanisms by acquisition of surface charge include dissociation of functional groups, adsorption of ions from solution, and adsorption of polyelectrolytes, ionic surfactants and charged macromolecules (Schaep and Vandecasteele 2001). These charging mechanisms could take place on the exterior membrane surface as well as the interior pore surface of the membrane. The sign of the membrane charge can be deduced from the chemical structure of the membrane material. For instance, Elimelech and Childress (1996) reported that for thin-film composite RO membranes, negative charge develops due to the carboxyl functional groups of the aromatic ring; while positive charge may develop because of pendant amino groups. It was also reported that for cellulose acetate RO membranes, negative charge develops because of one or more of the following: (1) remains of hydrolyzed acetic anhydride, (2) dissociation of di-carboxylic organic acid used in post treatment, or (3) adsorption of anions (hydroxyl, chloride); while Positive charge develops mostly because of impurities or divalent metals used in post treatment. Seidal *et al.* (2001)

found in their research that adsorption of SO_4^{2-} ions may also play a role in the surface charge acquisition. The sign and density of membrane surface charge is often evaluated by means of measurement of zeta potential in the laboratory.

Previous experimental data in literature show that the effective membrane charge density is not fixed, but is dependent on feed salt concentration (Aitkuliv *et al*. 1984; Tsuru *et al*. 1991b; Bowen *et al*. 1997; Bowen and Mohammad 1998a, 1998b; Schaep *et al*. 2001). Tsuru *et al*. (1991b) and Bowen and Mukhtar (1996) have pointed out that the membrane charge density increases with the feed salt concentration, which can be expressed in terms of a Freundlich isotherm as follows:

$$\log_{10}|X| = s\log_{10}C_b + q \tag{2.32}$$

However, Bowen and Mohammad (1998a, 1998b) presented their measured data in different forms and noted that the membrane charge density increases linearly with the concentration.

Boltzmann Distribution. The surface charges have an influence on the distribution of ions in the solution due to the requirement of the electroneutrality of the system, which leads to the formation of an electrical double layer, namely a charged surface and a neutralized excess of counter-ions in the adjacent solution. Figure 2.5 shows a simplified situation where a surface has a negative charge with uniform charge density Q (coul/m^2) and faces a solution containing bulk concentration C_i (mol/m^3). First, the negative surface charge would attract its counter-ions C^+, but repel its co-ions C^-. It then modifies the ionic concentrations near the surface, producing a negative electric

potential in the solution. The problem is assumed to be one-dimensional. That is, concentrations and potentials vary only with x, which is perpendicular to the surface.

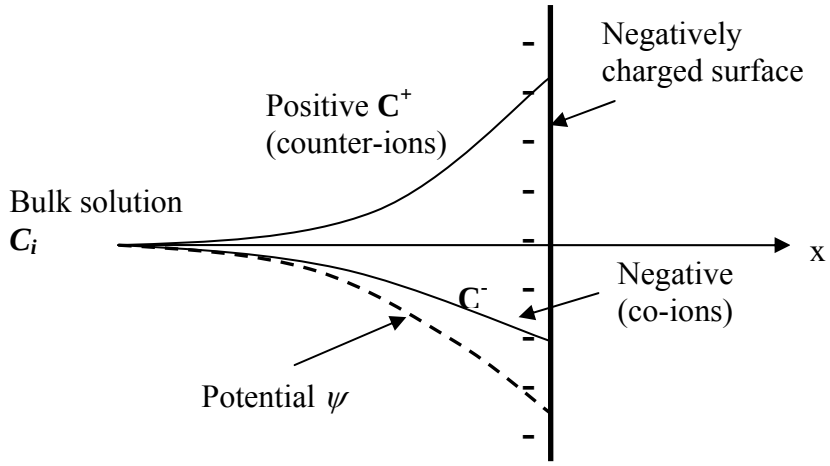

Figure 2.5 Concentration and Potential Profiles near Negatively Charged Surface

In order to solve both concentration and potential profiles, the ions are assumed to be in equilibrium in the vicinity of the surface, so that the electro-chemical potential is constant for each ion along the x-axis.

$$RT\ln C_i(-\infty) + z_i F\psi(-\infty) = RT\ln C_i(x) + z_i F\psi(x) \tag{2.33}$$

Hence, the ionic concentration in solution can be calculated by applying the condition that the electric potential is zero in the bulk solution, i.e. $\psi(-\infty)=0$:

$$C_i(x) = C_i(-\infty)e^{-z_i F\psi(x)/RT} \tag{2.34}$$

Equation (2.34) is a *Boltzman distribution*, in which the concentration of ion is exponentially related to the electric potential of the ion (Boltzmann 1868).

To solve for the electric potential, Poisson's equation is considered to relate $\psi(x)$ to the charge density $Q(x)$, which is the sum of the charges carried by various ions:

$$Q(x) = \sum_i z_i F C_i(x) \tag{2.35}$$

where the sum is taken over all ions in the solution. Combined with Equations (2.34) and (2.35), the Poisson's equation can be written as:

$$\frac{d^2\psi}{dx^2} = -\frac{1}{\varepsilon}\sum_i z_i F C_i(-\infty) e^{-z_i F\psi(x)/RT} \tag{2.36}$$

This is the *Poisson-Boltzman model* of the double layer.

Debye-Hückel Model and Debye Length. This non-linear differential Poisson-Boltzman equation cannot be solved in a closed form. Recall from calculus, exponential functions can be expressed as an infinite series of terms as follows:

$$e^x = 1 + x + \frac{x^2}{2!} + \frac{x^3}{3!} + \ldots \tag{2.37}$$

When the argument (x) of the exponential is small, the infinite series can be represented by just the first few terms, that is $e^x \approx 1 + x$, which holds for $x << 1$. When the potential is small:

$$\left|\frac{z_i F\psi(x)}{RT}\right| << 1 \qquad \text{or} \qquad \left|z_i F\psi(x)\right| << RT, \tag{2.38}$$

Equation (2.36) then becomes

$$\frac{d^2\psi}{dx^2} \approx -\frac{1}{\varepsilon}\left[\sum_i z_i F C_i(-\infty) - \sum_i z_i F C_i(-\infty)\frac{z_i F\psi(x)}{RT}\right] \tag{2.39}$$

The first sum in the brackets is zero because of the condition of electroneutrality in bulk solution. Hence, Equation (2.39) can be simplified as:

$$\frac{d^2\psi}{dx^2} = \frac{F^2\sum_i z_i{}^2 C_i(-\infty)}{\varepsilon RT}\psi(x) = \frac{1}{\lambda^2}\psi(x) \tag{2.40}$$

$$\lambda = \sqrt{\frac{\varepsilon RT}{F^2\sum_i z_i{}^2 C_i(-\infty)}} \tag{2.41}$$

where λ is the *Debye length* or the double-layer thickness. It is the length over which the imbalances and the potential sketched in Figure 2.5 will extend into the solution. It is dependent on physical-chemical properties of the solution such as dielectric constant and ionic concentrations. λ is also known as a characteristic distance which is the distance from the membrane surface at which the potential has decayed to 37 % of its surface potential (Clark 1996). The Debye length will be large and the surface potential will extend far into the bulk solution if ionic concentration is low in the solution (Bockris and Reddy 1970). Another important point is that divalent ions may have a much larger effect on the Debye length and surface potential than univalent ions, because of the z^2 term in Equation (2.41).

Applying the condition that the net excess charge in the solution should equal the charge on the surface (so that the total charge across the whole region sums to zero), the solution to Equation (2.40) takes the following form:

$$\psi(x) = \psi(0)e^{x/L} \qquad \text{and} \qquad \psi(0) = \frac{QL}{\varepsilon} \tag{2.42}$$

This is known as the *Debye-Hückel* approximation or theory (Debye and Hückel 1923; Clark 1996). The assumption of low potentials can be relaxed in an analysis known as *Gouy-Chapman* theory, which is not discussed here.

2.4 Electrodiffusion Theory of Ion Transport

2.4.1 Nernst-Planck Equation for Ionic Flux

Although introduced more than one century ago (Nernst 1888; Planck 1890), the Nernst-Planck flux equation still plays an important role in the study of ion transport processes through membranes. The Nernst-Planck equation can be derived from the

thermodynamics of irreversible processes. When a system is close to equilibrium, according to linear phenomenological laws, there is a linear relationship between flows and forces (Kondepudi and Prigogine 1999). Hence, membrane transport can be expressed by basic equation of linear thermodynamics. Transport rate in the direction *x* is proportional to the concentration × driving force, which is the gradient of electrochemical potential:

$$J_{ix} = -U_i c_i \frac{d\tilde{\mu}_i}{dx} \tag{2.43}$$

where J_{ix} = the flux of species *i* along the direction *x*, mol/(cm^{2}s)

U_i = mobility♣ of species *i*, $(cm/s)\cdot mol/N$, *or* $s\cdot mol/g$

c_i = concentration, mol/L

$\tilde{\mu}_i$ = the electrochemical potential, J/mol

$\frac{d\tilde{\mu}_i}{dx}$ = the driving force in the direction *x*, N/mol.

When ion or salt penetrates the membrane through its solution-membrane interface, it interacts chemically with the interfacial molecules (e.g., dissolving of ions into the membrane surface). The work connected with this type of interaction is called chemical potential of species *i* and is denoted as μ_i:

$$\mu_i = \mu_i^{\,0} + RT \ln a_1 \tag{2.44}$$

where $\mu_i^{\,0}$ is the standard chemical potential of species *i*; a_i is the chemical activity of species *i* in the membrane, $a_i = \gamma_i c_i$, and γ_i is the activity coefficient. The total work required for ion transfer is a sum of chemical and electrical work and is called the electrochemical potential $\tilde{\mu}_i$:

♣ U can be derived from $U = \frac{D}{RT} = \frac{\hat{u}}{zF}$. D: cm^2/s, ≈10^{-5} in water, R=8.314 J mol^{-1} K^{-1}, $\hat{u}$ is called electro mobility, m^{2}V^{-1}s^{-1}.

$$\tilde{\mu}_i = \mu_i + z_i F\psi = \mu_i^{\,0} + RT \ln a_1 + z_i F\psi \tag{2.45}$$

Assuming $a_i = c_i$, the driving force for moving ionic species across the membrane can be expressed as an electrochemical potential gradient:

$$\frac{d\tilde{\mu}_i}{dx} = RT \frac{d \ln c_i}{dx} + z_i F \frac{d\psi}{dx} \tag{2.46}$$

The well-known Nernst-Planck flux equation can be derived from Eqs. (2.43) and (2.46) and be expressed as follows:

$$J_i = -U_i c_i (RT \frac{d \ln c_i}{dx} + z_i F \frac{d\varphi}{dx}) = -U_i RT \frac{dc_i}{dx} - U_i c_i z_i F \frac{d\varphi}{dx} \tag{2.47}$$

The Nernst-Planck equation describes the electrodiffusion of a system of ions in an electric field and determines the electric current density due to gradients in the ionic concentration and external and internal forces.

2.4.2 Limitation and Extension in Membrane Applications

The main argument against validity of the Nernst-Planck equation arises from the macroscopic, smooth nature of the model used in its derivation (Buck 1984). The equation is one-dimensional, ignores edge effects and assumes that membrane is chemically-homogenous or coarse-grained in a random way. It has intrinsic limitations in dealing with bulk phase, finite-ion-size transport. In addition, the friction coefficients (mobilities and diffusion coefficients) cannot be microscopically defined by the Nernst-Planck equation.

Secondly, the equation is insufficient because it includes only the effects of the gradients of concentrations and electric potential. It does not explicitly account for the magnitude of the mobility in terms of solvent content or crossing-linking (Kato 1995). In phenomenological linear laws, the flux of a specific species is not only proportional

to its driving force, but also related to the contributions of non-conjugated forces. The Nernst-Planck equation neglects such coupling effects or "cross terms". Thirdly, the Nernst-Planck equation does not apply to ion transport through regions of space comparable in size with the moving species and its counter-ion atmosphere (i.e. the Debye length). The equation is only valid at time greater than 10^{-12} to 10^{-13} s. This is because prior to that time, the inertial ransom fluctuations are not yet averaged (Buck 1984).

Although use of the Nernst-Planck equation may not be strictly correct without the consideration of cross terms, random heterogeneities and high concentrations, these arguments would not limit the application of the equation. If the system size is much larger than the Debye length and the packing is randomly defective so that jumps sites are available, the Nernst-Planck equation can still be used safely in one dimension for membranes.

Schlögl (1964) and Dresner (1972) have described ionic transport through membranes using an extension of the Nernst-Planck equation that includes convection. The extended Nernst-Planck equation is a simplified version of the equations of irreversible thermodynamics, but it still take into account the three main mechanisms of ionic transport in membranes: diffusion, convection and electric migration, which can be expressed as follows:

$$J_i = -D^m{}_i \frac{\partial c_i}{\partial x} + k_{i,c} J_v c^m{}_i - D^m{}_i \frac{z_i F c^m{}_i}{RT} \cdot \frac{\partial \varphi_m}{\partial x} \tag{2.48}$$

where D_i^m is diffusion coefficient for species i, which equals to $U_i RT$. Analysis from Bowen and Mohammad (1998b) showed that the contribution of each transport

mechanism in membrane (i.e., diffusion, convection and electro-migration) is significant and should be taken into account together.

2.4.3 Electroneutrality and Donnan Equilibrium Assumptions

In the study of ion transport through membranes, a so-called local electroneutrality assumption is always involved. It assumes that the sum of charges carried by different ions is balanced by the local membrane charge density at each point through the membrane channel, that is $\sum_i z_i c_i(x) + X = 0$. It is much easier to solve the Nernst-Planck equation by using the local electroneutrality assumption than solving it with Poisson's equation simultaneously. However, this approach causes a physical paradox: a spatial electric field arises even in cases when the local electroneutrality is initially assumed (Hickman 1970; Jackson 1974; Martuzans and Skryl 1998). From electrostatics viewpoint, if the charge is neutral at each point along the membrane length, there should be no electric field.

While local electroneutrality is widely used in electrodiffusion of ions (Rubinstein 1990); it seems difficult to explain some calculated results from it. For instance, a non-zero electric potential would be obtained by solving the Nernst-Planck equation with local electroneutrality (Tsuru *et al.* 1991a). But taking into account the kinetic model underlying both Nernst-Planck and Poisson's equations, there could be no potential if there is no charge separation (Aguilella *et al.* 1987). Such a deviation indicates that the local electroneutrality cannot be strictly valid. The local electroneutrality assumption eliminates the electric interaction and that the electric field can only be obtained from the external applied one. This assumption is not realistic with respect to the operating condition for a RO/NF process. However, it was also reported that the assumption of

local electroneutrality was the limiting case of a certain dimensionless parameter which is related to the ratio of Debye length to membrane thickness, L^2/λ^2 (MacGillivray 1968). As L^2/λ^2 becomes larger, the electroneutrality condition becomes stronger and the charge density approaches zero (Kato 1995).

Another aspect in solving membrane transport requires the assumption of some boundary process. Under such circumstance, a Donnan equilibrium is usually assumed to exit between the interior and the exterior of the membrane (Tsuru *et al*. 1991a; Bowen and Mukhtar 1996; Hall *et al.* 1997; Peeters *et al.* 1998). In a charged membrane in contact with an electrolyte solution, the intrapore concentration of co-ions at the pore boundaries will be lower than that in the bulk solution, whereas the counter-ions have a higher concentration in membrane pores than in the solution. The Donnan potential, ψ_D is generated due to this concentration difference of the ions. By this potential, co-ions are repelled by the membrane, whereas counter-ions are attracted. The Donnan potential equals the potential difference between the electrical potential in the membrane and that in solution, which can be written as

$$\psi_{Don} = \psi^m - \psi = \frac{RT}{z_A F} \ln \frac{c_A}{C_A} = \frac{RT}{z_B F} \ln \frac{c_B}{C_B} \tag{2.49}$$

where C refers to the salt concentration in the membrane, while c refers to the salt concentration in the solution. The subscripts A and B refer to the charged components A and B in the solution. Combining Eq. (2.49) with the conditions of electro-neutrality in the solution and in the membrane, the distribution of co-ion B between the membrane and the solution can be derived as a function of the concentration of the fixed membrane charge X:

$$\frac{C_B}{c_B} = \left(\frac{|z_B| c_B}{|z_B| C_B + |z_X| C_X} \right)^{(|z_B|/|z_A|)} \tag{2.50}$$

where the concentration of fixed membrane charge is indicated by C_X and z_X. The ratio of C_B to c_B is termed as the Donnan partition coefficient of species B. It was reported by MacGillivary (1968) that the Nernst-Planck-Poisson system of equations would imply the existence of a Donnan equilibrium at the boundaries of the membrane.

Chapter 3

THE NERNST-PLANCK-DONNAN MODEL FOR LOOSE MEMBRANES

"Loose" RO membrane is a RO membrane with reduced salt rejection. It has been proven desirable for a number of applications where moderate salt removal is acceptable since operating pressures and power consumption are significantly lowered. So, in exchange for less than near complete salt removal, costs are reduced. In industry, NF membrane is commonly termed as a loose RO membrane; however this categorization is not real. The differences between two are subtle, but distinct. One notable difference is that NF membrane can mainly reject divalent or multivalent ions, but pass the mono-valent ions; while loose RO membrane still has a NaCl rejection ranging from 75% to 95%. In this study, both loose RO membranes and NF membranes are classified in a same category, in which the membrane is negatively charged with a pore size around 1 nm.

In this chapter, the solute transport characteristics under different operating conditions were simulated by using the Nernst-Planck-Donnan model, in which the electrostatic interaction was simplified as solely Donan exclusion. This numerical analysis requires the determination of three key parameters relating to membrane properties; namely,

effective membrane thickness, effective membrane pore radius, and effective membrane charge density, as well as the assumption of local electroneutrality. Results of the numerical analysis showed that membrane charge density played an important role in ion/salt transport behavior. Convection appeared to be the dominant mechanism involved in ion transport at low membrane charge. The salt retention rate decreased with increasing feed salt concentration, but remained unchanged when the ratio of membrane charge density to feed concentration was kept constant. It is noted that the extended model, obtained by incorporating the relationship between effective membrane charge density and bulk salt concentration into the Nernst-Planck-Donnan equation, is useful for describing and predicting membrane salt transport performance through loose RO/NF membranes.

3.1 The Nernst-Planck-Donnan Model

3.1.1 Transport equations inside the membranes

The extended Nernst-Planck equation forms the basis for modeling the transport of charged species through membrane pores (Bowen and Mukhtar 1996; Deen 1987) and it can be written as:

$$J_i = -D_{i,m}\frac{dc_i}{dx} + K_{i,c}J_v c_i - \frac{D_{i,m}F}{RT} z_i c_i \frac{d\psi}{dx} \tag{3.1}$$

where J_i is the flux of ion i, $D_{i,m}$ is the hindered diffusivity of ion i in the pores, c_i and z_i are the molar pore concentration and the valence of species i, $K_{i,c}$ is the hindrance factor for convection, J_v is the permeate flux, F is the Faraday constant, R is the gas constant, T is the absolute temperature, and ψ is the electrical potential, which is the driving force for the electrical migration of ions.

Rearranging Eq. (3.1) and noting that at steady state $J_i = J_v C_{i,p}$ (with $C_{i,p}$ being the concentration of ion *i* in the permeate), we obtain,

$$\frac{dc_i}{dx} = \frac{J_v}{D_{i,m}}\left(K_{i,c}c_i - C_{i,p}\right) - \frac{F}{RT} z_i c_i \frac{d\psi}{dx} \tag{3.2}$$

Electric potential gradient is common for all ions and it can be derived by multiplying Eq. (3.1) by $z_i/D_{i,m}$ and summating over all ions as follows:

$$\frac{d\psi}{dx} = \frac{\sum \frac{z_i J_v}{D_{i,m}}\left(K_{i,c}c_i - C_{i,p}\right)}{\frac{F}{RT}\sum\left(z_i{}^2 c_i\right)} \tag{3.3}$$

Electroneutrality in the membrane pores ($\sum_i z_i c_i + X = 0$, where *X* is the membrane charge density) was used to derive Eq. (3.3). Substituting Eq. (3.3) into Eq. (3.2), we obtain:

$$\frac{dc_i}{dx} = \frac{J_v\left(K_{i,c}c_i - C_{i,p}\right)}{D_{i,m}} - \frac{z_i c_i \sum z_i J_v\left(K_{i,c}c_i - C_{i,p}\right)/D_{i,m}}{\sum z_i{}^2 c_i} \tag{3.4}$$

The boundary conditions to Eq. (3.4) are:

$$x = 0 \qquad c_i = c_{i,m} \tag{3.5a}$$

$$x = \Delta x \qquad c_i = c_{i,p} \tag{3.5b}$$

where $c_{i,m}$ and $c_{i,p}$ are the pore concentrations of ion *i* on the feed side and permeate side surfaces of the membrane, respectively.

There is also a requirement for electroneutrality in permeate, which is expressed as:

$$\sum_i z_i C_{i,p} = 0 \tag{3.6}$$

and for no overall electrical current passing through the membrane:

$$I = \sum_i F z_i J_i = 0 \tag{3.7}$$

The ion concentration on the membrane surface is related to the bulk concentration by Donnan partition. The traditional Donnan partition accounts for the electrostatic effects in which the charged membrane will attract counter-ions and repel co-ions (Higa 1998; Bowen and ukhtar 1996; Deen 1987). In addition, the finite ion size results in steric partition of ions (Deen 1987; Palmeri *et al*. 1999; Bhattacharjee *et al*. 2001). Therefore, considering both Donnan and steric effects, the relation between intrapore concentration at the membrane surface and the bulk concentration can be expressed by the following equation:

$$\left[\frac{c_{i,m}}{C_{i,m}\left(1-\lambda_i\right)^2}\right]^{\frac{1}{z_i}} = \exp\left[-\frac{F\Delta\psi_D}{RT}\right] = cons\tan t \tag{3.8}$$

where $C_{i,m}$ is the concentration of ion i in the bulk solution, and λ is the hindrance coefficient, $\lambda = r_{i,s}/r_p$ with $r_{i,s}$ and r_p being the ionic species and pore radii, respectively (Palmeri *et al.*, 1999).

Eqs. (3.4)-(3.8) constitute a one-dimensional model for ion/solute transport in membrane pores. Given bulk salt concentration and permeate flux, the equations can be numerically solved by using the Runge-Kutta-Gill method. That is, membrane transport performance (e.g. ion fluxes and permeate concentrations) can be predicted through a simulation exercise.

3.1.2 Calculations of hindrance factors

Solutes moving in free solution experience a drag force exerted by the solvent. When solutes move in confined spaces, such as membrane pores, the drag is modified and the transport may be considered to be hindered (Deen 1987). Such effects can be expressed in terms of hindrance factors for diffusion:

$$K_{i,d} = \frac{D_{i,m}}{D_{i,\infty}} = -1.705\lambda_i + 0.946 \tag{3.9}$$

and for convection:

$$K_{i,c} = \frac{v_i}{J_v} = -0.301\lambda_i + 1.022 \tag{3.10}$$

where both hindrance factors are functions of λ (Bowen and Mukhtar 1996; Bhattacharjee *et al*. 2001; Bowen and Cao 1998). The ionic radii, $r_{i,s,}$ and bulk ion diffusivity, $D_{i,\infty,}$ can be estimated by Stokes-Einstein equation as follows:

$$D_{i,\infty} = \frac{RTu_i}{|z_i|F} \tag{3.11}$$

$$r_{i,s} = \frac{RT}{6\pi\mu D_{i,\infty} N_A} \tag{3.12}$$

where u_i is the ion mobility, μ is viscosity, and N_A is the Avogadro number. The calculation of hindrance factors and hindered diffusivity for r_p = 1.0 nm are summarized in Table 3.1.

Table 3.1 Ionic properties and hindrance factors used in this study (for r_p = 1.0 nm)

Ionic type	Na^+	Cl^-	SO_4^{2-}
Charge, z	+1	-1	-2
Ionic mobility, $u_i \times 10^8$ ($m^2V^{-1}s^{-1}$)	5.19	7.91	8.29
Diffusivity, $D_{i,\infty} \times 10^9$ (m^2s^{-1})	1.333	2.031	1.062
Ionic radius, $r_{i,s}$ (nm)	0.1840	0.1207	0.2309
λ	0.184	0.121	0.231
Hindrance factor for diffusion, $K_{i,d}$	0.632	0.740	0.552
Hindrance factor for convection, $K_{i,c}$	0.967	0.986	0.952
Hindered diffusivity, $D_{i,m} \times 10^9$ (m^2s^{-1})	0.842	1.503	0.586

3.1.3 Relationship between effective membrane charge density and bulk salt concentration

The use of the above model as a predictive method requires the determination of three parameters relating to membrane properties. These are the effective charge density, the effective membrane thickness, and the membrane pore radius. The effective membrane charge can be obtained by calculating zeta potential from measurement of the streaming potential using the Helmholtz-Smoluchowski equation (Childress and Elimelech 1996; Bowen and Cao 2001; Ariza *et al*. 2001; Childress and Elimelech 2000; Ariza and Benavente 2001; Seidel *et al*. 2001). Previous experimental data in literature show that the effective membrane charge density is dependent on feed salt concentration (Bowen and Mukhtar 1996; Aitkuliev *et al*. 1984; Tsuru *et al*. 1991b; Bowen *et al*. 1997; Bowen and Mohammad 1998b; Schaep *et al*. 2001). As illustrated

in Figure 3.1, the relationship between membrane charge density and bulk salt concentration can be expressed in terms of a Freundlich isotherm (Bowen and Mukhtar 1996; Tsuru *et al*. 1991b) as follows:

$$\log_{10}|X| = s\log_{10}C_b + q \tag{3.13}$$

where s and q are empirical constants that could be obtained from least-square analysis. The data from Tsuru *et al*. (1991b) show that, for NTR-7450 and NTR-7410 RO membranes, NaCl and Na_2SO_4 solutions have typical s values of around 0.674 and 0.524, respectively. The corresponding values of q are 1.486 and 1.772, respectively. Similarly, for NF membranes, Bowen and Mukhtar (1996) reported that the s values for CA20, HC50, and PES5 membranes are 0.499, 0.875, and 0.521, respectively. The corresponding values for q are 0.859, 0.999, and 0.881, respectively.

Although no mechanistic model for the relationship between effective membrane charge density and electrolyte concentration is currently available, it has been noted that membrane charge increases with increasing electrolyte concentration. This phenomenon might be caused by ion adsorption in or on the membrane or by the influence of ionic strength on the dissociation rate of the charged groups present at the membrane (Peeters *et al*. 1998). To investigate the effect of feed salt concentration on membrane rejection, different Freundlich isotherms were used in this study. Table 3.2 summarizes the different s and q values used in the simulation study. Since s and q values in literature ranged from 0.5 to less than 1.0, and 0.5 to less than 2.0, respectively, six pairs of data were chosen to cover these ranges; while case 7 and case 8 represented some real cases in NF membranes.

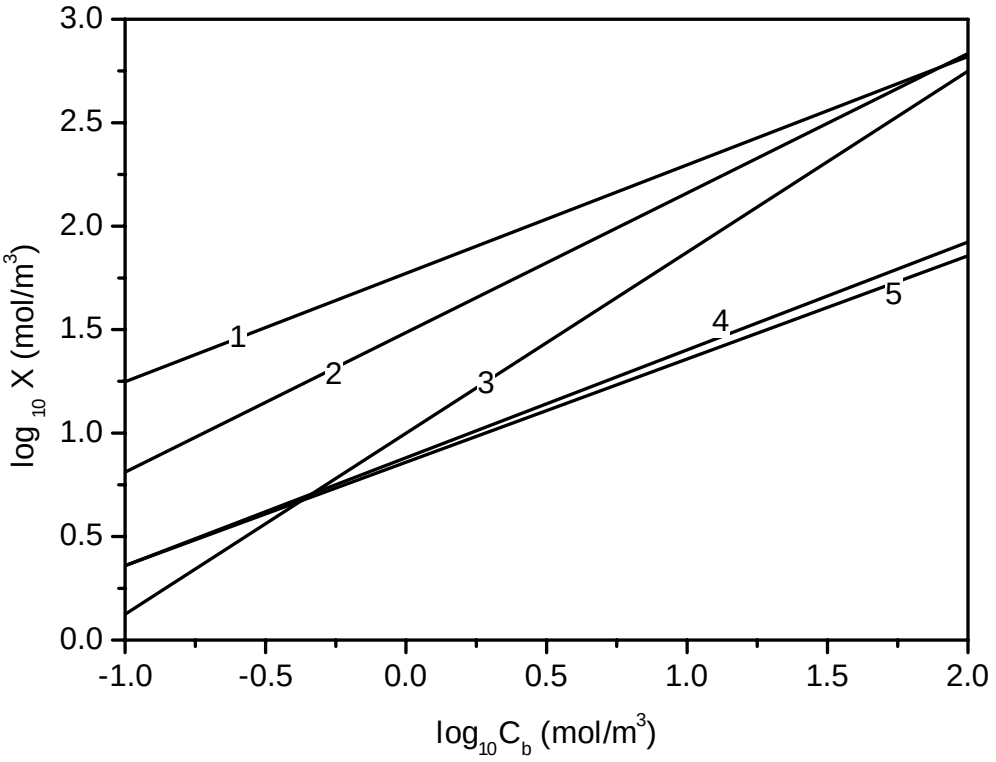

Figure 3.1 Freundlich isotherm of the effect membrane charge density as a function of the bulk salt concentration 1: NTR-7450 membrane, Na_2SO_4 (from Tsuru *et al.* 1991b); 2: NTR-7450 membrane, NaCl (from Tsuru *et al.* 1991b); 3: HC50 membrane; 4: PES5 membrane; 5: CA20 membrane; NaCl/Na_2SO_4 mixture (from Bowen and Mukhtar 1996)

Table 3.2 The values of s and q used in this study

	Case 1	Case 2	Case 3	Case 4	Case 5	Case 6	Case 7	Case 8
s	0.5	0.5	0.5	1.0	1.0	1.0	0.499	0.875
q	0.5	1.0	2.0	0.5	1.0	2.0	0.859	0.999

3.2 Contribution of Electromigration

As discussed in section 3.1, the Nernst-Planck-Donnan model assumes that charges are neutral at each point of membrane. Such a local electroneutrality assumption could cause a theoretical paradox. As illustrated in Figure 3.2, an electric field arises across the membrane while there are no net charges. The electric field can be induced only by the externally applied electric field when charges are neutral along the membrane. In this case, due to the membrane charge, co-ions and counter-ions have a different distribution on membrane-solution interfaces, where the Donnan potentials are induced. In the Nernst-Planck-Donnan model, the Donnan potentials on both sides of membrane act as the applied electric field, which causes a constant electric field along the membrane.

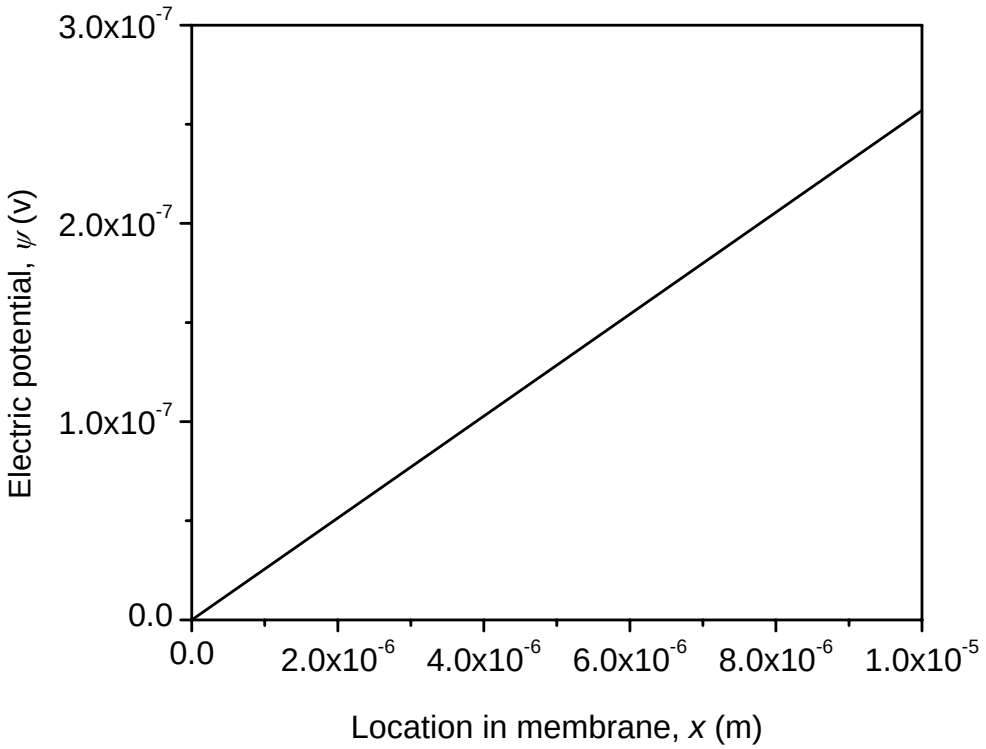

Figure 3.2 Electric potential profiles within the charged membrane: X=-10 mol/m^3, C_b=1.0 mol/m^3

However, such an induced electric field is very weak. It can be found from Table 3.3 that convection play a predominant role in ionic flux when the membrane charge density is low. On the contrary, the contribution of electro-migration dependent on electric field strength is hard to be detected. Thus from this discussion, it can be pointed out that the Nernst-Planck-Donnan model inherent with local electroneutrality assumption overlooks the electrostatic interaction between membrane and ions by ignoring the effects of electro-migration of ions resulting from the weak induced electric field.

Table 3.3 Contribution of diffusion, convection and electro-migration for a 1.0 mol/m^3 NaCl solution

J_v	X= -1.0 mol/m^3			X= -10 mol/m^3		
(m/s)	J_d (%)	J_c (%)	J_e (%)	J_d (%)	J_c (%)	J_e (%)
10^{-6}	49.46	50.46	7.69×10^{-2}	94.47	5.52	8.42×10^{-3}
10^{-5}	48.89	51.10	7.79×10^{-3}	93.51	6.48	9.78×10^{-4}
5×10^{-5}	43.82	56.18	1.71×10^{-3}	82.91	17.09	5.20×10^{-4}
8×10^{-5}	40.02	59.98	1.14×10^{-3}	74.61	25.39	4.83×10^{-4}
10^{-4}	37.60	62.40	9.51×10^{-4}	69.49	30.51	4.64×10^{-4}

3.3 Volume Flux Effects

The effect of the volume flux on rejection of NaCl and Na_2SO_4 in a single electrolyte solution is plotted in Figure 3.3. As shown in this figure, salt rejection increases with increasing permeate flux. The separation behavior of the ions under increasing permeate flux condition is predominated by the so-called "dilution effect" (Seidel *et al*. 2001). When the permeate flux through the membrane increases while the ion flux remains relatively unchanged, the increased permeate flux will dilute the salt concentration in the permeate. This will result in a lower ion concentration in the permeate and thereby lead to a higher salt rejection efficiency.

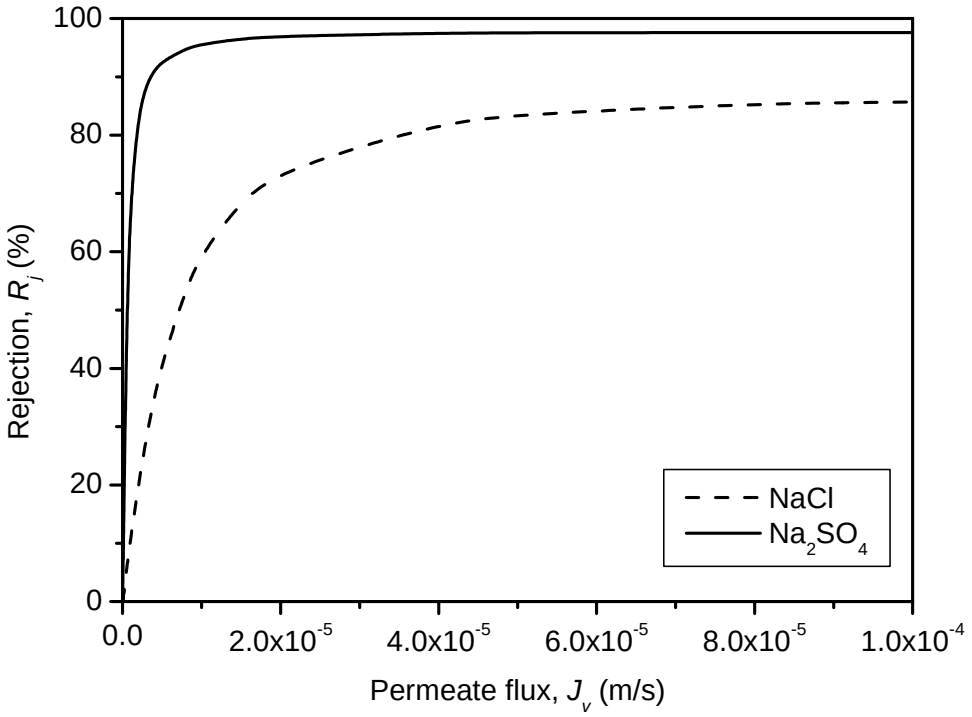

Figure 3.3 Rejection as a function of volume flux for a 1.0 mol/m^3 single electrolyte (membrane charge density X = -10.0 mol/m^3)

It is also shown in Figure 3.3 that for a given permeate flux, electrolyte with divalent co-ion (e.g. Na_2SO_4) has a higher rejection efficiency than the corresponding value of monovalent co-ion (e.g. NaCl). Under the same conditions, the rejection of Na_2SO_4 is higher than that of NaCl. This result can be further illustrated by the ion distribution on the membrane interface and the concentration profile of ions in the membrane, which are shown in Figure 3.4.

Due to the Donnan partition, the concentrations of co-ions (Cl^-, SO_4^{2-}) are very low, whereas that of counter-ions (Na^+) is nearly equal to the membrane fixed charge density. The concentration of SO_4^{2-} is even lower than that of Cl^- because of the difference in their valences. In addition, the concentration of SO_4^{2-} decreases faster inside the membrane than that of Cl^-. This phenomenon in turn results in an even lower salt concentration at the exit membrane interface and hence a lower permeate salt concentration. The higher rejection efficiency for divalent co-ions could be attributed to the co-effect of the Donnan partition of ions on both the entrance and exit sides of the membrane interfaces and the steric effect of ions in the membrane pores.

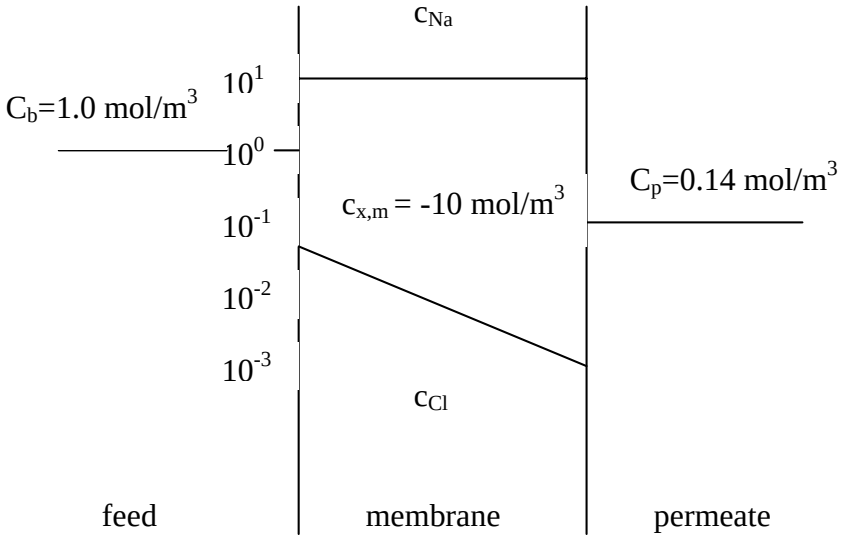

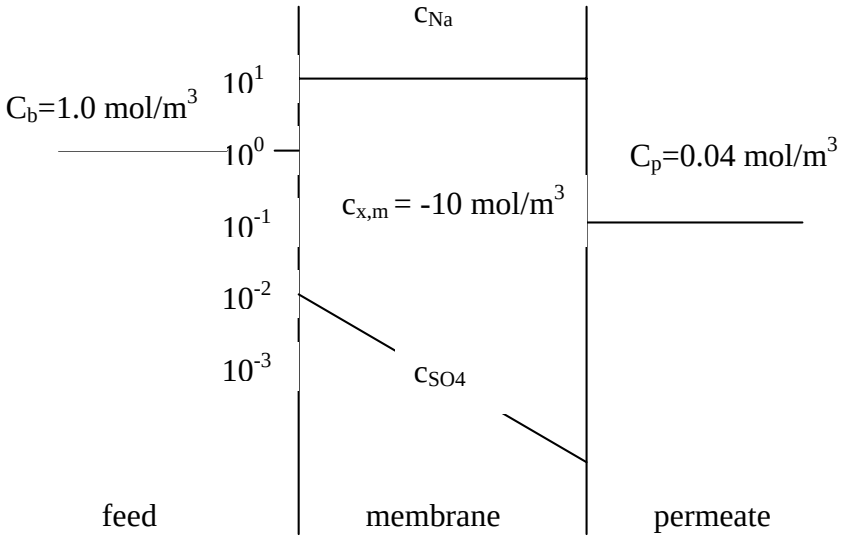

Figure 3.4 Concentration gradients of (a) Na^+ and Cl^- and (b) Na^+ and $SO4^{2-}$ in a negatively charged membrane with a fixed charge of -10.0 mol/m^3

3.4 Feed Concentration Effects

3.4.1 Effect of feed salt concentration on salt rejection at fixed membrane charges

Figure 3.5 shows the effect of feed salt concentration on rejection efficiency at a fixed membrane charge density. The salt rejection efficiency decreases drastically with the increase in feed concentration when the salt concentration is at the lower range. It is noted from Figure 3.5 that salt rejection efficiency remains virtually unchanged when feed salt concentration is increased beyond certain value. One of the possible explanations to this observed phenomenon can be deduced from the Donnan exclusion. This is because an increase in salt concentration in the solution will render the concentration of the co-ions (Cl^- or SO_4^{2-}) in the membrane to increase too. According to Eq. 3.8, the higher the co-ion concentration in the membrane, the lower the Donnan potential will be. The rejection of salt is largely determined by the concentration of co-ions on the membrane surface (Peeters *et al*. 1998; Bardot 1995). More specifically, a reduction in Donnan exclusion of co-ions from the membrane surface will lead to a lower rejection of salt. As a result, an increasing feed salt concentration will cause a reduction in salt rejection. As shown in Figure 3.5, for a given salt concentration, the rejection efficiency of NaCl is lower than that of Na_2SO_4. This finding indicates that co-ion concentration in the membrane would also increase with decreasing co-ion valence.

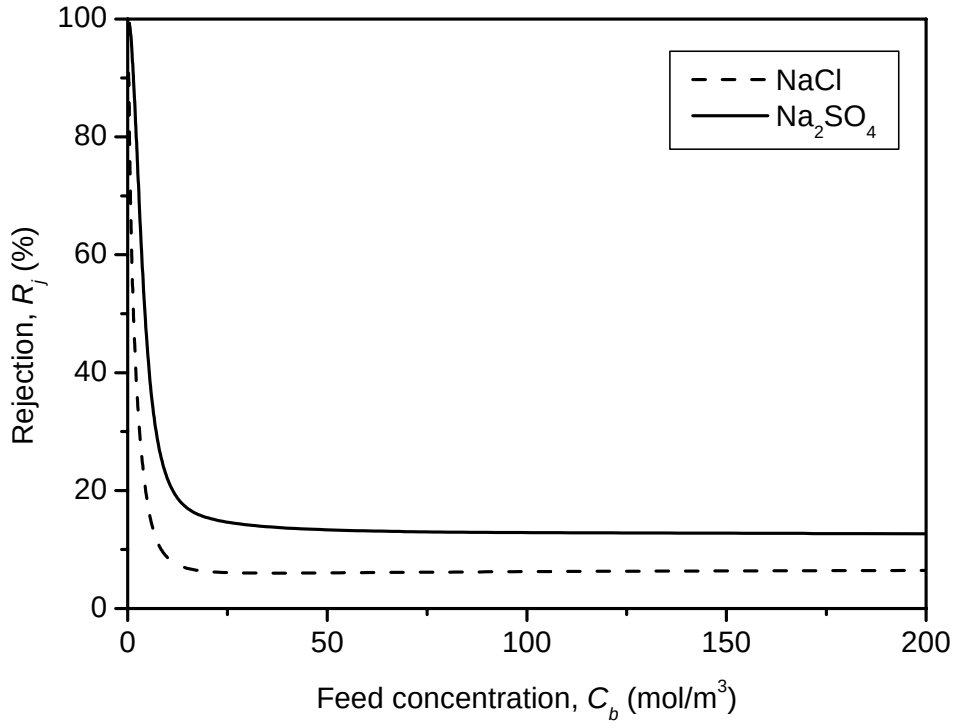

Figure 3.5 Salt rejection in single electrolyte solution as a function of its bulk concentration (J_v = 10^{-5} m/s; membrane charge density X = -10.0mol/m^3)

The effect of effective membrane pore radius on the rejection of NaCl and Na_2SO_4 solution is shown in Figure 3.6. It is clear from Figure 3.6 that the efficiency of salt rejection decreases with an increase in membrane pore radius. This observation can be attributed to the steric effect. For a given ion, the ratio of ion radius to membrane pore radius, λ ($\lambda = r_{i,s}/r_p$), will decrease with increasing membrane pore radius. As shown in Eqs. (3.9) and (3.10), a reduction in λ will increase the hindrance factors for diffusion and convection, $K_{i,d}$ and $K_{i,c}$. From Eq. (3.1), it is seen that higher hindrance factors will lead to a higher ion flux and thus a lower rejection of the ions concerned. It is interesting to note from Figure 3.6 that the variation associated with the predicted values of Na_2SO_4 rejection, with respect to membrane pore radius, is greater than the

corresponding variation associated with NaCl. This observation could be attributed to the smaller change in the magnitude of λ resulting from the smaller ionic radius of chloride ions.

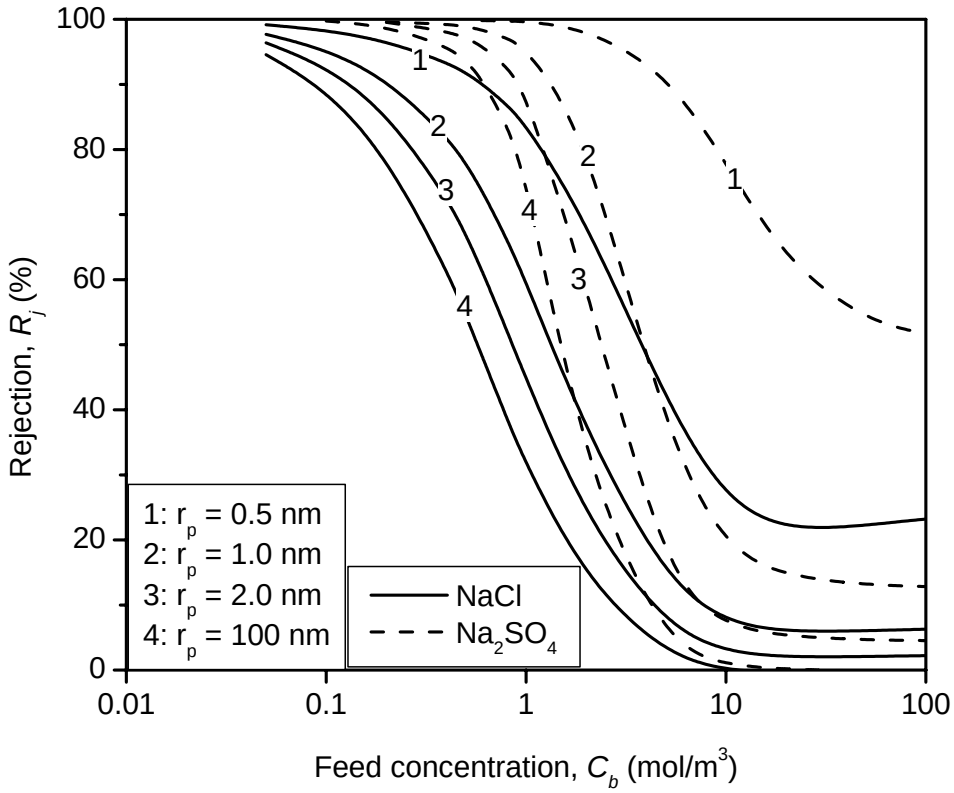

Figure 3.6 Salt rejection in NaCl and Na_2SO_4 solutions as a function of feed salt concentration at various effective membrane pore radius, r_p (J_v = 10^{-5} m/s; membrane charge density X = -10.0mol/m^3)

3.4.2 Effect of the Freundlich isotherm of feed concentration and membrane charge

It has been recognized that membrane charge density is not constant but increases with increasing bulk ion concentration (Bowen and Mohammad 1998a; Donnan 1995; Tsuru *et al.* 1991b). Figure 3.7 shows the relationship between feed salt concentration and salt rejection by incorporating the effect of bulk ion concentration on effective membrane charge for Cases 1, 2, and 3 as summarized in Table 3.2 (charge density for Case 3 > Case 2 > Case 1). It is noted from Figure 3.7 that for both NaCl and Na_2SO_4 solutions, the efficiency of salt rejection obtained for Case 3 is greater than the corresponding value for Case 2. Likewise, the salt rejection efficiency obtained for Case 2 is greater than that for Case 1. This observation indicates that at a given feed salt concentration, the membrane with a higher charge density will yield higher salt rejection efficiency. The increase in effective membrane charge density with salt concentration is possibly due to the adsorption of co-ions taking place at the membrane-solution interface (Peeters *et al*. 1998; Bowen and Mukhtar 1996). As Donnan potential increases with the effective membrane charge, an increase in effective membrane charge density will result in an increase in salt retention. Thus, co-ion adsorption increases the ability of the membrane to reject salts at high concentration. It is noted from Figure 3.7 that the efficiency of salt rejection associated with Na_2SO_4 solution increases more significantly from Case 1 to Case 3 than that in NaCl solution. This observation suggests that the effect of feed salt concentration on membrane charge plays a more important role for divalent co-ions than for monovalent co-ions.

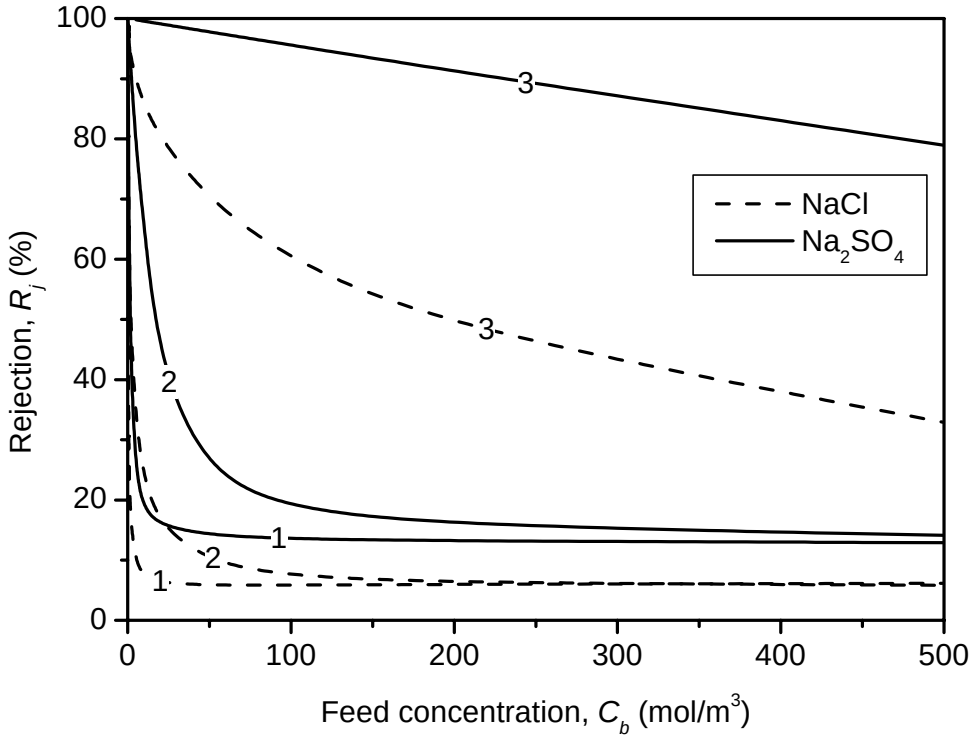

Figure 3.7 Salt rejection in single NaCl and Na_2SO_4 solutions as a function of feed salt concentration for the Cases 1, 2, and 3 shown in Table 3.2.

1: $\log_{10}|X| = 0.5\log_{10}C_b + 0.5$ **; 2:** $\log_{10}|X| = 0.5\log_{10}C_b + 1.0$ **;**

3: $\log_{10}|X| = 0.5\log_{10}C_b + 2.0$

Figure 3.8 shows the relationship between salt rejection and feed salt concentration for Cases 4, 5, and 6 (shown in Table 3.2). It is interesting to note from Figure 3.8 that when the parameter *s* in Freundlich isotherm (Eq. (3.13)) for membrane charge density is equal to 1, salt rejection efficiency does not change with the feed salt concentration. It is noted from Eq. (3.13) that when *s* = 1, the effective membrane charge density can be written as follows:

$$|X| = 10^{q} \times C_b \tag{3.14}$$

For a given value of *q*, the ratio of membrane charge density to the feed salt concentration ξ (= $|X|/C_b$) becomes a constant (= 10^q). As the salt rejection is only dependent on the ratio of charge density to salt concentration, it is not affected by salt concentration when *s* = 1. In this case, salt rejection is only governed by *q*.

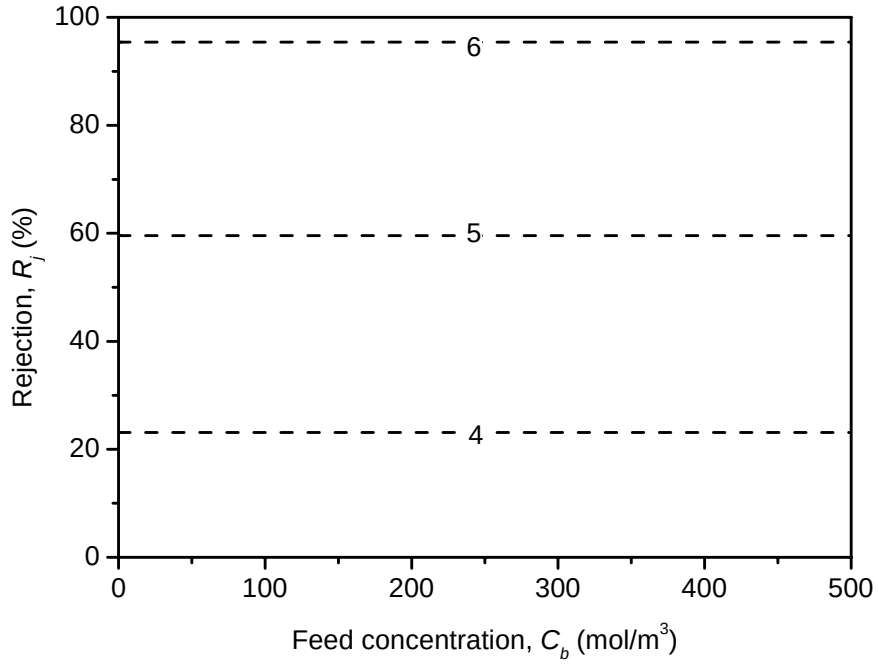

Figure 3.8 Salt rejection in single NaCl solutions as a function of feed salt concentration for the Cases 4, 5, and 6 shown in Table 3.2.

4: $\log_{10}|X| = 1.0\log_{10}C_b + 0.5$**; 5:** $\log_{10}|X| = 1.0\log_{10}C_b + 1.0$**;**

6: $\log_{10}|X| = 1.0\log_{10}C_b + 2.0$

3.4.3 A quantitative method for predicting membrane separation behavior

The application of the membrane processes would be greatly facilitated if quantitative methods for predicting salt rejection become available. Incorporated with the relation between the effective membrane charge density and the feed salt concentration, the Nernst-Planck-Donnan model can provide a feasible method for predicting the salt retention under different operation conditions.

Salt rejections as a function of feed salt concentration are calculated for single electrolyte solutions of NaCl and Na_2SO_4 and the results are plotted in Figure 3.9. The parameters used in these calculations (Cases 7 and 8 of Table 3.2) were obtained from the typical values of NF membranes reported by Bowen and Mukhtar (1996). The effect of feed concentration on the salt rejection can be expressed in the empirical equations obtained by trend lines as shown in Figure 3.9. Such empirical equations can be used to estimate the rejection efficiency in the single electrolyte solution under different concentrations. Figure 3.10 shows the relationship between the efficiency of salt rejection and the ratio of membrane charge to feed concentration (ξ). It is noted from Figure 3.10 that the salt rejection increases with ξ.

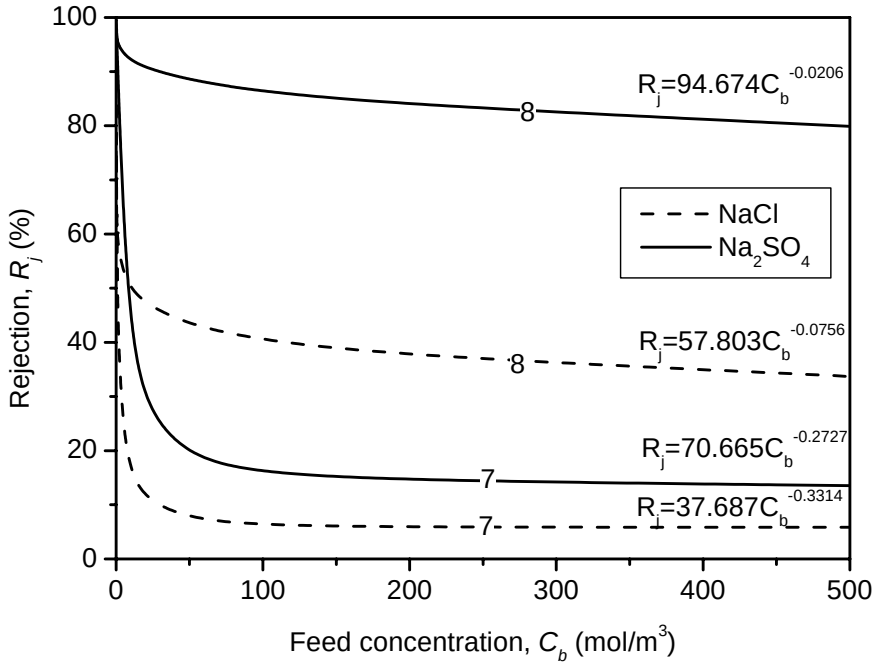

Figure 3.9 Salt rejection in single NaCl and Na_2SO_4 solutions as a function of feed salt concentration for the Cases 7 and 8 shown in Table 3.2

7: $\log_{10}|X| = 0.499\log_{10}C_b + 0.859$ **8:** $\log_{10}|X| = 0.875\log_{10}C_b + 0.999$

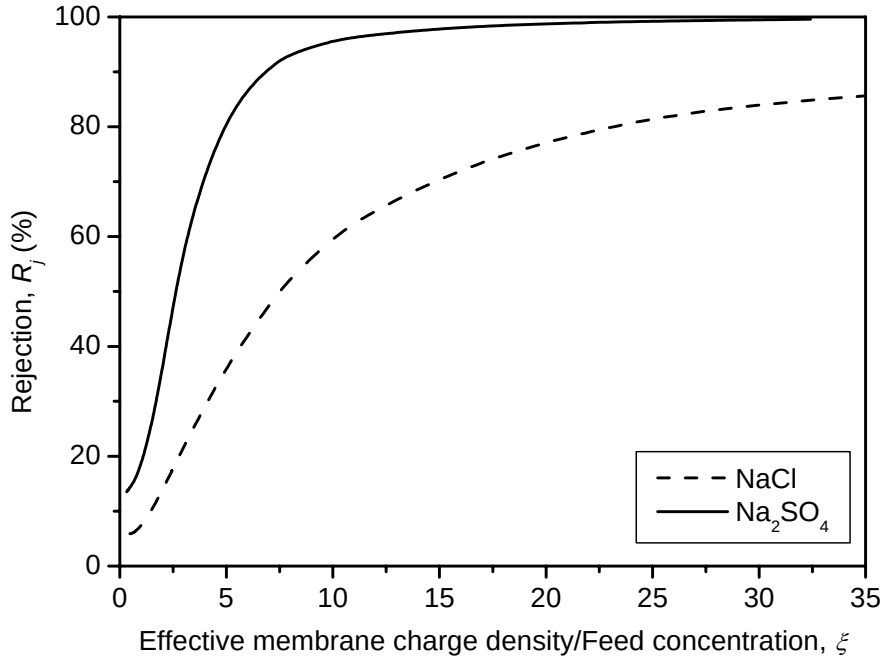

Figure 3.10 Salt rejection in single NaCl and Na_2SO_4 solutions as a function of the ratio of effective membrane charge density to the feed salt concentration (ξ)

3.5 Ion/Salt Rejections in Mixed NaCl/Na_2SO_4 Solution

Figure 3.11 shows the calculated results of ion rejections in a mixed NaCl/Na_2SO_4 solution. The rejection of sulfate ions is higher than that of chloride ions and increases with the permeate flux, which is similar to the case of single electrolyte solutions. However, rejection of sulfate ions is higher than that obtained in a single-electrolyte solution (shown in Figure 3.5 (b)), while rejection of chloride ions is lower than that in a single electrolyte solution (shown in Figure 3.5 (a)). Monovalent co-ions, which receive less repulsive force than divalent co-ions, show a higher capability to transport through the membranes. Hodgson (1970) suggested that in multiple electrolyte solutions, the rejection of a type of ions could be improved by the presence of another type of more permeable ions of the same charge. Thus, the monovalent chloride ions and the divalent sulfate ions can be effectively separated by a membrane from their mixed solution.

Furthermore, there can be a negative rejection for chloride ions at low permeate flux. It is also noted that the magnitude of negative rejection increases with permeate flux initially and then decreases as permeate flux increases further. Eventually, the rejection becomes positive and continues to increase with increasing permeate flux. The negative rejection for some ions means that the concentration of these ions in the permeate is higher than that in the feed. Since the membrane is usually negatively charged, the cations can penetrate the membrane much more readily than the anions due to the effect of Donnan exclusion. The negative rejection of chloride ions is required to maintain the electroneutrality in the permeate. Figure 3.11 also shows the effect of membrane pore radius on salt rejection in multi-electrolyte solutions. The rejection rate decreases with increasing effective pore radius. In contrast, the rejection

of chloride ions shows a greater variation that is contradictory to the case in the single electrolyte solutions. This implies that divalent co-ions have greater influence on rejection of monovalent co-ions in a multi-electrolyte solution.

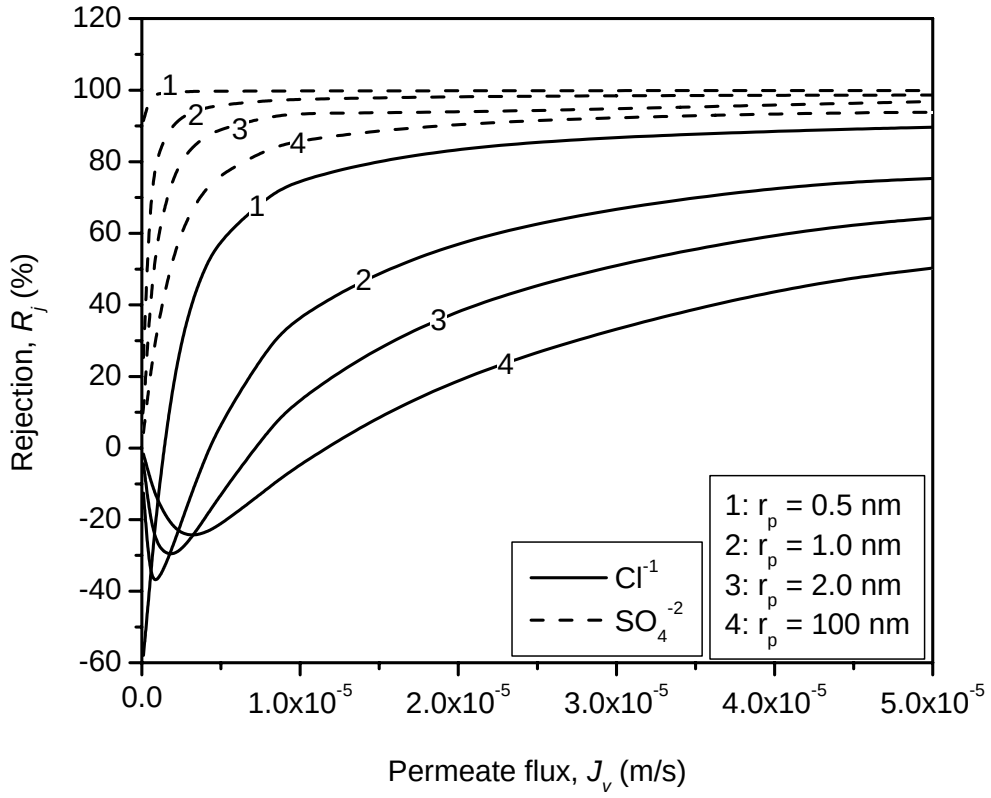

Figure 3.11 Effect of the volume flux (J_v) on rejection of anions in 1.0 mol/m^3 mixed NaCl/Na_2SO_4 solution at different membrane pore radius, r_p (NaCl fraction = 0.5; membrane charge density X = -10.0mol/m^3)

The relationship between the ion rejection and the ratio of the effective membrane charge to the feed salt concentration (ξ) is illustrated in Figure 3.12. The ion rejection rate does not increase with ξ monotonically in mixed solutions. The rejection of the monovalent chloride co-ions shows the greatest variance with respect to ξ. Figure 3.13 shows the effect of feed concentration on the ion rejection for (a) Case 7 and (b) Case 8 in mixed $NaCl/Na_2SO_4$ solutions. Unlike the monotonic decreasing rejection in a single electrolyte, the rejection of chloride ions (for Case 7) decreases first and then increases with the feed concentration in mixed solutions. The increasing phase of salt rejection does not occur when the *s* value in the Fruendlich isotherm is sufficiently high, as shown in Figure 3.13 (b).

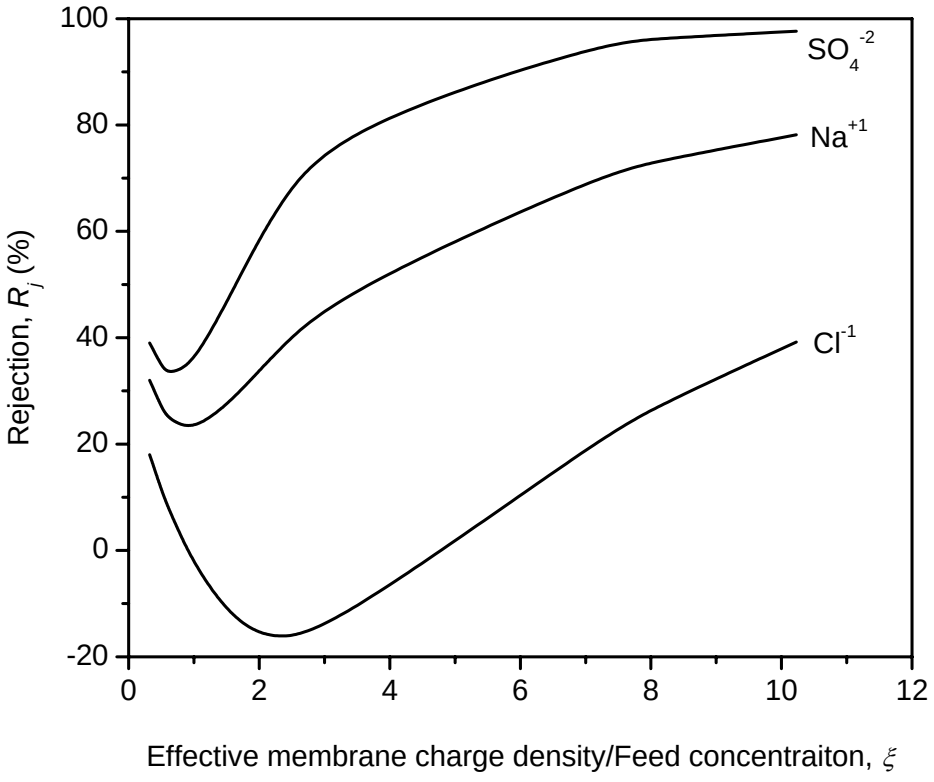

Figure 3.12 Rejection of ions in mixed $NaCl/Na_2SO_4$ solutions as a function of the ratio of effective membrane charge density to the feed salt concentration (ξ)

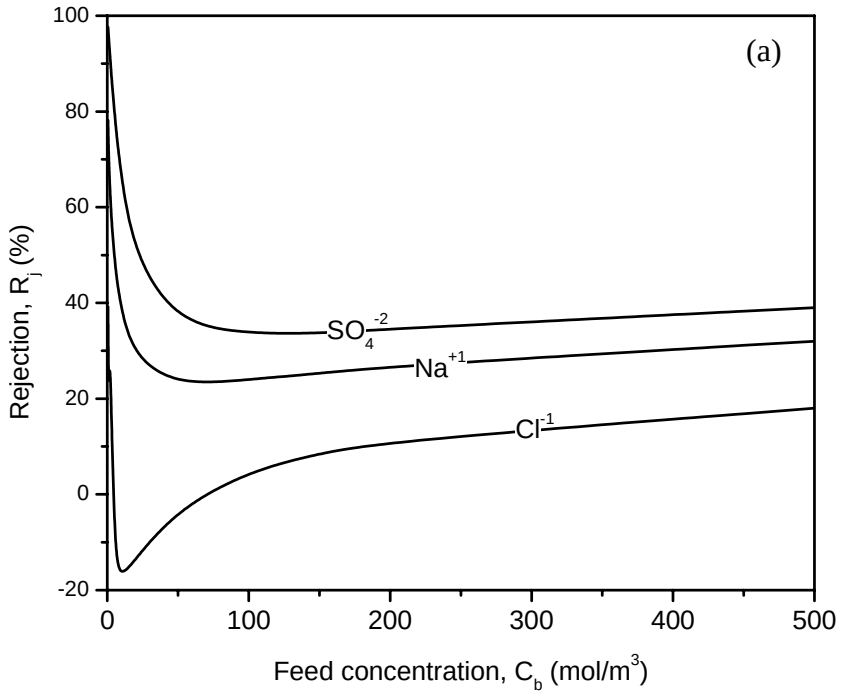

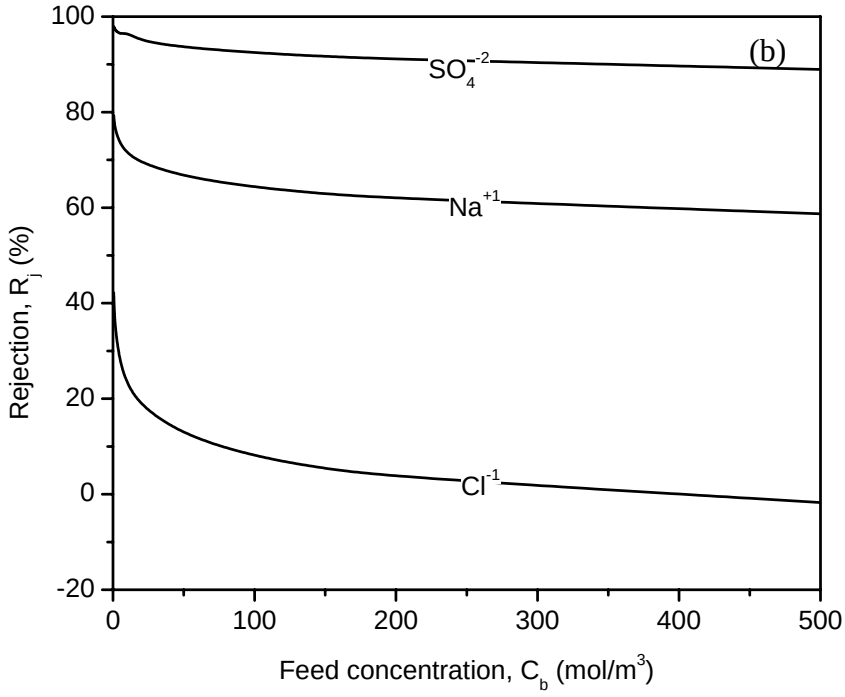

Figure 3.13 Rejection of ions in mixed NaCl/Na_2SO_4 solutions as a function of feed salt concentration (a) for Case 7 in Table 3.2: $\log_{10}|X| = 0.499\log_{10}C_b + 0.859$ **and (b) for Case 8 in Table 3.2:** $\log_{10}|X| = 0.875\log_{10}C_b + 0.999$

3.6 Summary

The Nernst-Planck-Donnan model is a feasible method for analyzing and predicting salt transport through loose RO/NF membranes, although the inherent local electroneutrality assumption overlooks the phenomena of electrostatic interaction between membrane and ions by eliminating the effects of electro-migration of ions due to the weak induced electric field. It can be concluded that the salt/ion rejection by the membranes is strongly affected by the membrane charge density, which can be related to the feed salt concentration with an empirical formula similar to the Freudlich isotherm. For a single-electrolyte solution, the ratio of membrane charge density to feed salt concentration is a major factor controlling the solute rejection through RO/NF membranes.

The empirical relationship between the ion/salt rejection and feed salt concentration for single- and multi-electrolyte solutions can be obtained from the calculation based on the Nernst-Planck-Donnan model. It may provide a new angle to understand membrane transport and a new method to estimate the solute transport through NF and RO membranes.

Furthermore, for a multi-electrolyte solution, preliminary simulations show that under certain conditions, rejection to some ions can be negative (concentration of the ions in the permeate is higher than in the feed). However, the phenomena of multi-ion transport are very complex and, therefore, more efforts are needed to further explore on this rather interesting subject.

Chapter 4

A NEW FORMULATION FOR ION TRANSPORT THROUGH DENSE RO MEMBRANES

In Chapter 3, it has been shown that the Nernst-Planck-Donnan model only considers the electrostatic interactions as Donnan exclusion on membrane surfaces. When the ions move across the membrane, electrostatic interactions are actually unrealistically eliminated. It is also noted from the literature review presented in Chapter 2 that the other existing models cannot be realistically used to quantitatively predict the transport behaviors of ions across dense RO membrane. In view of this, the objective of this study was to develop a valid formulation, which can be used to explain ion transport behaviors through RO membranes.

Membrane submerged in liquid media usually develops electric charge as a result of membrane-solution interaction or imbalanced ion transport. The charged membrane will in turn strongly affect ion transport across the membrane by its electrostatic interaction with the charged ions. Although it is well established that the ion transport can be adequately described by the Nernst-Planck and Poisson equations, the boundary conditions for the problems of practical importance are not as readily defined. In this chapter, a comprehensive theory of ion transport and electrostatic interaction in

membranes was developed from solid fundamental principles. Special effort was made to determine the boundary conditions of the unsteady-state ion transport problem. The invalid electroneutrality assumption was avoided by applying the classic Poisson's equation and well-defined boundary conditions at unsteady state condition. Finally, simulation results were presented to demonstrate (i) the ion transport process until steady state is established, (ii) the development of unbalanced charges and electric potential, and (iii) the concentration and potential profile within the membrane. This model could provide a new understanding of ion transport through membranes.

4.1 Model Development

4.1.1 Ion Transport through RO membrane

The ion transport problem typically encountered in RO membrane processes can be generally presented as shown in Figure 4.1. A RO membrane separates two electrolyte solutions of different concentration. The concentration of ion *i* in the feed solution on the left-hand-side of membrane has a higher concentration (C_{0i}) than that in the permeate solution (C_{pi}) on the right-hand-side of the membrane. The ions in the feed solution will transport through the membrane under the chemical gradient. However, because ions are charged, the ion transport process is much more involved than that of non-electrolytes. Firstly, the membrane may be initially charged or acquire electric charge due to unbalanced ion transport. There are therefore electrostatic interactions existing between the membrane and the ions. Secondly, owing to the charges associated with the ions, the general electroneutrality for solutions on both sides of the membrane has to be maintained. This will lead to the NO-NET-CURRENT

requirement for ion transport through the membrane at steady state. In other words, the transports of various ions are not independent but coupled with each other.

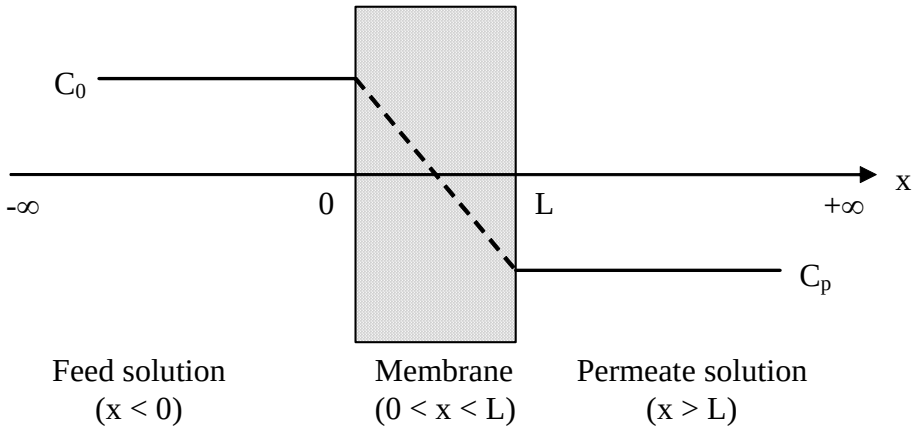

Figure 4.1 One-dimensional coordinate diagram

Furthermore, owing to the electric charge on the membrane, the concentrations of ions on the membrane surfaces are different from the ion concentrations in the bulk solutions. The ion concentrations on the membrane surfaces cannot be specified without knowing the charge distribution along the membrane thickness. Charge distribution along the membrane thickness can only be known when the transport equations are solved for concentrations of all ions, which in turn requires the concentration boundary conditions on the two membrane surfaces be specified. The coupling between the surface ion concentrations and the charge property of the membrane has not been properly solved yet. The assumption of electroneutrality on every point of the membrane and the use of Donnan potential are examples of desperate effort in overcoming this difficulty.

To overcome the difficulty in specifying the boundary conditions for ion transport through RO membrane at steady state, a formulation for unsteady state ion transport will be developed in the remaining part of this section. The unsteady state transport problem has much higher flexibility in selecting boundary conditions. The steady state transport problem can be solved by running the unsteady state transport problem sufficiently long. As a membrane is a film that can have huge surface but with a thin thickness, the transport through membrane can be adequately described in one-dimension (i.e., concentrations, fluxes and electric field vary only with x) which is perpendicular to the membrane surface (as shown in Figure 4.1).

4.1.2 Electrochemical Equilibrium in Boundary Layers

As stated before, the boundary conditions on the membrane surfaces are very difficult to be specified due to the electrostatic interaction between the charged membrane and ions. However, the interface between the membrane and the liquid can be generally described with the known physical principles by considering a thin boundary layer adjacent to the membrane surface. While electroneutrality can be generally assumed in the bulk solution far away from the charged membrane, unbalanced charge will be developed in a thin boundary layer adjacent to the membrane. The ions are distributed in the boundary layer such that the total electrochemical potential remains constant (no gradient) in the boundary layer.

Based on the electrochemical equilibrium, the ion concentrations in the boundary layer adjacent to the membrane can be related to the local electric potential according to Boltzmann distribution (Boltzmann 1868), in which the potential ψ is assumed to be zero in the bulk solution far from the membrane surface:

$$C_i(x) = C_{ib} e^{-\frac{z_i F \psi(x)}{RT}} \tag{4.1}$$

where $C_i(x)$ and C_{ib} are the concentrations of ion *i* at *x* and in the bulk respectively, z_i is the charge number of ion *i*, *F* is the Faraday constant, *R* is the universal gas constant, *T* is the absolute temperature, and $\psi(x)$ is the electric potential in the solution. The distribution of mobile ions in solution is represented as a continuous charge density.

Hence, a classical description of electrostatic interaction in solution can be given by the Poisson-Boltzmann equation (PB):

$$\frac{d^2\psi}{dx^2} = -\frac{1}{\varepsilon_a \varepsilon_0} \sum_i z_i F C_{ib} \exp\left[-z_i F \psi(x)/RT\right] \tag{4.2}$$

where ε_a is dielectric constant for solutions and ε_0 is permittivity of free space (= 9×10^{-12} coul/volt-m).

Eq. (4.2) cannot be solved analytically, except for some special cases. However, if $\left|z_i F \psi(x)\right| < RT$, the PB equation can take the form known as the Debye-Hückel approximation (Debye and Hückel 1923; Clark 1996). That is:

$$\frac{d^2\psi}{dx^2} = \frac{1}{\lambda^2}\psi(x) \tag{4.3}$$

where λ is the Debye length or the double-layer thickness

$$\lambda = \sqrt{\frac{\varepsilon_a \varepsilon_0 RT}{F^2 \sum_i z_i^2 C_{ib}}} \tag{4.4}$$

The solution to Eq. (4.3) gives the potential profile in the solution near the membrane:

$$\psi(x) = -\frac{Q\lambda}{\varepsilon_0 \varepsilon_a} e^{\frac{x}{\lambda}} \tag{4.5}$$

where Q is the net charge in the solution expressed as surface density at membrane-solution interface. If the potential of the bulk solution in the feed side is taken as zero (i.e., the reference), the potential at the membrane-feed interface is:

$$\Delta\psi_0 = \psi(0) - \psi(-\infty) = -\frac{Q_0\lambda_f}{\varepsilon_0\varepsilon_a} \tag{4.6}$$

where Q_0 is the net charge in the feed solution expressed as surface density at membrane-feed interface, and λ_f is the Debye length in the feed solution. Similarly, the potential difference between the membrane-permeate interface and the permeate bulk solution is:

$$\Delta\psi_L = \psi(\infty) - \psi(L) = \frac{Q_L\lambda_p}{\varepsilon_0\varepsilon_a} \tag{4.7}$$

where Q_L is the net charge in the permeate solution expressed as surface density at membrane-permeate interface and λ_p is the Debye length in the permeate side.

When the potential at the interface is known, the ion concentration distributions in the boundary layers adjacent to the membrane are fully defined. Substituting Eqs. (4.6) and (4.7) into Eq. (4.1), the ion concentrations at the interfaces (i.e., both feed and permeate sides) can be obtained as follows:

$$C_{i0} = C_i(0) = C_{if}e^{-\frac{z_iF\Delta\psi_0}{RT}} \tag{4.8}$$

$$C_{iL} = C_i(L) = C_{ip}e^{\frac{z_iF\Delta\psi_L}{RT}} \tag{4.9}$$

where C_{i0} and C_{iL} are ion concentrations at the membrane-feed and membrane-permeate interfaces, respectively; C_{if} and C_{ip} are ion concentrations in the bulk solutions at the feed and permeate sides, respectively.

4.1.3 Governing Equation for Ionic Transport through Membrane

Within the membrane ($0 \le x \le L$), the flux of ions is described by the so-called extended Nernst-Planck equation (Schlögl 1966; Dresner 1970; Tsuru *et al.* 1991a; Bowen and Mukhtar 1996):

$$J_i = -D_i \frac{dc_i}{dx} - \frac{D_i F}{RT} z_i c_i \frac{d\psi}{dx} + k_{i,c} J_v c_i \tag{4.10}$$

where J_i is ionic flux; D_i and $k_{i,c}$ are diffusivity and convective factor of species I respectively; c_i is ionic concentration in the membrane; and J_v is permeate flux. Eq. (4.10) shows that the total flux consists of three components, namely diffusion, electro-migration, and convection. They are driven by the gradients in concentration, electric potential, and pressure, respectively.

From mass conservation principle and extended Nernst-Planck equation, the governing equation for ion transport through membrane at unsteady-state is derived as:

$$\frac{dc_i}{dt} = D_i \frac{d^2 c_i}{dx^2} + \frac{D_i F}{RT} z_i \frac{d}{dx}\left(c_i \frac{d\psi}{dx} \right) - k_{i,c} J_v \frac{dc_i}{dx} \tag{4.11}$$

Eq. (4.11) is the general equation for ion transport across RO membranes and may be reduced to simpler forms for some special cases. For example, when the ion transport is completely independent of solvent (water) transport, the third term on the right-hand-side of the equation can be discarded. The time dependent term on the left-hand-side of the equation is zero for ion transport at steady state.

The potential distribution on the membrane is related to the charge distribution by Poisson's equation:

$$\varepsilon_0 \varepsilon_m \frac{d^2 \psi}{dx^2} = -F\left(\sum z_i c_i + X \right) \tag{4.12}$$

where ε_m is dielectric constant of the membrane material and X is the (volumetric) fixed charge density in membrane.

Ion transport through RO membranes can be completely defined with the governing equations (4.11) and (4.12), and the boundary conditions specified by Eqs. (4.6) - (4.9). In this formulation, instead of the invalid local electroneutrality assumption and the ill-defined Donnan potential, fundamental principles of Boltzmann-Poisson distribution and Poisson equation are used to specify the boundary conditions. However, the charges in the boundary layers (Q_0 and Q_L in the feed and permeate sides of the membrane) have not be determined yet. This task will be done in the following section.

4.1.4 Electroneutrality in Membrane System

Membranes acquire net charge while in contact with solution because of unbalanced exchange of cations and anions with the solution. The two major mechanisms contributing to ion exchange between the membrane and solution are: (1) the differential transport fluxes in cations and anions through membrane, and (2) exclusion effect of the fixed or bounded charge of the membrane (Purcell 1985; Griffiths 1999). Membrane can also acquire an electric charge on surfaces through adsorption of ions from solution and/or dissociation of functional groups (Schaep 2001). This can be included into the second mechanism as a special case.

In a membrane system, both the membrane and the boundary layers in the solution adjacent to the membrane surface are initially neutral before the ion transport starts. The charges developed in the membrane and the boundary layers are a result of unbalanced movement of the cations and anions across the membrane-feed and

membrane-permeate interfaces. Therefore, the net charge in any region can be calculated by taking account of the cumulative charge across the interfaces, i.e.,

$$Q = \left[\int_0^t \left(\sum_i z_i F J_i \right) dt \right]_{in} - \left[\int_0^t \left(\sum_i z_i F J_i \right) dt \right]_{out} \tag{4.13}$$

Thus the total cumulative charge in the membrane, Q_m, over time period t can be obtained as:

$$Q_m = \int_0^t \left(\sum_i z_i F J_i \right)\Big|_{x=0} dt - \int_0^t \left(\sum_i z_i F J_i \right)\Big|_{x=L} dt \tag{4.14}$$

As both boundary layers in the solutions each have only one interface across which there is charge flow, the cumulative charge in the boundary layers during time period t are given as:

$$Q_0 = -\int_0^t \left(\sum_i z_i F J_i \right)\Big|_{x=0} dt \tag{4.15}$$

$$Q_L = \int_0^t \left(\sum_i z_i F J_i \right)\Big|_{x=L} dt \tag{4.16}$$

where Q_0 and Q_L are membrane surface charge at the feed and permeate side, respectively.

From the charge conservation law and electroneutrality in the whole system, there is a fundamental relationship between all the charges:

$$Q_0 + Q_m + Q_L = 0 \tag{4.17}$$

Eq. (4.17) is a mathematical statement of electroneutrality for the membrane system (i.e., the membrane and the two boundary layers adjacent to the membrane in feed and permeate solutions). The charge neutrality is always held for the whole membrane system even though there are net charges on the membrane and the boundary layers.

4.1.5 Electric Current and Non-equilibrium Steady State

A Membrane system is in thermodynamic equilibrium state when ionic flux, J_i, is equal to zero. Non-equilibrium steady state, on the other hand, is characterized as a time-independent system with a flow going through it. When a system reaches its steady state, flows, concentrations and potentials become constant. Owing to different ionic diffusivity, different ions have different ionic fluxes. This phenomenon in turn creates a surface potential on membrane-solution interface and an electric field across the membrane. The resulting time-dependent potential will reach a constant when and only when the net ionic flux is equal to zero ($J_+ = J_-$) along the membrane length. Therefore, no electric current will be produced when a membrane system has attained steady state phenomenon, i.e,

$$\sum_i z_i J_i = 0 \tag{4.18}$$

At steady state, ionic concentration is independent of time. The following expression can be derived from continuity equation:

$$\frac{\partial J_i}{\partial x} = -\frac{\partial c_i}{\partial t} \tag{4.19}$$

The above equation implies that ionic flux is independent of its position within the membrane. That is, the flux flowing into the membrane equals the flux flowing out of the membrane. Accordingly, the following expression is obtained:

$$J_{i,x=0} = J_{i,x=L} \tag{4.20}$$

Eq. (4.20) is the steady-state constraint used in this study.

4.2 Numerical Procedures

The coupled governing equations (Eq. (4.11) and Eq. (4.12)) with the complicated boundary conditions are a problem to which an analytical solution is practically impossible to obtain. A numerical procedure was developed in this study instead. The non-steady state transport equation and Poisson equation were discretized into finite difference form using the Crank-Nicolson scheme (Tannehill et al. 1997; Cheney and Kincaid 1999) and a central difference scheme. The resulting tri-diagonal matrix was then solved by a specialized Gaussian Elimination technique known as the Thomas Algorithm (Anderson 1995; Epperson 2002; Mahan 2002).

A flow diagram of the computer program was shown in Figure 4.2. The parameters and initial ion concentrations were the required input to the program. An iterative scheme was employed to decouple the difference equations for concentrations and membrane potential. At any time step, the iteration started with the potential at the previous time step as an initial guess. The ion concentration profiles were determined from the numerical solution of Eq. (4.11). With the ion concentration profiles, a new potential profile was subsequently obtained from the numerical solution of Eq. (4.12). Once the iteration converged, the concentration and potential at this time were determined and the calculation would go on to the next time step. The no-electric-current condition was used as the indicator for the steady state and the program would stop when the steady state was reached.

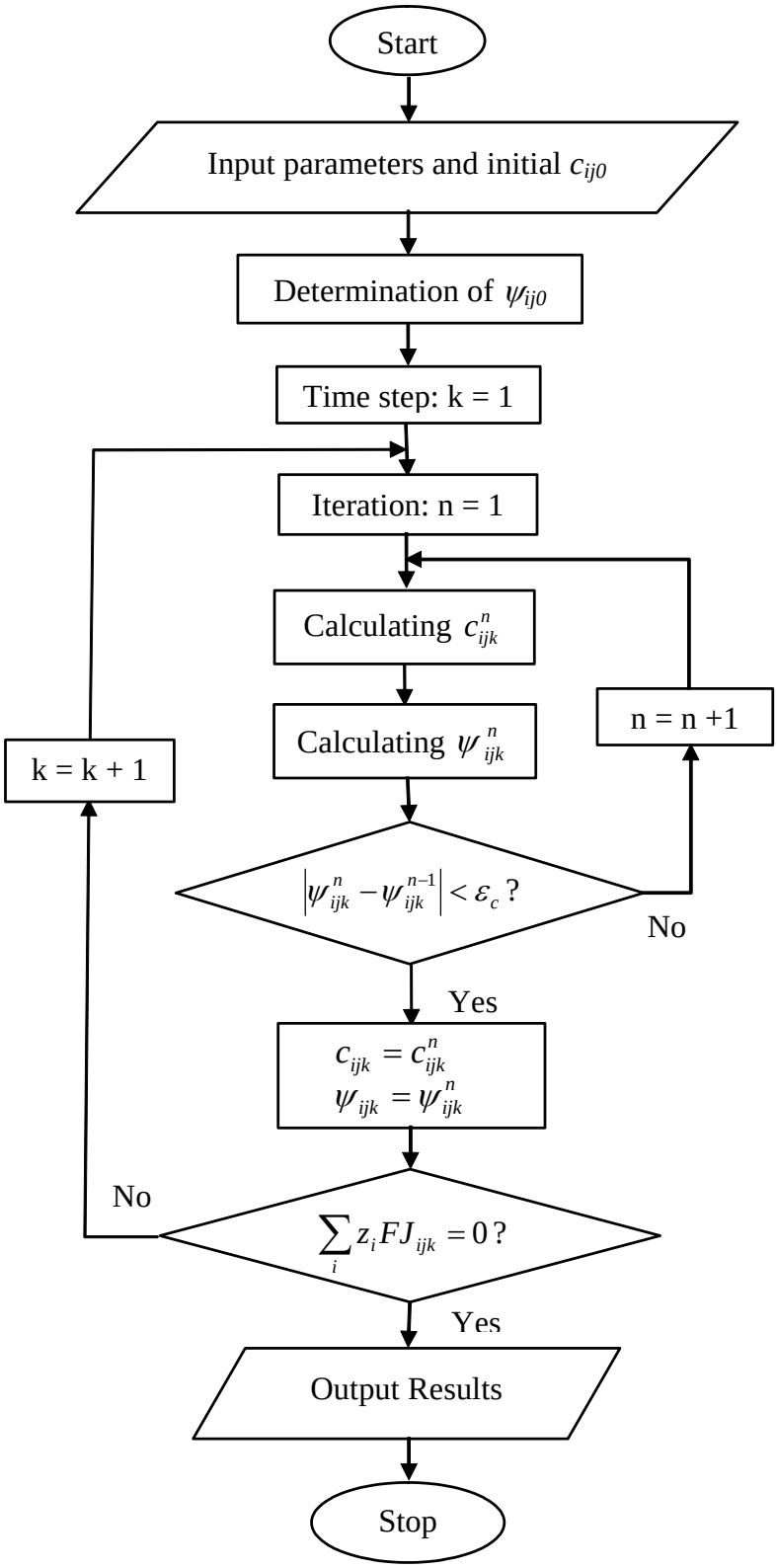

Figure 4.2 Flowchart of iteration scheme

4.3 Results and Discussions

Some fundamental phenomena or aspects of ion transport through RO membranes were investigated and discussed below with a simple salt consist of one cation and one anion. These include the time scale of the transport to reach steady state, the magnitude of the acquired membrane potential, and charge distribution throughout the membrane. The following initial conditions were used in most of the simulation studies:

$$c_i(x) = C_{if} - \frac{x}{L}\left(C_{if} - C_{ip}\right) \tag{4.21}$$

This equation gives continuous concentration profiles across the membrane thickness with the ion concentrations on the membrane surfaces equal to the feed and permeate concentrations, respectively. The use of these initial concentrations could significantly shorten the computation time to reach the steady state than the uniformly distributed ones. Unless other stated, the parameters summarized in Table 4.1 would be used in the numerical simulations.

Table 4.1 Parameters used in simulation studies

Ionic type	Cation	Anion
Charge, z	+1	-1
Feed concentration, C_0 (mol/m^3)	0.1	0.1
Diffusivity, $D_i \times 10^{12}$ (m^{2}s^{-1})	1.0	5.0
Coefficient for convection, k_c	0	0
Membrane thickness, L (m)	1×10^{-5}	
Dielectric constant of membrane, ε_m	20	
Dielectric constant of solutions, ε_a	80	
Fixed membrane charge density, X (mol/m^3)	0	

4.3.1 Transient Behaviors of Ion Transport

Although membrane performance at steady state is usually the main concern in most transport studies, the dynamic process from unsteady state to steady state will reveal some useful information about ion transport. Figure 4.3 shows the time-dependent ion fluxes entering the feed surface (a) and leaving the permeate surface (b) of the membrane. In this time scale, the differences between the cations and anions could not be seen. At the very beginning of ion transport, the ion fluxes entering the membrane are much higher than those leaving the membrane. As transport proceeds, the ion fluxes entering the membrane decrease while the ion fluxes leaving the membrane increase until reaching a steady state. The ion transport in this example reached its steady state in less than 40 seconds. However, it should be pointed out that in realistic setting of actual membrane transport problems, the time that the ion transport process takes to reach the steady state will be strongly dependent on membrane thickness and the mobility of ions within the membrane.

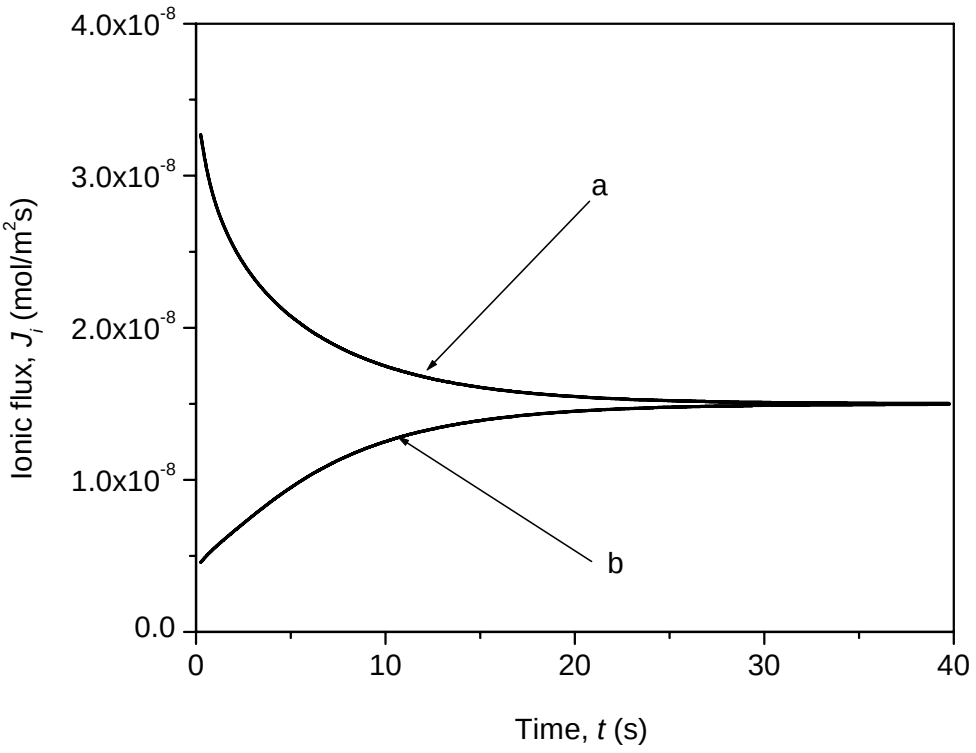

Figure 4.3 Profiles of ionic fluxes with time: (a) inward flux for cation and anion at the membrane-feed interface and (b) outward flux for cation and anion at membrane-permeate interface

Figure 4.4 shows the fluxes of the anion and cation at both (a) membrane-feed interface and (b) membrane-permeate interface in a much shorter time scale. It clearly illustrates that the anion fluxes at both interfaces are higher than those of cation in the beginning due to the higher mobility of the anions. The anion fluxes decrease with time while the cation fluxes increase with time. As illustrated in Figure 4.4, the two fluxes equalize with each other within 0.005 sec. The process is so quick that the difference between the anion and cation fluxes could not be seen in Figure 4.3 using a much larger time scale. The unbalanced ionic fluxes would induce electric current, and subsequently, the unbalanced charge at both membrane-solution interfaces with

the feed and permeate solutions. More discussions on the induced membrane potential and its relation with ion fluxes will be present in the subsequent sections.

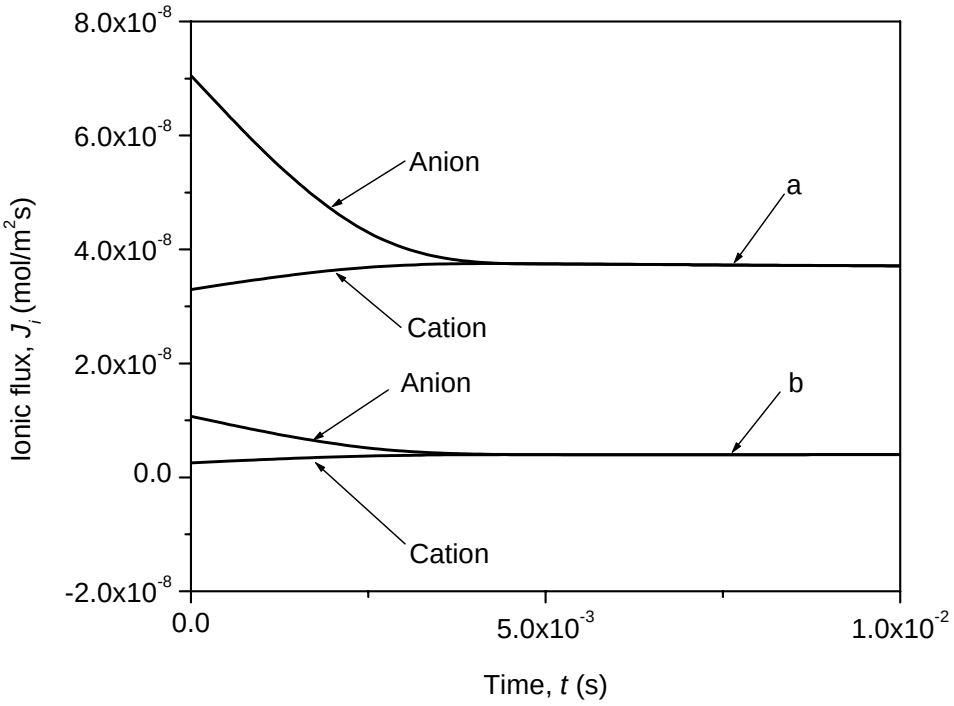

Figure 4.4 Transient behaviors of ionic flux at (a) the membrane-feed interface and (b) membrane-permeate interface

4.3.2 Acquirement of Membrane Potential

Owing to different mobility between cations and anions, the initially uncharged membrane can acquire membrane potential as a result of ion transport through the membrane. The membrane potential is usually comprised of three components: (i) potential difference between the feed solution and the membrane surface ($\Delta\psi_0$), (ii) potential difference across the membrane ($\Delta\psi_m$), and (iii) potential difference between the membrane surface and the permeate solution ($\Delta\psi_L$). The potential acquiring

process is presented in Figures 4.5 and 4.6. Figure 4.5 shows the time-dependent $\Delta\psi_0$ and $\Delta\psi_L$ calculated with Eqs. (4.6) and (4.7), respectively. The higher fluxes of negative charge across the membrane-solution interfaces result in negative values for both $\Delta\psi_0$ and $\Delta\psi_L$. It could be seen from Figure 4.5 that the absolute values of the potential differences at both membrane interfaces increase with time. The potential difference across the membrane thickness $\Delta\psi_m$ is a direct result of the numerical solution. As shown in Figure 4.6, the absolute value of $\Delta\psi_m$ decreases with time with a decreasing rate and stabilizes at a constant value.

Both Figures 4.5 and 4.6 shows that the increasing rates of the potential differences are high in the beginning and level off with time till reaching their respective stable values. This phenomenon reflects regulation effect of the membrane potential on ion transport. The net effect of the membrane potential is to accelerate the less mobile ions and to hinder the more mobile ions so that the charges carried by cations and anions are equal to each other at steady state. Figures 4.5 and 4.6 also show that it takes about 30 sec for the potential differences to stabilize. As the ion fluxes are much less sensitive than the potential differences (with a factor about 1000, i.e., $F\lambda/\varepsilon_a\varepsilon_0$), such a small flux difference could not be detected from Figure 4.4. The results shown in Figures 4.5 and 4.6 imply that the true no-electric-current condition could only be applicable when the membrane system had attained the steady state.

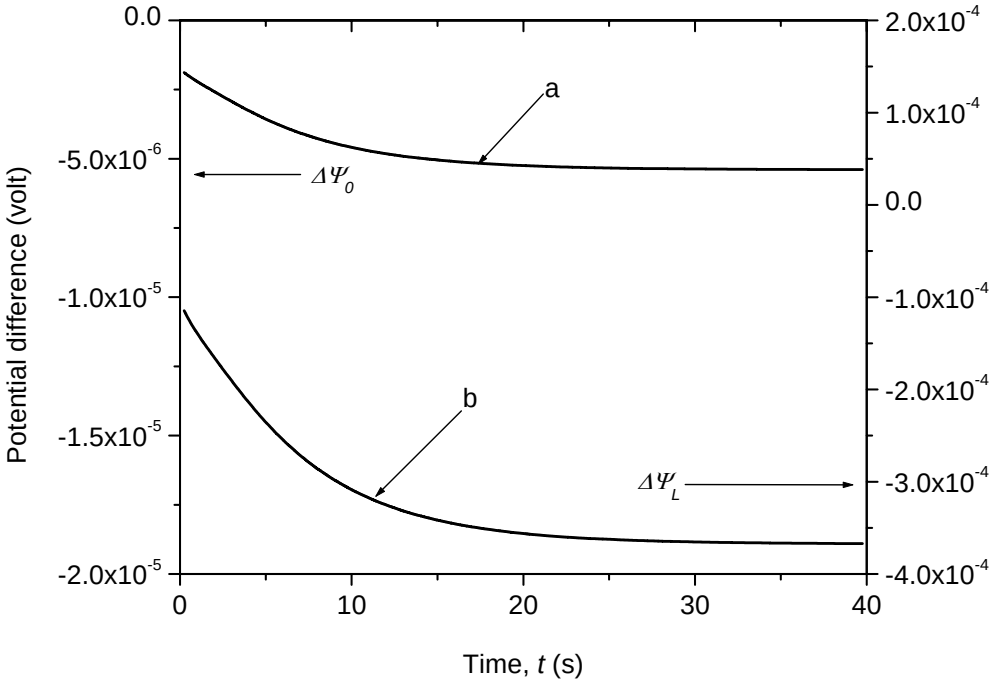

Figure 4.5 Transient behaviors of potential difference between (a) the feed and membrane interface and (b) the permeate and membrane interface

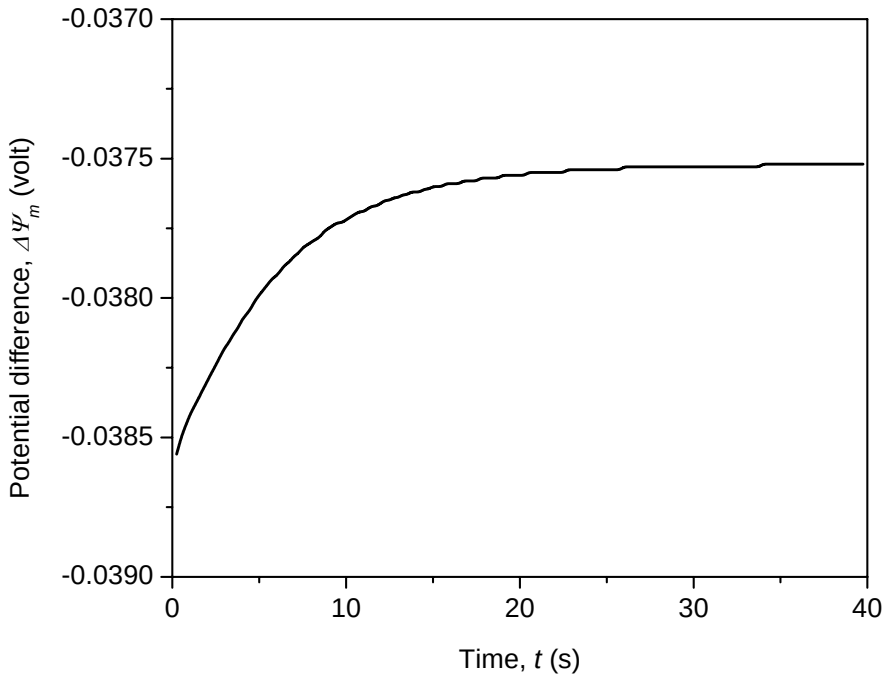

Figure 4.6 Profile of potential difference across the membrane with time

Comparing the magnitudes of the three potential differences, it is found that the potential difference across the membrane is orders larger in magnitude than the other two. In this current case, the potential differences at steady state are around -0.005 mv and -0.37 mv at the two interfaces, respectively. The corresponding potential across the membrane is -37.5 mv, which is 99.0% of the total membrane potential. The decrease of potential from the feed side towards the permeate side is schematically presented in Figure 4.7.

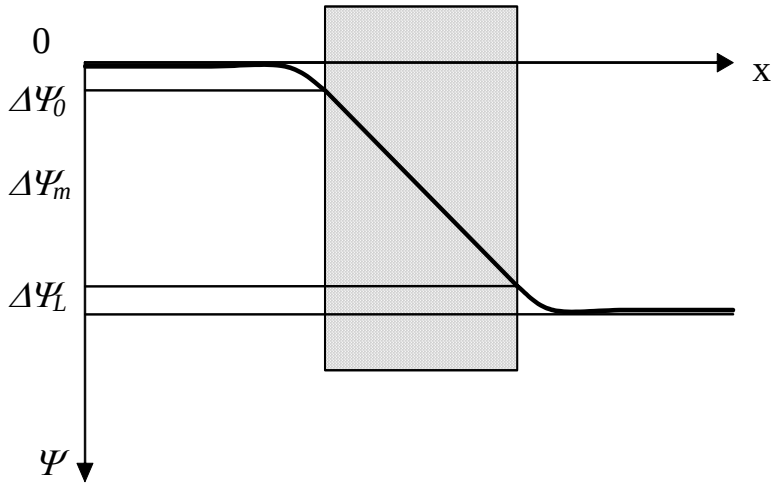

Figure 4.7 Schematic diagram of potential difference

4.3.3 Net Charge Distribution in Membrane System

Net charge in the feed and permeate solutions were readily calculated with Eq. (4.5) combined with Eqs. (4.15) and (4.16). The net charge density (mol/m^3) at any location (x) in the membrane was calculated as $\sum_i Fz_i c_i(x)$ directly from the numerical solutions of the ion concentration distributions.

As showed in Figures. 4.8(a) and 4.8(b), both feed and permeate solutions have net charges (not neutral) and the signs of the net charges are opposite. This observation could be explained with the different mobility of the anion and cation. Owing to the higher mobility of the anion used in the simulations, more anions would enter the membrane from the feed solution in an initial period of ion transport. Net positive charge resulted from the excessive cations remains in the feed solution. For the same reason, the permeate solution would obtain net negative charge as more anions would enter the permeate solution in the same period. It is found from the figures that the net charge densities decrease rapidly to zero in very narrow boundary layers. It could also be seen from Figure 4.8 that the net charge densities in both solutions increase with time initially and reach the steady state in about 40 seconds.

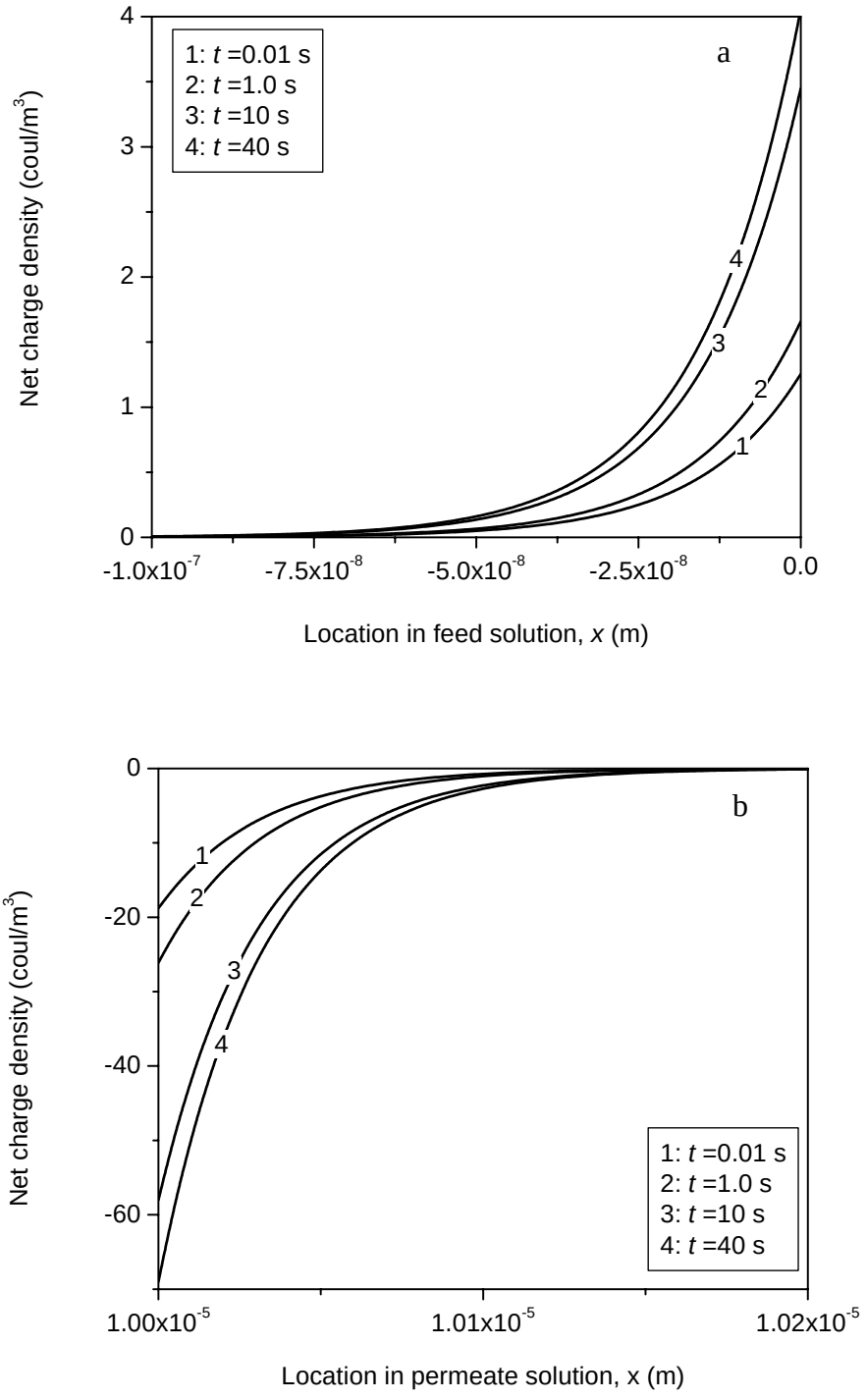

Figure 4.8 Net charge profiles in (a) feed and (b) permeate solutions

The net charge density across the membrane at steady state is presented in Figure 4.9. Although the net charge density is almost zero (but not zero) in most part across the membrane, there is relatively large amount of unbalanced charges in a narrow region of each membrane surface, as indicated by the two circles shown on the figure. The two-circled regions are enlarged in Figures 4.10(a) and 4.10 (b) to show the detailed variations of the net charge density toward the membrane surfaces. It could be seen from these two figures that charge densities are 4.0 coul/m^3 of positive charge near the feed interface of the membrane and 15 coul/m^3 of negative charge near the permeate interface of the membrane. This result deviates substantially from the common assumption of electroneutrality on every point across the membrane. It is these unbalanced charges that induces the membrane potential, which regulates the ions with different mobility to travel through the membrane at the same fluxes.

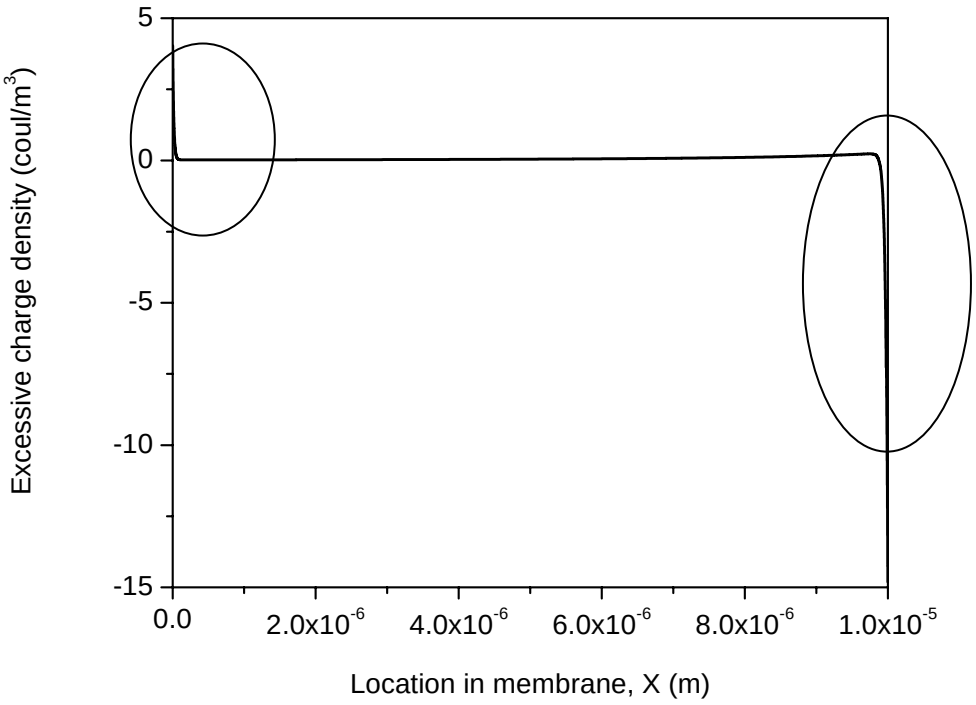

Figure 4.9 Net charge profiles within the membrane

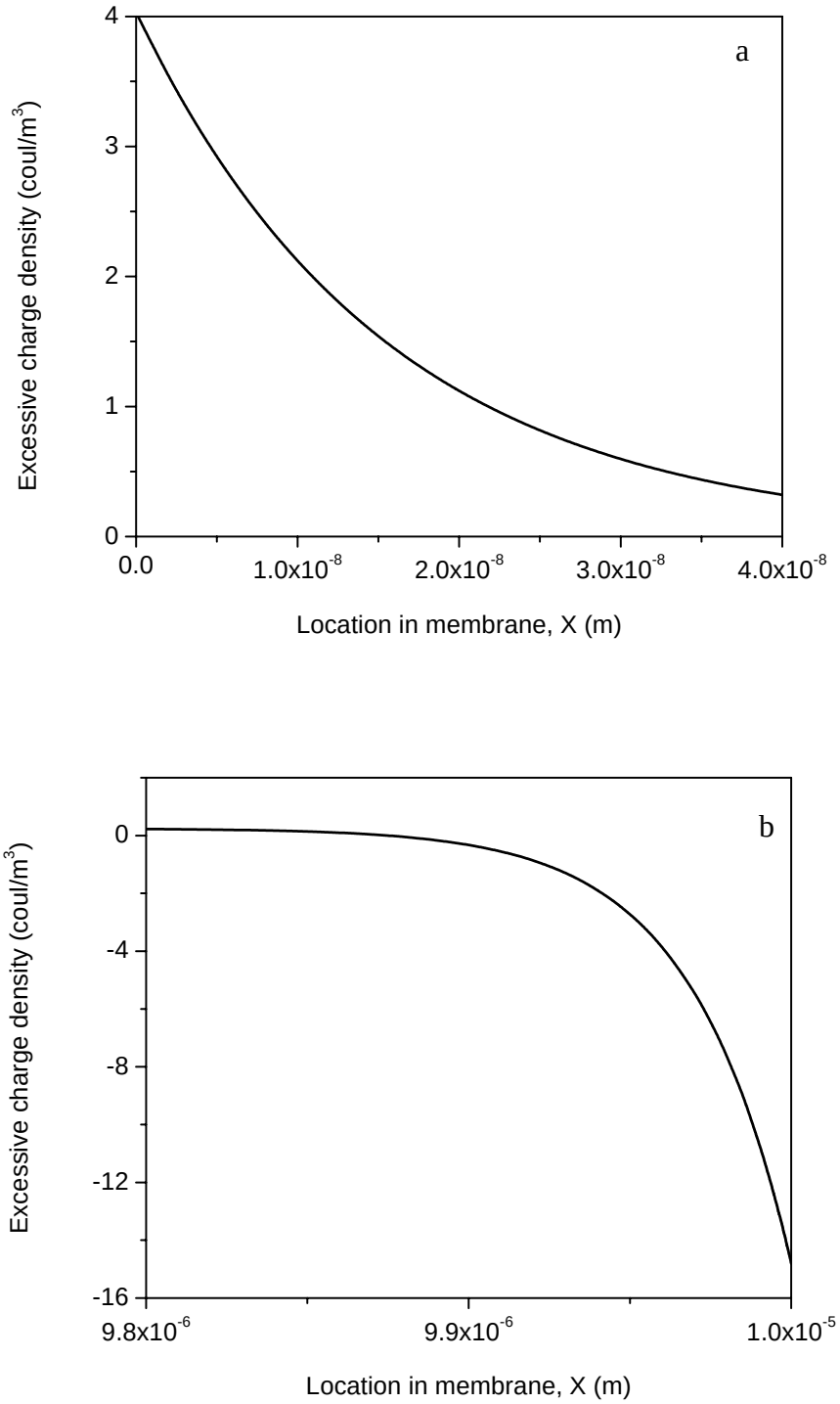

Figure 4.10 Unbalanced charges at (a) the membrane-feed interface and (b) the membrane-permeate interface

4.3.4 Concentration and Potential Profiles at Steady State

The concentration distributions of ions on the membrane and in the solutions adjacent to the membrane surfaces at steady state are a result of ion transport across the membrane. At the same time, they are responsible for maintaining the membrane potential and sustainable ion transport across the membrane. The information on ion concentration and potential profiles at steady state is therefore of fundamental importance for understanding membrane potential and ion transport.

The concentration distributions of cation and anion in the feed and the permeate solutions at steady state were calculated with Eqs. (4.1) and (4.5) and plotted in Figures. 4.11(a) and 4.11(b). Concentration profiles of the two ions within the membrane as shown in Figure 4.12 were directly derived from the numerical solution. It is noted that the anion concentration is lower than cation concentration in a region around the membrane-feed interface and the opposite occurs at the membrane-permeate interface. The net charges of two regions are the major source of the induced membrane potential.

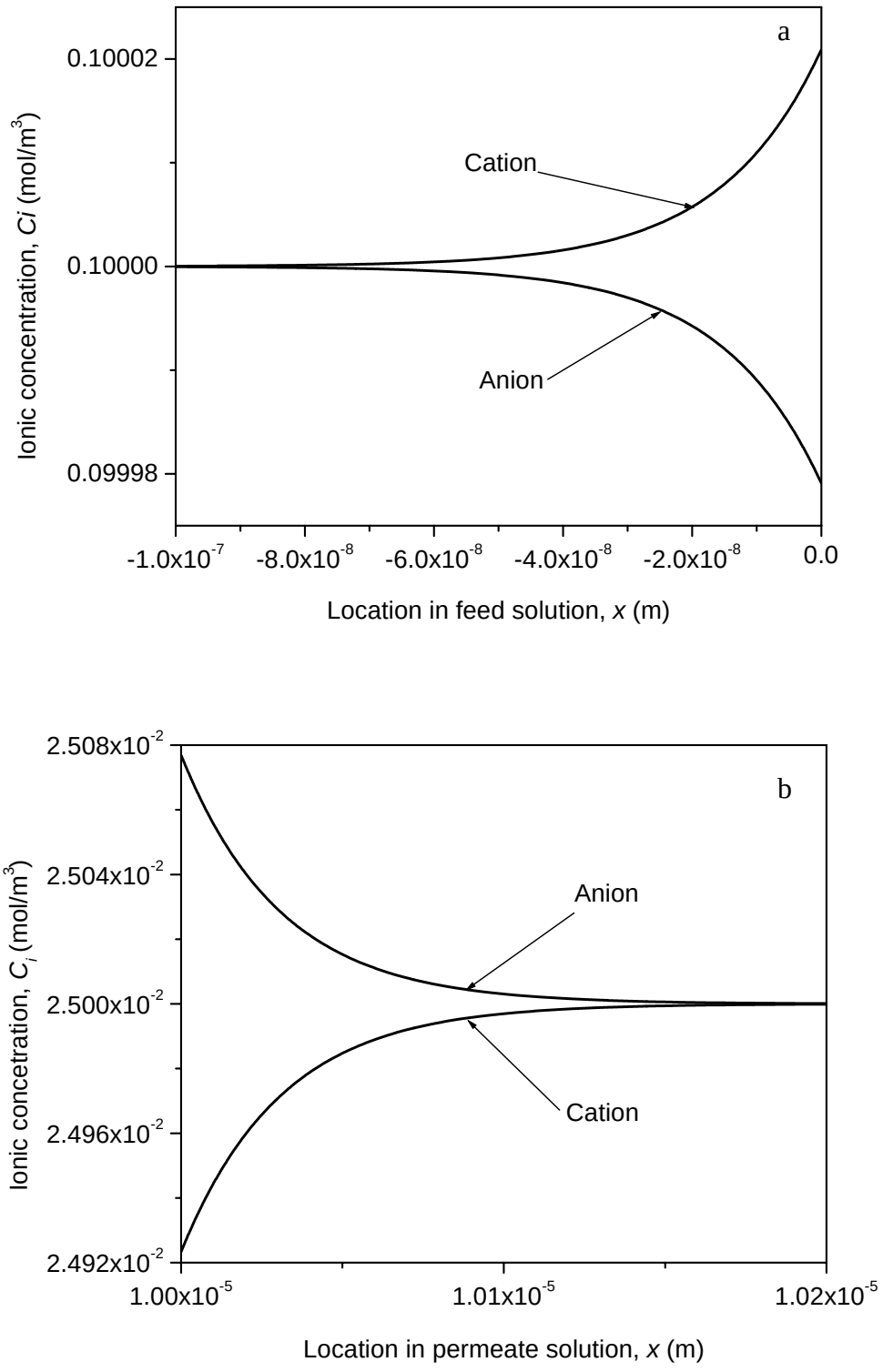

Figure 4.11 Ionic concentration profiles in (a) the feed solution and (b) the permeate solution

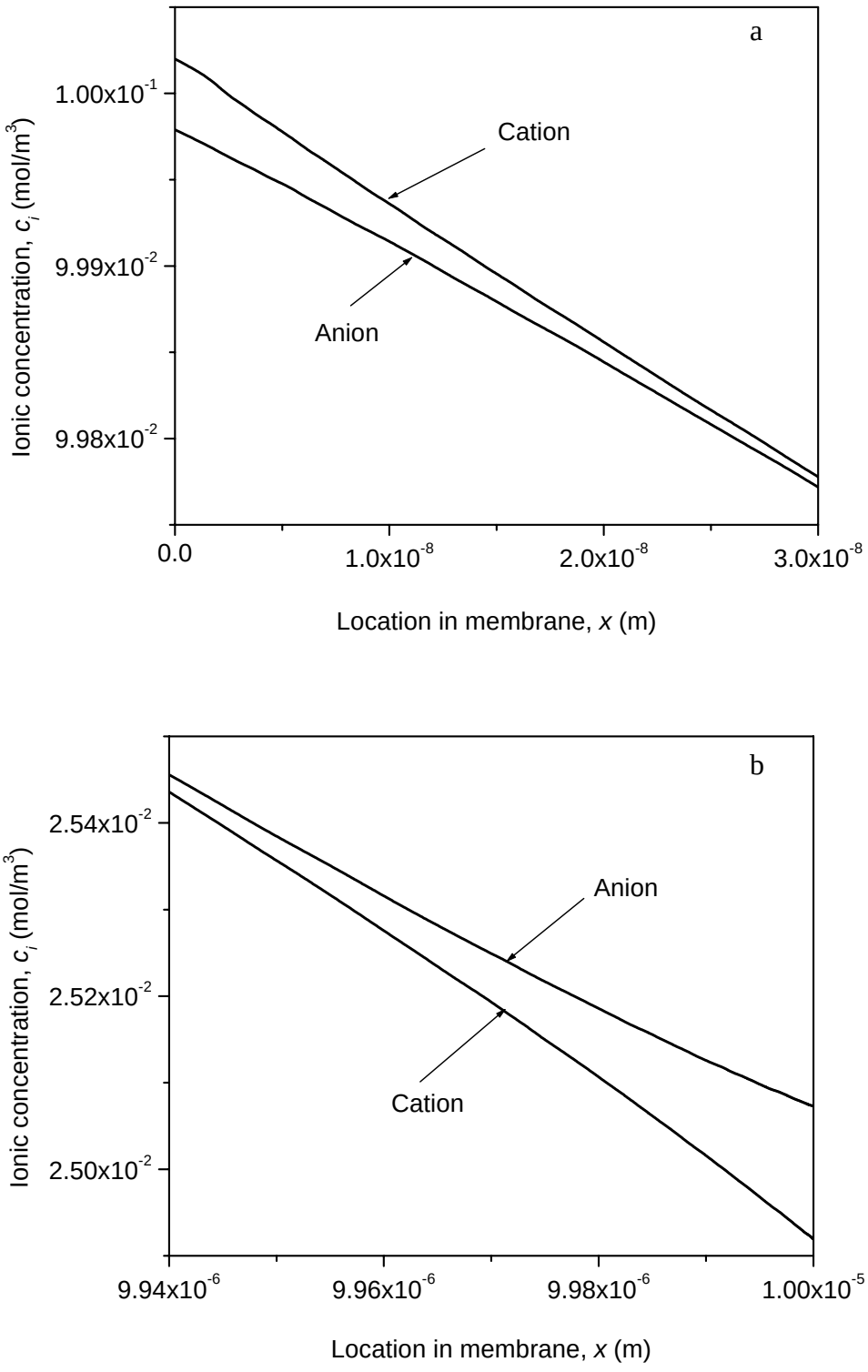

Figure 4.12 Ionic concentration profiles in the membrane (a) near to the feed interface and (b) near to the permeate interface

The induced potential profile within the membrane at the steady state is shown in Figure 4.13. The potential decreases (with an increasing rate) towards downstream (in the membrane) due to the positive charge on the feed side and negative charge on the permeate side of the membrane. The decline in potential indicates that the electrostatic force would work for cations but against anions to transport across the membrane. This feature of the induced membrane potential is of fundamental importance for ion transport across the membrane. The built-up of the membrane potential provides a mechanism such that the ion transport can be self-regulated to basically maintain the electroneutrality in feed and permeate solutions even though the mobility is quite different between cations and anions.

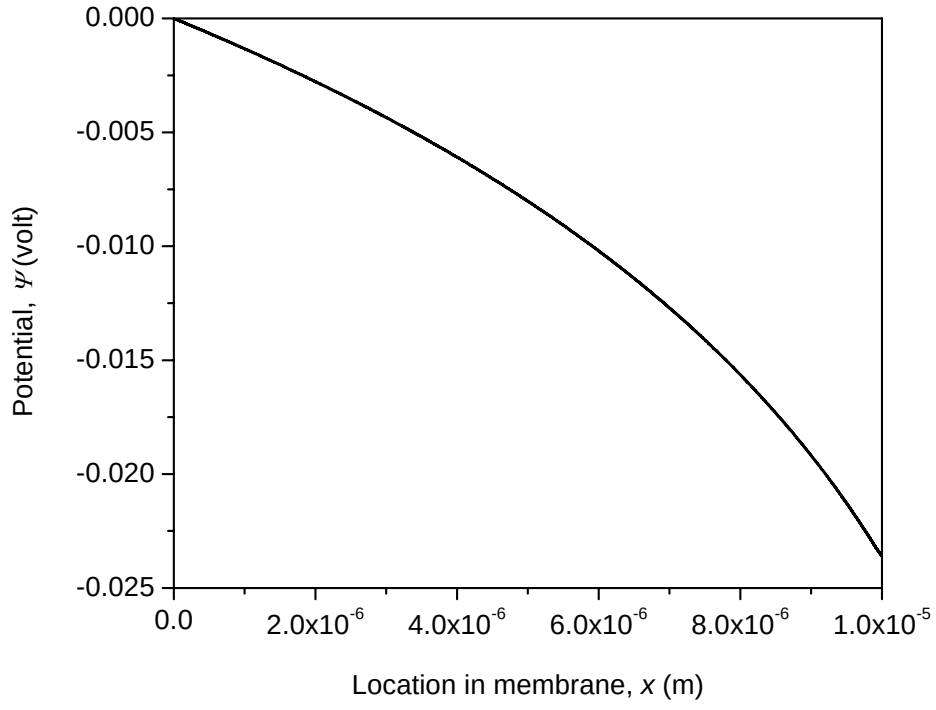

Figure 4.13 Potential profiles within the membrane

With the above simulation study, a clearer picture of ion transport across the initial uncharged membrane can be obtained, which is schematically presented in Figure 4.14. In the bulk solution far away from the membrane surfaces (*region a* and *region e*), electroneutrality is maintained and there is no electrostatic force on ions. In the membrane system (*region b + region c + region d*), two regions of net charge are developed as a result of unbalance ions transport due to the difference in the ion mobility. Positive charge is developed on the left side and negative charge is developed on right side of the membrane system. The membrane potential induced by this unbalanced charge distribution provides a necessary regulation mechanism for maintaining no-current condition at steady state.

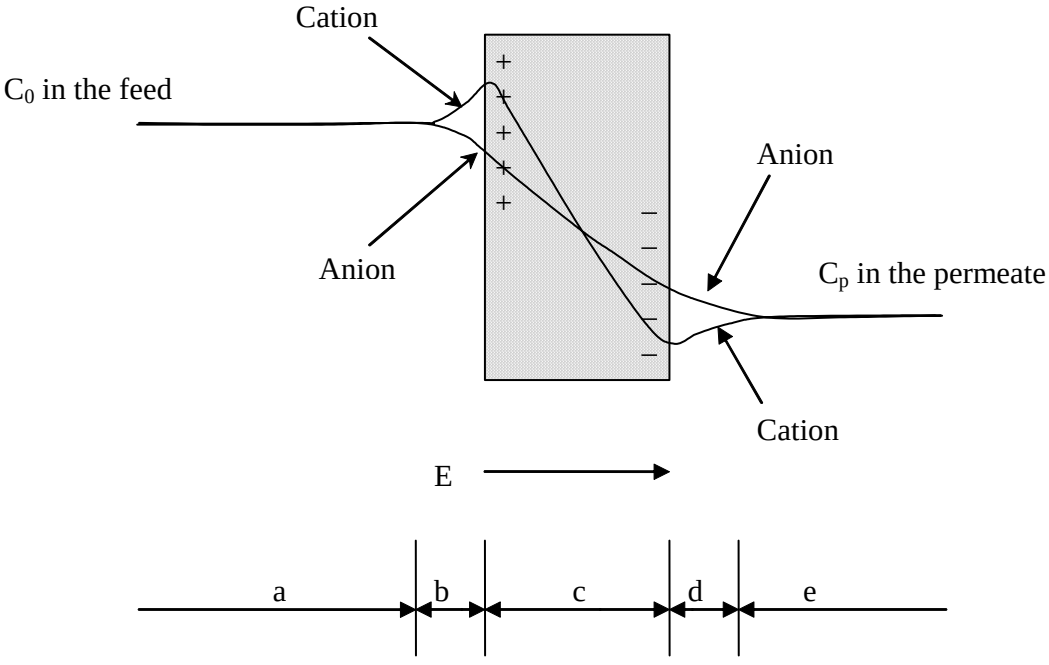

Figure 4.14 Illustrative scheme of ion transport through a membrane with zero fixed charge

4.4 Summary

Ion transport across RO membranes is a complex problem because of the involvement of the induced membrane charge or potential. A particular difficulty in the specification of the boundary conditions arises from the modification of the ion concentrations at the membrane surfaces by the induced membrane charge. Owing to the induced membrane charge, the ion concentrations on membrane surfaces are not fixed values but variables dependent on membrane charge. As *a priori* knowledge of the membrane charge at the steady state is usually not available, the ion concentrations on the membrane surfaces cannot be specified.

The unsteady state model for ion transport developed in this study can effectively overcome the difficulty in specifying boundary conditions. In this model, only initial value of the membrane charge that is *a priori* knowledge is required. The membrane charge or potential will be updated at every time step so that the boundary conditions can always be well defined. The ion concentrations in the solution with contact to the membrane surfaces are determined with Boltzmann-Poisson equation. Ion transport across the RO membrane at steady state can be obtained with the proposed model by running it for sufficient long time.

Numerical simulations with the unsteady state model were carried out in this study as demonstrations of applicability of this model. It can be concluded from the simulation study that the time scale for the transport to attain steady state is less than 1 min (for the conditions used in the simulations). Net electrical charge or potential develops in the initially uncharged membrane due to different mobility of the cations and anions. The induced membrane potential or the electrostatic force hinders the fast ions while

accelerates the slow ions to transport across the membrane. The ultimate state of the electrical charge built up or membrane potential acquirement is that the charges of cations and anions fluxes across the membrane are equal to each other. The acquirement of membrane charge or potential is actually a self-regulation mechanism to maintain electroneutrality in the bulk solutions on both sides of the membrane.

Chapter 5

MECHANISMS FOR ION TRANSPORT THROUGH RO MEMBRANES

The unsteady-state Nernst-Planck-Poisson model for ion transport through dense RO membrane has been presented in Chapter 4. The objective of this work was to investigate the mechanisms of ion transport through RO membranes by this newly developed model. It aimed to investigate (1) the electrostatic interaction between the membrane and ions and its influence on ion transport, (2) the mechanism of coupled transport by different ions, and (3) the effects of different parameters such as salt concentration, fixed membrane charge, diffusion coefficients, permeate flux, and electrolyte valences on the contribution of diffusion, electro-migration and convection to the ion flux.

In this chapter, transport mechanisms for ions in RO membranes were investigated in terms of diffusion, electro-migration and convection. The unsteady-state Nernst-Planck-Poisson model was briefly introduced first and the simulation results under different conditions were then presented. It is believed that the findings from this work would reveal the transport mechanisms at a deeper level and provide a better understanding for ion transport.

5.1 Coupled Transport Mechanisms

Ion flux through RO membranes can be adequately described by the extended Nernst-Planck equation:

$$J_i = -D_i \frac{dc_i}{dx} - \frac{D_i F}{RT} z_i c_i \frac{d\psi}{dx} + k_{i,c} J_v c_i \tag{5.1}$$

where J_i is ionic flux; D_i and $k_{i,c}$ are diffusivity and convective factor of species i respectively; c_i is ionic concentration in the membrane; F is the Faraday constant; R is the ideal gas constant; T is the absolute temperature; z_i is the valence of species i; ψ is the electric potential; and J_v is water flux. Eq. (5.1) shows that the total flux consists of three components of diffusion, electro-migration, and convection, driven by the gradients in concentration, electric potential, and pressure, respectively. The three individual fluxes can be calculated by Eqs. (5.2a), (5.2b) and (5.2c), respectively.

$$J_{d,i} = -D_i \frac{dc_i}{dx} \tag{5.2a}$$

$$J_{e,i} = -\frac{D_i F}{RT} z_i c_i \frac{d\psi}{dx} \tag{5.2b}$$

$$J_{c,i} = k_{i,c} J_v c_i \tag{5.2c}$$

where $J_{d,i}$, $J_{e,i}$, and $J_{c,i}$ stand for the flux due to diffusion, electro-migration and convection for species i, respectively.

The schematic diagram of concentration profile, electric field and representation of diffusive, electromigrative and convective fluxes is shown in Figure 5.1. This study is focused on the electrolyte solution with one cation and one anion. The limiting species is defined as the ion, which may have a smaller diffusion coefficient or may be repelled by the electrostatic forces from the membrane interfaces (i.e., the co-ion of the

membrane). In order to illustrate the coupled transport mechanism, it is assumed in Figure 5.1 that the anion has a higher mobility than the cation, so the cation in this case is the limiting species.

As shown in Figure 5.1, the concentration of the electrolyte solution in feed bulk C_f is higher than that in the permeate bulk solution C_p. Owing to the negative concentration gradient within the membrane from feed to permeate side, the diffusive fluxes for both ions are oriented towards the permeate side. The water transports from feed side to permeate side under the driving force of the pressure difference. As a result, the convective fluxes for both ions direct towards the permeate side. As expressed in Eq. (5.2b), the electromigrative flux is more complicated and its direction depends on the electric field within the membrane and the valence of the species. Firstly, due to the unbalanced ion transport resulted from the difference in the ion mobility, net electric charge is acquired across the membrane; secondly, an electric potential is then induced by the net charge: in this case, the anion is more mobile than the cation, causing an electric field (E) directing to the permeate side. The electromigrative flux for cation and anion is consequently oriented towards the permeate and the feed side, respectively. It is this induced electric field that couples the transport of two ions by exerting a negative electromigrative flux on the more mobile ion but a positive electromigrative flux on the less mobile ion. In other words, the limiting species is the ion having a positive contribution of electro-migration. The flux of two ions is thus regulated by the induced electric field and the non-electric-current condition is maintained at steady state within the membrane.

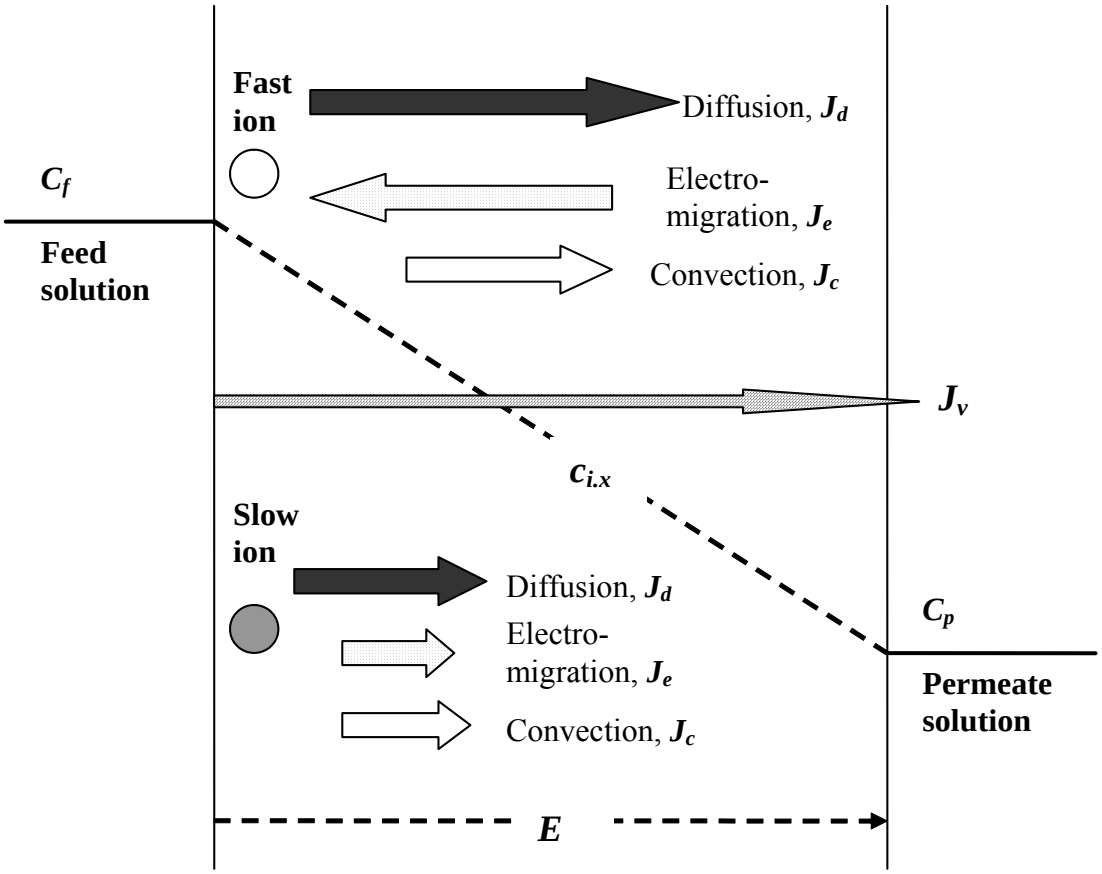

Figure 5.1 Schematic diagram of ionic flux due to diffusion, electro-migration and convection

5.2 Mathematical Model

The governing equation for the unsteady-state Nernst-Planck-Poisson model is the continuity equation:

$$\frac{dc_i}{dt} = D_i \frac{d^2 c_i}{dx^2} + \frac{D_i F}{RT} z_i \frac{d}{dx}\left(c_i \frac{d\psi}{dx} \right) - \frac{d}{dx}\left(k_{i,c} J_v c_i \right) \tag{5.3}$$

while the potential distribution on the membrane is related to the charge distribution by Poisson's equation:

$$\varepsilon_0 \varepsilon_m \frac{d^2 \psi}{dx^2} = -F\left(\sum z_i c_i + X \right) \tag{5.4}$$

with ε_0 the permittivity of free space (= 9×10^{-12} coul/volt-m), ε_m the dielectric constant of the membrane material, and X the (volumetric) fixed charge density in membrane.

The boundary conditions for Eq. (5.3) and (5.4) are formulated in Eqs. (5.5a-b) and (5.6a-b), respectively:

$$x = 0, \quad C_{i0} = C_{if} e^{-\frac{z_i F \Delta\psi_0}{RT}} \tag{5.5a}$$

$$x = L, \quad C_{iL} = C_{ip} e^{\frac{z_i F \Delta\psi_L}{RT}} \tag{5.5b}$$

with L the membrane thickness; C_{if} and C_{ip} the ion concentrations in the bulk solutions at the feed and permeate sides, respectively; $\Delta\psi_0$ the potential difference between the membrane-feed interface and the feed solution; and $\Delta\psi_L$ the potential difference between the membrane-permeate interface and the permeate solution.

$$x = 0, \quad \psi_0 = \frac{\lambda_f}{\varepsilon_0 \varepsilon_a} \int_0^t \left(\sum_i z_i F J_i \right)\Big|_{x=0} dt \tag{5.6a}$$

$$x = L, \quad \left.\frac{d\psi}{dx}\right|_L = \frac{1}{\varepsilon_0 \varepsilon_a} \int_0^t \left(\sum_i z_i F J_i \right)\Big|_{x-L} dt \tag{5.6b}$$

with ε_a the dielectric constant for solutions and λ_f the Debye length in feed solution.

Ion transport through RO membranes can be completely defined with the governing equations (5.3) and (5.4), and the boundary conditions specified by Eqs. (5.5) - (5.6). The model was solved in this study with the following initial condition for Eq. (5.3):

$$t = 0, \quad c_i(x) = C_{if} - \frac{x}{L}\left(C_{if} - C_{ip}\right) \tag{5.7}$$

There is also a non-electric-current requirement for the membrane:

$$\sum_i z_i J_i = 0 \tag{5.8}$$

as well as the steady-state restriction:

$$J_{i,x=0} = J_{i,x=L} \tag{5.9}$$

5.3 Numerical Calculations

The numerical procedure for the unsteady-state Nertnst-Planck-Poisson model was developed by Song *et al.* (2003). The non-steady state transport equation and Poisson equation were discretized into finite difference form using the Crank-Nicolson scheme and a central difference scheme. The resulting tridiagonal matrix was then solved by a specialized Gaussian Elimination technique known as the Thomas Algorithm. An iterative scheme was employed to decouple the difference equations for concentrations and membrane potential. At any time step, the iteration started with the potential at the previous time step as an initial guess. The ion concentration profiles were determined from the numerical solution of Eq. (5.3). With the ion concentration profiles, a new potential profile was subsequently obtained from the numerical solution of Eq. (5.4). Once the iteration converged, the concentration and potential at this time were determined and the calculation would go on to the next time step. The no-electric-current condition was used as the indicator for the steady state and the program would stop when the steady state was attained.

The concentration and potential profile at steady state could be obtained through the above procedure and the total flux (J_i), the flux due to diffusion ($J_{d,i}$), electro-migration ($J_{e,i}$) and convection ($J_{c,i}$) could be calculated by using Eqs. (5.1), (5.2a), (5.2b) and (5.2c), respectively; while the contributions of three fluxes to the overall ion flux were calculated by $J_{d,i}/J_i$, $J_{e,i}/J_i$, and $J_{c,i}/J_i$, respectively.

As discussed before, the Nernst-Planck-Poisson model provides a quantitative method for predicting process performance of ion transport through membranes. However, to solve the unsteady-state Nernst-Planck-Poisson model as described above, one needs to input feed salt concentrations as well as permeate concentrations. Since the concentration of permeate is usually unknown initially, in order to predict the solute rejection rate or permeate concentration by using the Nernst-Planck-Poisson model, the golden section search method was applied in this study. As shown in Figure 5.2, the optimal C_p value was searched in the interval (0, c_0) and the objective function was the absolute value of difference between the initial guessed C_p and the calculated C_p values. The idea is to divide the current bracketed line to three parts by the golden section ratio (i.e., 0.618 and 0.382). The two points here are X_1 and X_2 and then calculate which one's function value is smaller. New end points will be chosen so that the smaller value is between those points, i.e. the other endpoint is one of the previous endpoints (the one with the smaller value) and the other end point is a fraction distance 0.382 from the one with the greater value. The root of the objective function is then searched within the new interval until an optimal C_p value is reached.

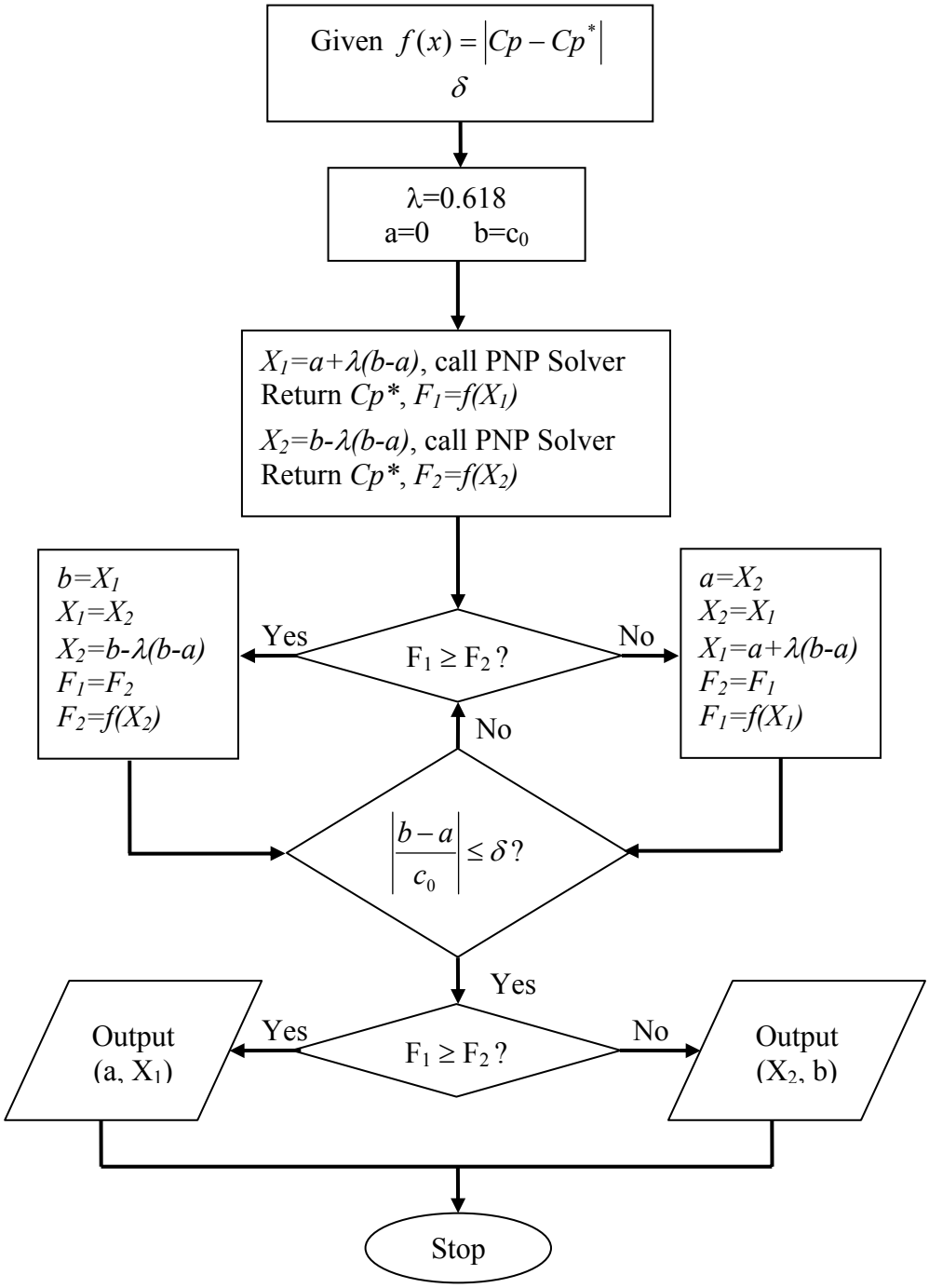

Figure 5.2 Flowchart of golden section approach to optimization of permeate concentration

5.4 Results and Discussions

Since a RO membrane can usually be regarded as a dense thin layer without pores in it, convective flow resulted from bulk water flux through the membrane is not a significant contributor to ion flux compared to diffusion and electro-migration. In this work, the relative importance to membrane transport was analyzed mainly for diffusion and electro-migration in Sections 5.4.1 and 5.4.2. The effect of convective flow on ion transport was discussed later in Section 5.4.3.

In a membrane system, there are generally two types of volumetric charges: the charge carried by the mobile ions moving in the membrane ($\sum_i Fz_i c_i$) and the charge fixed in membrane matrix, usually indicated with charge density X. The mobile ions contribute to the built up of electric field and, at the same time, the concentration of ions is affected by the electric field. The fixed membrane charge is not affected by electric field but determined by the properties of the membranes. Simulations of ion transport were carried out below for both membranes with and without fixed charge to investigate the electrostatic interactions between membrane and ions and the coupling between different ions.

5.4.1 Transport through membranes with no fixed charge

Initiating coupled transport of ions

The first case simulated was a symmetric electrolyte (1-1) with cation and anion having the identical diffusion coefficients ($D_+ = D_- = 5\times10^{-12}$ m^2/s). Simulation shows the cation and anion concentrations are identical through the membrane thickness and no net charge and electric field induced. The electromigrative flux is zero for both ions, so that diffusion is the only mechanism for ion transport in this case. The consequent

diffusive flux maintains constant across the membrane. As plotted in Figure 5.3, the diffusive flux of cation and anion equal to each other, and the value increases linearly with the feed salt concentration.

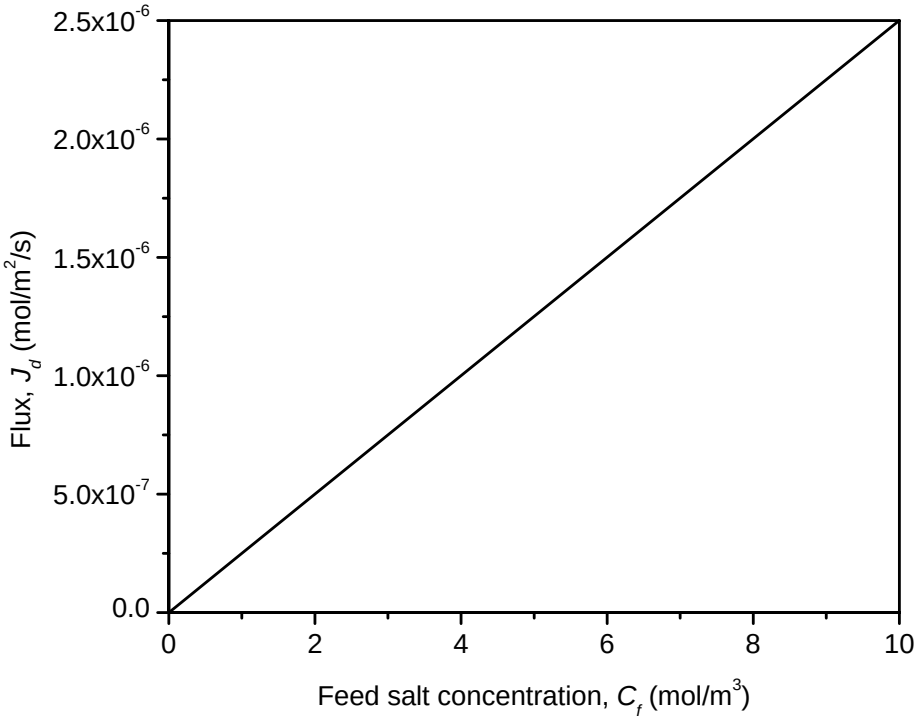

Figure 5.3 Ion flux versus feed salt concentration: X= 0, D_+= D_-= 5×10^{-12} m^2/s, J_v=5×10^{-7} m/s

The transport of ions with different diffusion coefficients were investigated next and resultant net charge density and electrical field strength were plotted in Figure 5.4. It can be seen from Figure 5.4 that two regions of net charge are developed in this case as a result of unbalance ions transport in the initial stage due to the difference in the ion nobilities (D_+ = 1× 10^{-12}m^2/s, D_-= 5×10^{-12} m^2/s). Positive charge is accumulated on the feed side of the membrane while the negative charge is accumulated on the permeate

side. Consequently, an electric field is developed toward the permeate side. Such an induced electric field will accelerate the transport of the less mobile cations by a positive contribution from electro-migration as well as slow down the transport of the more mobile anions with a negative electromigrative flux. As shown in Figure 5.5, both diffusion and electro-migration play important roles in the ion transport when the cations and anions have different mobility.

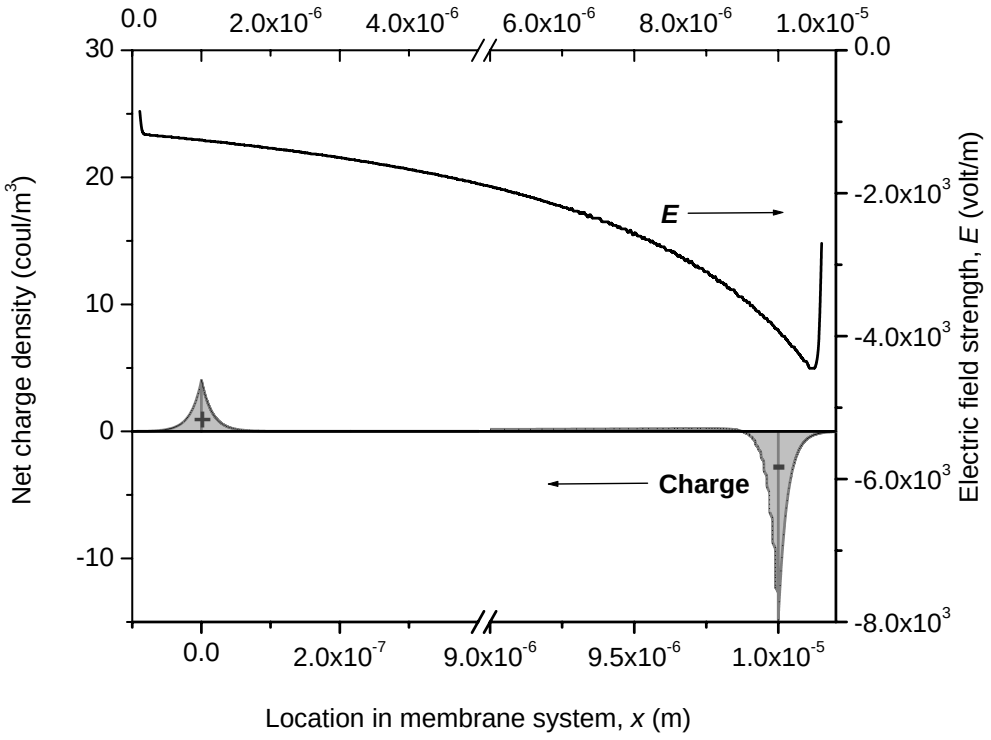

Figure 5.4 Profile of net charge density and electric field strength in the membrane system: X= 0, D_+ = 1× 10^{-12}m^2/s, D_- = 5×10^{-12} m^2/s, J_v= 5×10^{-7} m/s, C_f = 0.1 mol/m^3

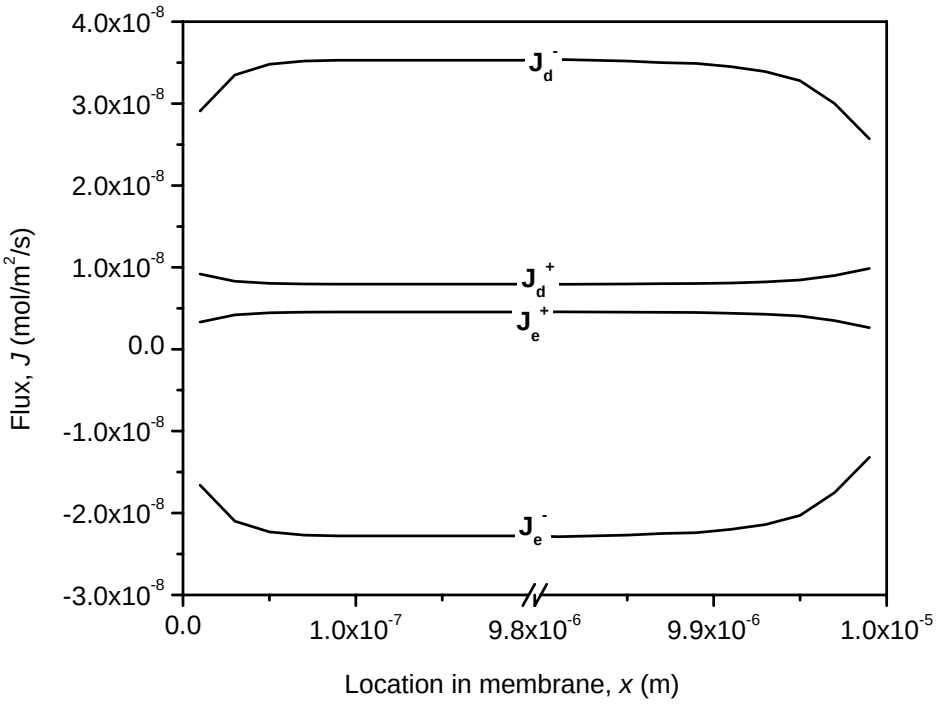

Figure 5.5 Ion flux profiles across the membrane: X= 0, D_+ = 1× 10^{-12}m^2/s, D_- = 5×10^{-12} m^2/s, J_v= 5×10^{-7} m/s, C_f = 0.1 mol/m^3

Moreover, both the diffusive and electromigrative fluxes are not constant, but changes within the membrane. At the feed side of the membrane, the net positive charge exerts an increase in value of concentration gradient for anions and a decrease in value for cations. This phenomenon leads to an increase in the diffusive flux for the anion but a decrease in diffusive flux for the cation. Meanwhile, the relatively steeper increase in electric field strength at the feed end causes an increase in values of electromigrative flux for both anions and cations. Analogically, diffusive and electromigrative fluxes have the opposite trends at the permeate side of the membrane. The fluxes level off when the local net charge within the membrane is eliminated and the increasing rate of electric field strength offsets the decreasing rate of ion concentration in the membrane.

Although the overall ionic flux is conservative along the membrane, the diffusive and electromigrative fluxes vary with the transmembrane coordinate. Hence, in later discussion, unless otherwise specified, the values of fluxes presented were the stable quantities occurred in the middle of the membrane (i.e., the values at $x = 5 \times 10^{-6}$ m).

Flux regulation between ions

Contribution of diffusive and electromigrative fluxes to ion flux under different ratios of ionic diffusion coefficients were simulated, the results of which are shown in Figure 5.6. When the cation has the same diffusion coefficient with the anion ($D_-/D_+ = 1.0$), diffusion contributes 100 % to the total flux while electro-migration contributes zero. When $D_-/D_+ > 1$, anions diffuse faster than cations, resulting in a higher diffusive flux of anion than that of cation. The limiting species in this case is the cation. The induced electric field acting as a "flux regulator" could make up the difference in diffusion fluxes. This phenomenon leads to a positive contribution of electromigrative flux for cation. Such a contribution would increase with the ratio of diffusion coefficients of two ions (D_-/D_+). As shown in Figure 5.6, as the ratio of D_-/D_+ increases, the diffusive contribution to total flux of cations decreases while the electromigrative contribution increases. When the ratio of D_-/D_+ is large enough, both contributions of diffusion and electromigration for the limiting species would become identical (i.e., 50 % of total ionic flux). Symmetrically, as shown in Figure 5.6, when $D_-/D_+ < 1$, the limiting species is anion and the induced electric field exerts a positive contribution on anion flux. Such a contribution would also increase with the difference between the diffusion coefficients of cations and anions.

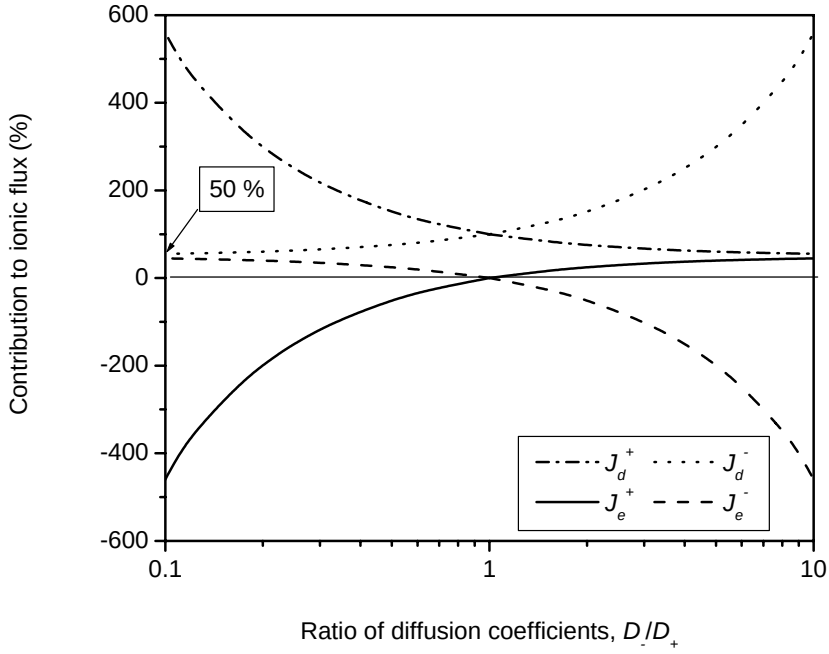

Figure 5.6 Contribution of diffusive and electromigrative fluxes to ionic fluxes versus ratio of diffusion coefficients D_-/D_+: X= 0, C_f = 0.1 mol/m^3

"Flux regulator" the induced electric field will manage the fluxes for two ions by means of electro-migration. It is the electromigrative flux that makes up the differences in diffusive fluxes between two ions. In the case of D_-/D_+ =10 (as shown in Figure 5.7), the diffusive flux for anion (~10J_d^+) is roughly 10 times that of cation (J_d^+). Although the two ions transport under the same induced electric field, their electromigrative fluxes do not take the same value with opposite signs (i.e., 4.5J_d^+). The anion has a larger value of electromigrative flux (~8.18J_d^+) while the cation has a smaller electromigrative flux (~0.82 J_d^+). By mathematical induction, when the ratio of two ionic diffusivities is N (D_-/D_+ =N), to offset the difference, the electromigrative flux for cations and anions is roughly $\left(\frac{N-1}{N+1}\right)$ of their respective diffusive flux. The

mathematical expressions for diffusive, electromigrative and total fluxes are summarized as follows:

$$J_d^- = NJ_d^+ \tag{5.10a}$$

$$J_e^+ = \frac{N-1}{N+1} J_d^+ \tag{5.10b}$$

$$J_e^- = N\frac{N-1}{N+1} J_d^+ \tag{5.10c}$$

$$J = J_d + J_e = \frac{2N}{N+1} J_d^+ \tag{5.10d}$$

When N$\rightarrow\infty$, $\left(\frac{N-1}{N+1}\right)\rightarrow 1$. It is therefore clear why both contributions of diffusion and electro-migration tend to become identical (i.e., reach 50 % as shown in Figure 5.6) when the ratio of diffusion coefficients increases. It can be indicated that for membrane with no fixed charge, diffusion is likely to be the primary mechanism for ion flux, while ion transport would be coupled and regulated by electro-migration due to the induced electric field by different ion diffusivities.

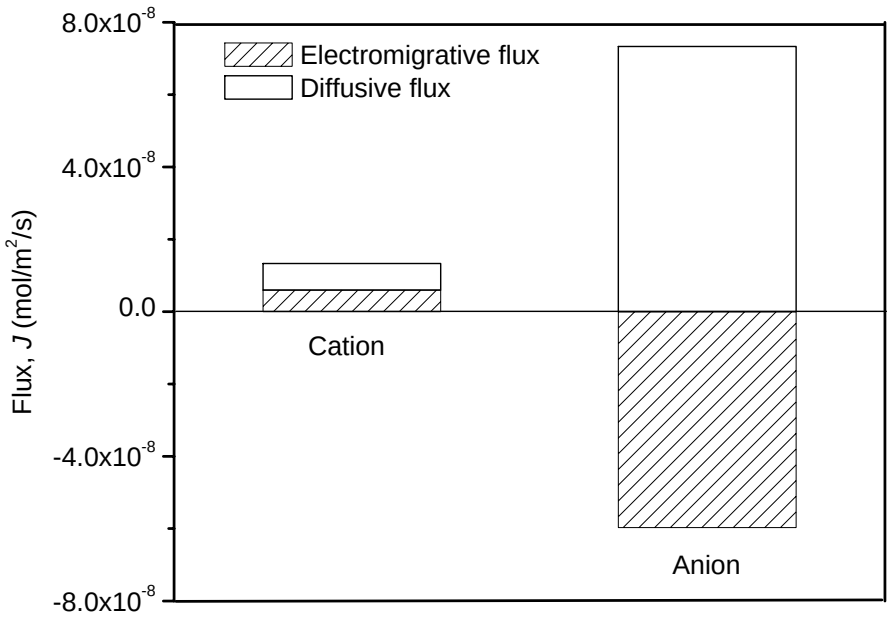

Figure 5.7 Diffusive and electromigrative fluxes for cation and anion: D_-/D_+ =10, X= 0, C_f = 0.1 mol/m^3, J_v= 5×10^{-7} m/s

Effect of feed concentration

Figure 5.8 shows the fluxes under different salt concentrations for uncharged membranes. The diffusive flux, electromigrative flux and total fluxes increase linearly with the feed salt concentration. Although electric field is induced due to the different ion mobility and ions are coupled with each other, the linearity between salt flux and concentration indicates that salt concentration has no effect on salt retention for the non-charged membranes.

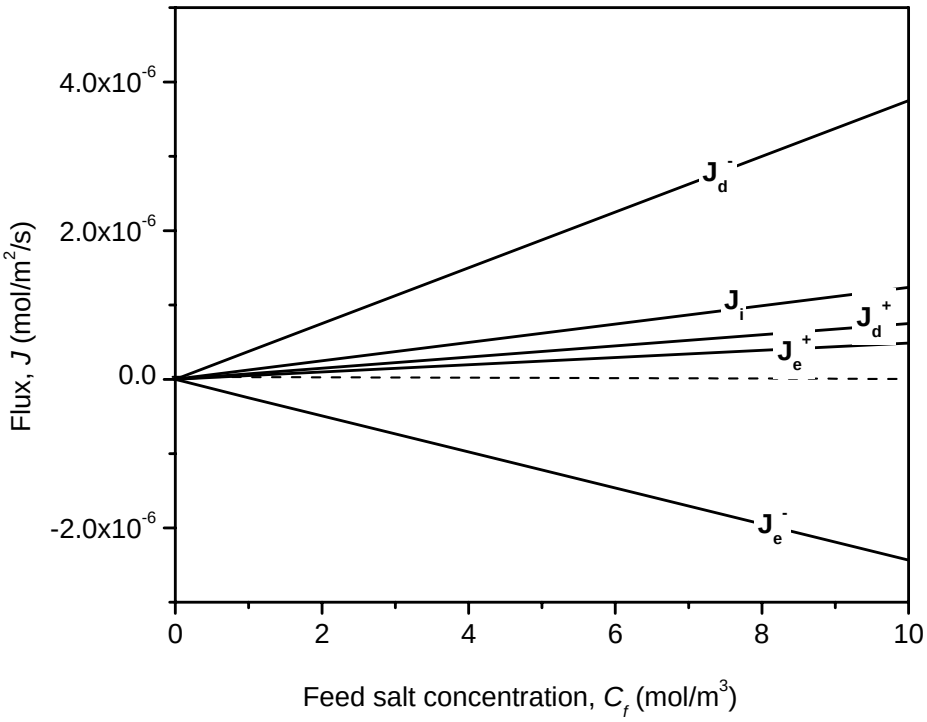

Figure 5.8 Ion flux versus feed salt concentration: X= 0, D_+ = 1× $10^{-12}$$m^2$/s, D_- = 5×10^{-12} m^2/s, J_v= 5×10^{-7} m/s

5.4.2 Transport through membranes with fixed charge

Effect of fixed membrane charge density

The fixed membrane charge is an important membrane property that affects strongly ion transport through the membrane. In order to investigate the effect of the fixed membrane charge, the transport of cations and anions in an electrolyte solution (1-1) with identical diffusivity through a negatively-charged membrane was first simulated. The negative fixed membrane charge attracts counter-ions (cations) and repels co-ions (anions) from the membrane surfaces. As a result, con-ions (anions) are the limiting ions in this case. The exclusion of co-ions from the membrane-solution interface by the fixed membrane charge causes a decrease in co-ion concentration within the membrane. The concentration profiles are shown in Figure 5.9. Unlike in the non-charged

membrane, the concentration of anions is much smaller than that of cations in the charged membrane. However, such a difference is roughly balanced by the fixed membrane charge *X*, which results in a zero net charge within the membrane, while imbalanced charges are developed at both side regions of the membrane. The electric field is induced not because of different ion diffusivities but the electrostatic interaction between membrane and ions via the fixed membrane charge.

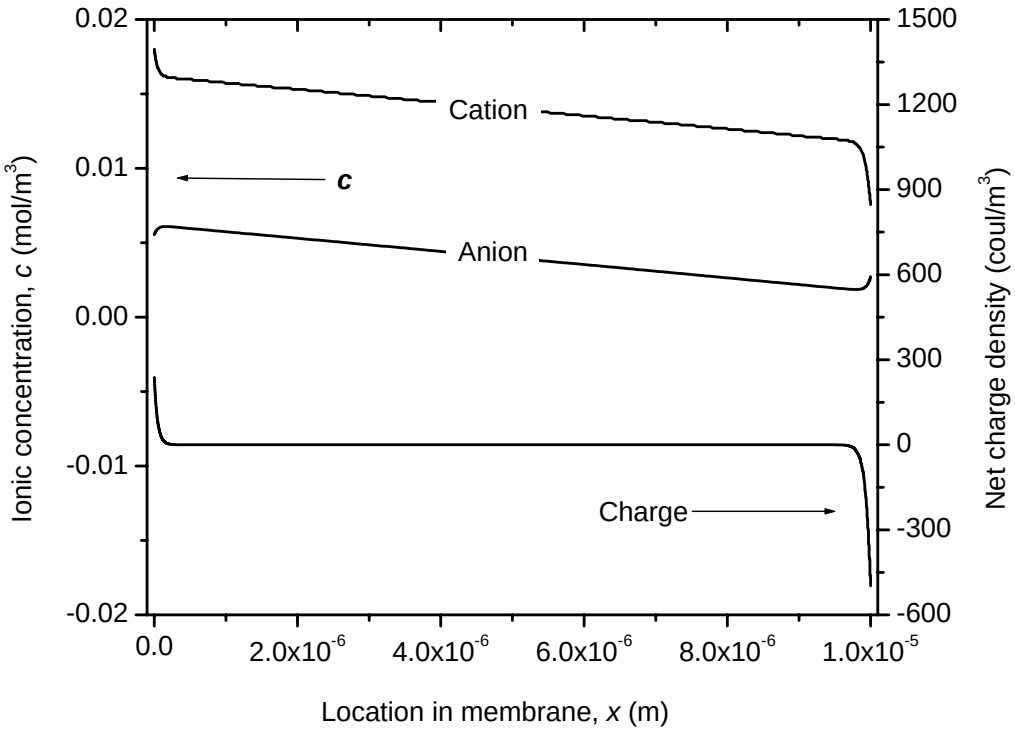

Figure 5.9 Concentration and charge profiles across the membrane: $D_+ = D_- = 5\times10^{-12}$ m^2/s, $X = -0.01$ mol/m^3, $C_f = 0.01$ mol/m^3, $J_v = 5\times10^{-7}$ m/s

Figure 5.10 shows the contributions of diffusion and electro-migration to ionic flux under different membrane charges. When the value of fixed membrane charge density ($|X|$) increases, more co-ions are repelled from the membrane surface, resulting in a lower concentration of anions but a higher concentration of cations in membrane. As

imbalanced net charges at both sides of the membrane increase, an electric field with higher potential gradient is therefore developed. In addition, the stronger electrostatic interaction between membrane and ions causes a higher cation concentration gradient but a lower anion concentration gradient across the membrane. Diffusive flux for cations increases while that for anions decreases, arousing a bigger difference between them. Such a difference is made up by the higher electromigrative flux resulted from the stronger induced electric field. Thus for anions, the increase in membrane charge ($|X|$) leads to an increase in contribution of electro-migration, but a decrease in contribution of diffusion to ion transport. It can be found in Figure 5.10 that unlike the uncharged membrane where diffusion always contributes more than half to ion transport, in charged membranes with a high charge density (X= -0.05 mol/m^3), the "regulation medium" electro-migration may contribute more than 50 % of ion flux.

The effect of salt concentration can be illustrated in Figure 5.10. When salt concentration increases, the contribution of diffusion decreases to a valley value and then increases with the feed salt concentration. In contrast, the contribution of electro-migration increases first to a peak value and then decreases with the concentration. As the electromigrative flux is a function of both electric field strength and the ion concentration in membrane (although the electric field strength could increase with the feed concentration), the counteraction of electric field on co-ions would cause a decrease in electromigrative flux due to the decrease in co-ion concentration in membrane. As a result, the electromigrative contribution increases with $|X|/C_f$, when $|X| << C_f$, but decreases when $|X| >> C_f$.

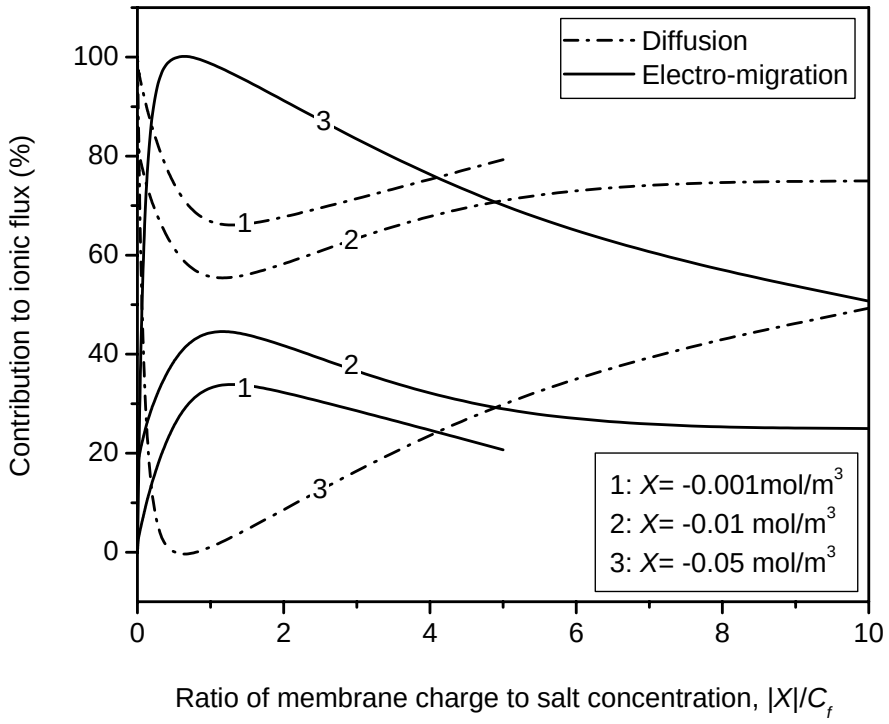

Figure 5.10 Contribution of diffusive and electromigrative flux versus ratio of membrane charge to feed salt concentration $|X|/C_f$: $D_+ = D_- = 5\times10^{-12}$ m^2/s, $J_v = 5\times10^{-7}$ m/s

Effect of diffusion coefficients and feed concentration

As discussed above, the electric field is induced due to the imbalanced transport of different ions in a transient period. The rate of ion transport is dependent on its diffusivity and the fixed membrane charge density. The limiting species are the ions with the lower diffusivity for the non-charged membrane; while for charged membrane, co-ions become the limiting ions if both ions having the same diffusivities. The transport of ions having different diffusivities through membrane with fixed charge as presented below is more complicated.

Figure 5.11 (a) shows the ion flux versus ratio of diffusion coefficients D_-/D_+. When cations and anions have the identical diffusivities (i.e., $D_-/D_+=1$), anions (co-ions) are the limiting species, resulting in a negative contribution of electro-migration to cation flux. When the anions have a greater diffusion coefficient than cations, the limiting species would be transferred from anions to cations with lower diffusivity. As illustrated in Figures 5.11 (a) and (b), there exits a critical value of ratio of diffusion coefficients termed as *transition ratio* $[D_-/D_+]_T$, where the electro-migration contributes zero for both ion transport. When diffusion coefficient ratio is smaller than transition ratio, the anions are the limiting ions, causing an electric field with direction pointing towards the feed side of membrane. However, when D_-/D_+ is higher than the transition ratio, the limiting species are the cations and the induced electric field is oriented to the permeate side. At the transition point, the induced electric fields from both charge sources of fixed membrane charge and different diffusivities counteract each other, reaching a nil electrical potential across the membrane. This point is also defined as isoelectric point. As can be seen in Figure 5.11 (b), contribution of diffusion decreases with the ratio of D_-/D_+; while contribution of electro-migration increases. The contributions of the two mechanisms involved in ion transport level off at high ratio of D_-/D_+, but would not reach an identical value as for the non-charged membrane (see Figure 5.6). It implies that even at a low membrane charge density (e.g., -0.01 mol/m^3), the electro-migration might predominate over the diffusion when co-ion has a sufficiently high diffusivity than counter-ion.

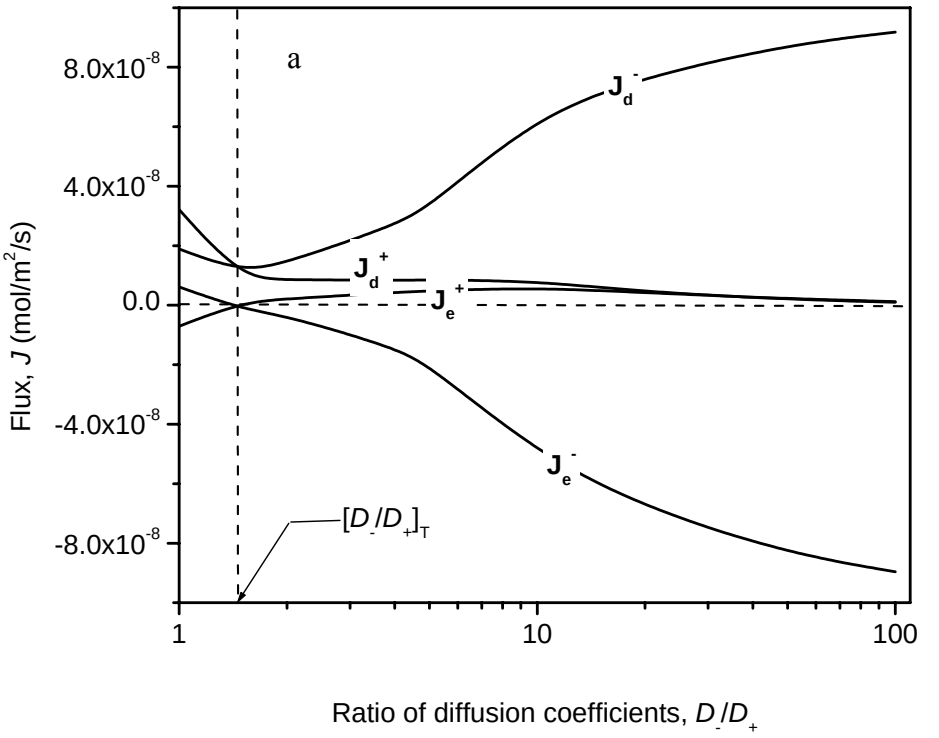

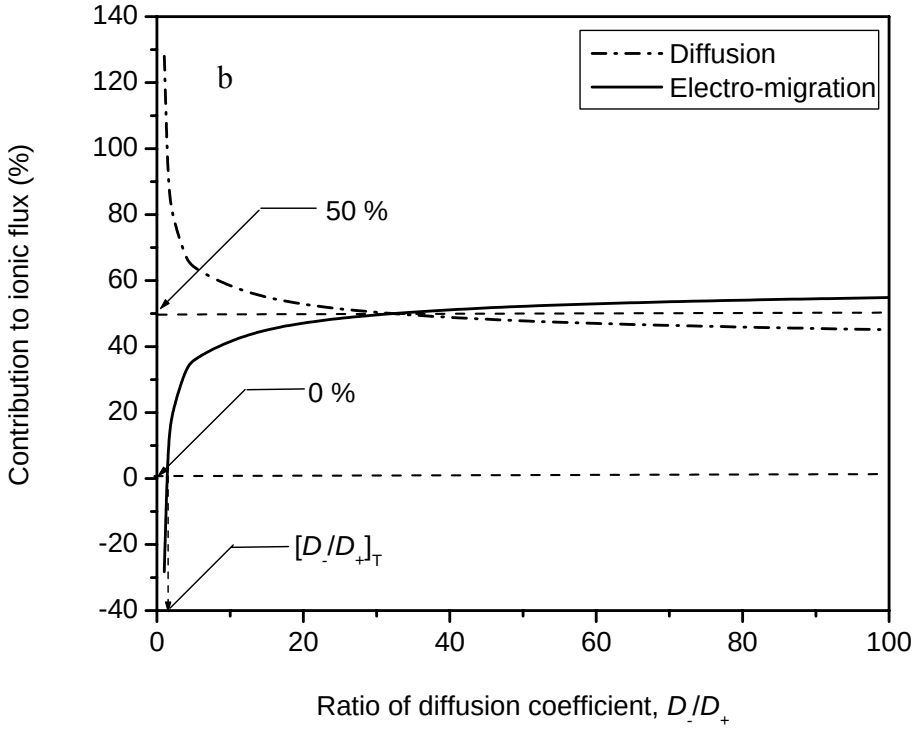

Figure 5.11 Effect of diffusion coefficient on (a) ion flux due to diffusion and electro-migration and (b) their contributions to ion flux: X= - 0.01 mol/m^3, C_f = 0.1 mol/m^3, J_v= 5×10^{-7} m/s

Figure 5.12 presents the contributions of diffusion and electro-migration to transport of an electrolyte with co-ion diffusion coefficient larger than that of counter-ion. It is noted that diffusion is the dominant mechanism involved in ion transport over the range of feed concentration investigated. In addition, contribution of electro-migration arises with the concentration and approaches a constant value at a high feed concentration. There is also a transition feed concentration $[C_f]_T$, which divides the concentration into two regions: (i) when $C_f<[C_f]_T$, the limiting species are anions; and (ii) when $C_f>[C_f]_T$, the limiting species are changed to cations. The induced electric fields in these two regions have opposite signs with a value of zero at isoelectric point $[C_f]_T$.

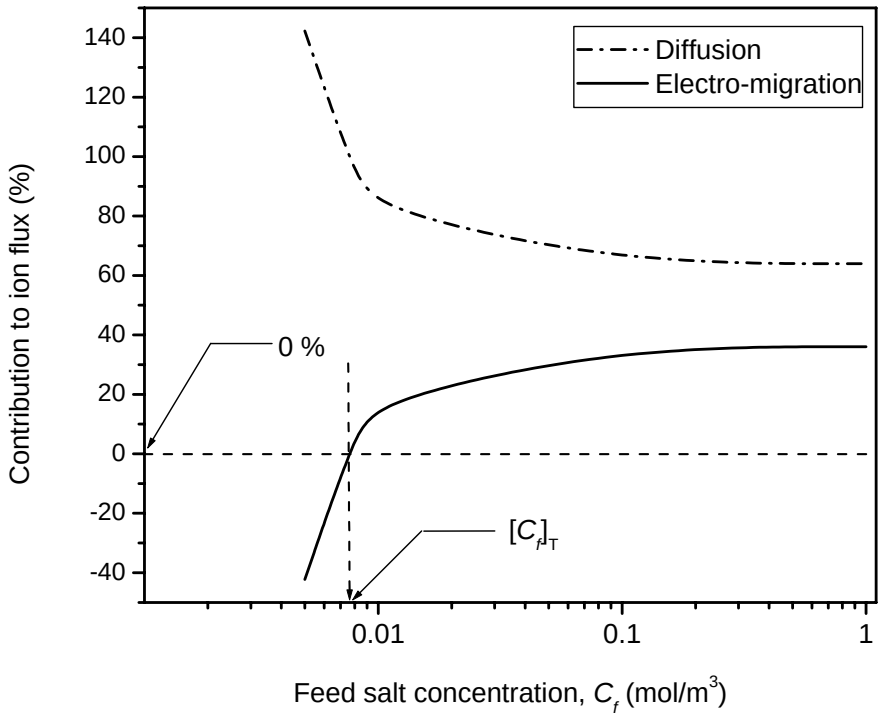

Figure 5.12 Contribution of diffusive and electromigrative flux versus feed salt concentration: X= - 0.01 mol/m^3, D_+ = 1× 10^{-12}m^2/s, D_- = 5×10^{-12} m^2/s, J_v= 5×10^{-7} m/s

Effect of valence

To investigate the influence of ion valence on ion transport, the simulations have been conducted for different electrolyte solutions with same salt concentration and identical ionic diffusivity. The higher valence in co-ions causes a more significant degree of exclusion of co-ion by the charged membrane that in turn leads to a bigger difference in diffusive fluxes between two ions and inducing a stronger electric field across the membrane. Consequently, as illustrated in Figure 5.13, for electrolytes 1-1, 1-2, and 1-3, the higher co-ion valence leads to a higher contribution of electro-migration, but a lower contribution due to diffusion. However, the increase in counter-ion valence has the reverse effect: it increases the co-ion concentration within the membrane and reduces the electric field strength. Compared to 1-1 electrolyte, 2-1 electrolyte has an even smaller contribution of electro-migration. Another group of electrolytes with multivalent cations and anions are also shown in this figure. Although electrolyte 2-4, 2-2 and 4-2 has the same ratio of valence ($|z_+|/|z_-|$) as electrolyte 1-2, 1-1 and 2-1, respectively, the same salt concentration lead to a higher charge density for the former, which results in a higher electric field and a higher electromigrative contribution.

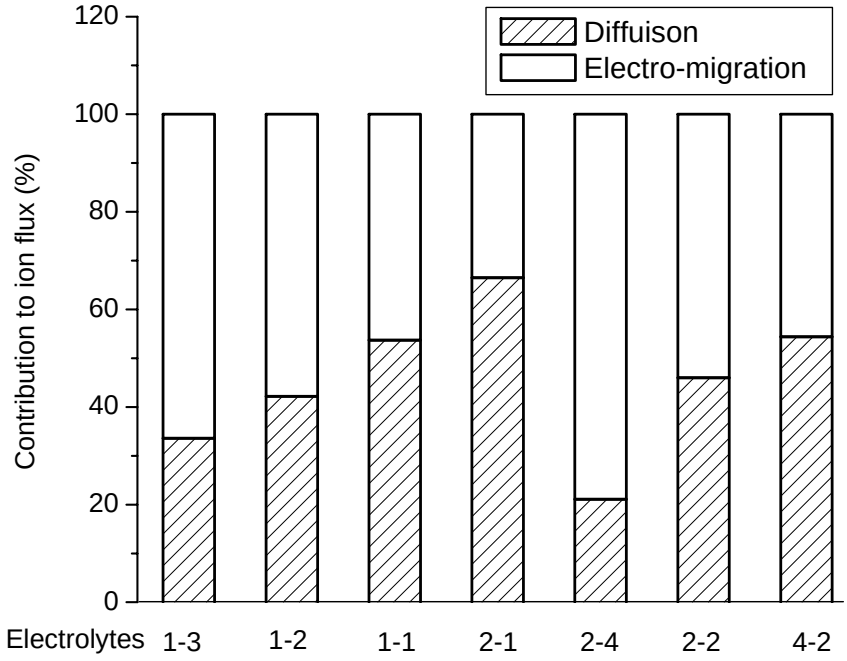

Figure 5.13 Contribution of diffusive and electromigrative flux for electrolyte solutions with different valences: X= - 0.01 mol/m^3, D_+= D_-= 5×10^{-12} m^2/s, C_f = 0.01 mol/m^3, J_v= 5×10^{-7} m/s

5.4.3 Contribution of convective flow

Effect of convective factor

Convective mechanism is associated with the transport of electrolyte by the water flux through the membranes. Some former research showed that convection has a dominant effect on solvent transport and might be a major contribution to solute transport (Meares 1976; Jonsson 1980; Soltanieh and Gill 1981). Convection is always considered as the consequence of micropores within the membranes. However, RO membrane usually has no pores and the convective ion flux is related to water flux by the convective factor k_c, which is defined as the ratio of ion flux by convective mechanism (J_c) to the total ion flux associated with the permeate flux (cJ_v).

Figure 5.14 (a) presents the influence of convective factor on diffusive, electromigrative, convective, and total ionic flux. An increase in convective factor leads to an increase in both convective and total ionic flux, but a decrease in diffusive and electromigrative flux. When there are defected pores in membranes, salt passage will increase, causing a lower salt retention. Hence, the increase in convective factor leads to an increase in ion concentration in the membrane, but a decrease in concentration gradient. The decrease in diffusive fluxes for both ions reduces their difference, while the difference of convective fluxes between two ions remains invariant. The imbalanced charge is then reduced, resulting in less work for electro-migration. In other words, convection can reduce the imbalanced ion transport by sacrificing the salt retention efficiency. It can even reverse the transport rates of two ions. When convective factor is small, the limiting species is the cation, the electromigrative flux of which is positive. The anion will become the limiting species at a sufficiently high convective factor, where a negative electromigrative flux is obtained for cation. Induced electric field thus changes its sign at high convective factors where contribution from electro-migration for cation approaches the negative value.

As illustrated in Figure 5.14 (b), when convective factor increases, the contribution of convection increases, but both contributions of diffusion and electro-migration decrease. There are three regions over the k_c ranging from 0 to 1.0:

(1) $k_c < [k_c]_{T1}$ J_d contribution > J_e contribution > J_c contribution;

(2) $[k_c]_{T1} < k_c < [k_c]_{T2}$ J_d contribution > J_c contribution > J_e contribution; and

(3) $[k_c]_{T2} < k_c$ J_c contribution > J_d contribution > J_e contribution.

Calculation for porous RO/NF membranes by Donnan models normally showed that the convection appeared to be the dominant mechanism, which is only considered the cases in 3rd region, with a k_c value higher than 0.9 (Bowen and Mukhtar 1996; Peeters *et al.* 1998; Bowen and Mohammad 1998; Fievet *et al.* 2002; Szymczyk *et al.* 2003).

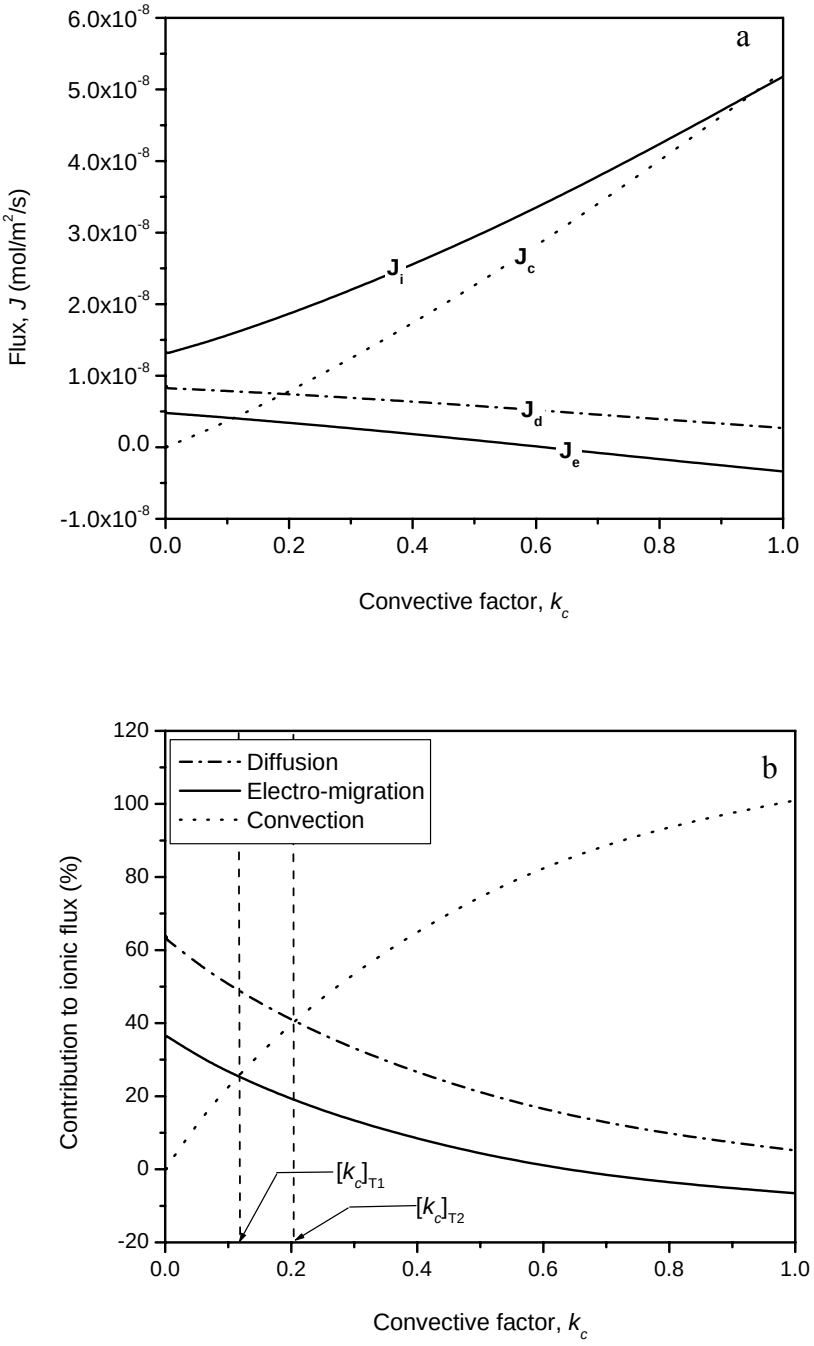

Figure 5.14 Effect of convective factor on (a) diffusive, electromigrative and convective fluxes and (b) their contribution to ion flux: X= - 0.01 mol/m^3, D_+ = 1× 10^{-12}m^2/s, D$_-$ = 5×10^{-12} m^2/s, C_f = 0.1 mol/m^3, J_v= 5×10^{-7} m/s

Effect of water flux

Convective ion flux is proportional to the product of concentration and water flux. As presented in Figure 5.15 (a), the convective flux increases linearly with water flux, while the diffusive flux keeps almost constant. The dilution effect of water flux will reduce the permeate concentration and increase the salt retention. On the other hand, the convective salt passage will also increase with the water flux. As water flux increases, the electromigrative flux increases till a peak value and then decreases, its contribution to ion flux follows the same trend as shown in Figure 5.15 (b). It can also be seen from Figure 5.15 (b) that the diffusion mechanism dominates the ion transport, but its contribution decreases with water flux, while the contribution of convection increases.

Effect of salt concentration

Figure 5.16 illustrates the effect of feed salt concentration on contributions of diffusion, convection and electro-migration. It is found from Figure 5.16 that feed salt concentration plays an important role for ion transport based on the mechanism of diffusion and electro-migration, but has no significant effect on convection. Over the feed concentration range being investigated, diffusion is likely to be the major mechanism involved in ion transport, which is regulated by the electro-migration of ions via the induced electric field. At a low feed concentration, the anions are limiting species with an electric field directing toward the feed side. When concentration increases, the induced electric field changes its direction and cations become the limiting ions, having a positive contribution from electro-migration. The contribution of diffusion decreases with feed salt concentration, while the contribution of electro-

migration increases. This change is within so narrow a range of concentration that both contributions become constant at whatever feed concentration.

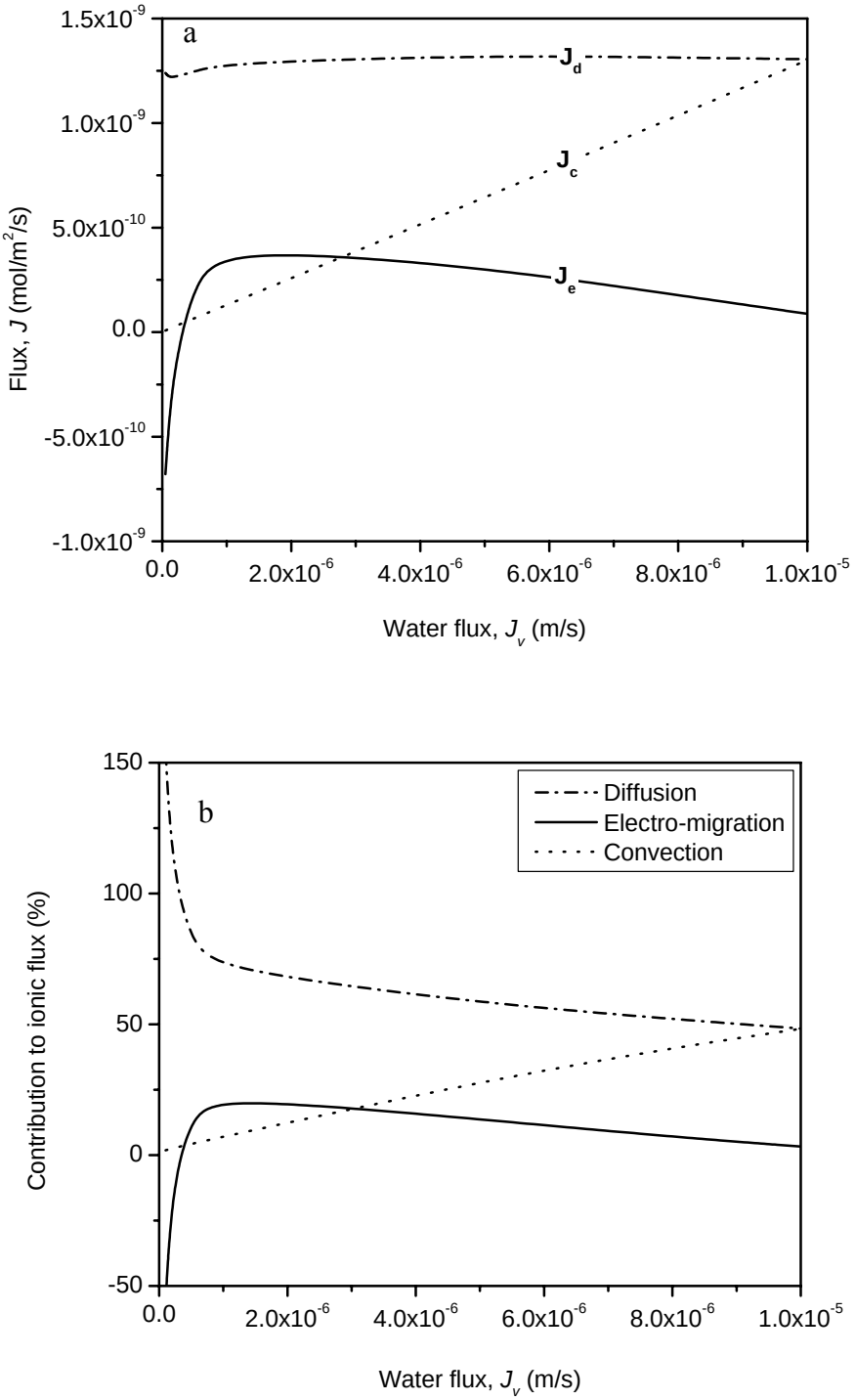

Figure 5.15 Effect of water flux on (a) diffusive, electromigrative and convective fluxes and (b) their contribution to ion flux: X= - 0.01 mol/m^3, D_+ = 1× 10^{-12}m^2/s, D$_-$ = 5×10^{-12} m^2/s, C_f = 0.01 mol/m^3, k_c= 0.01

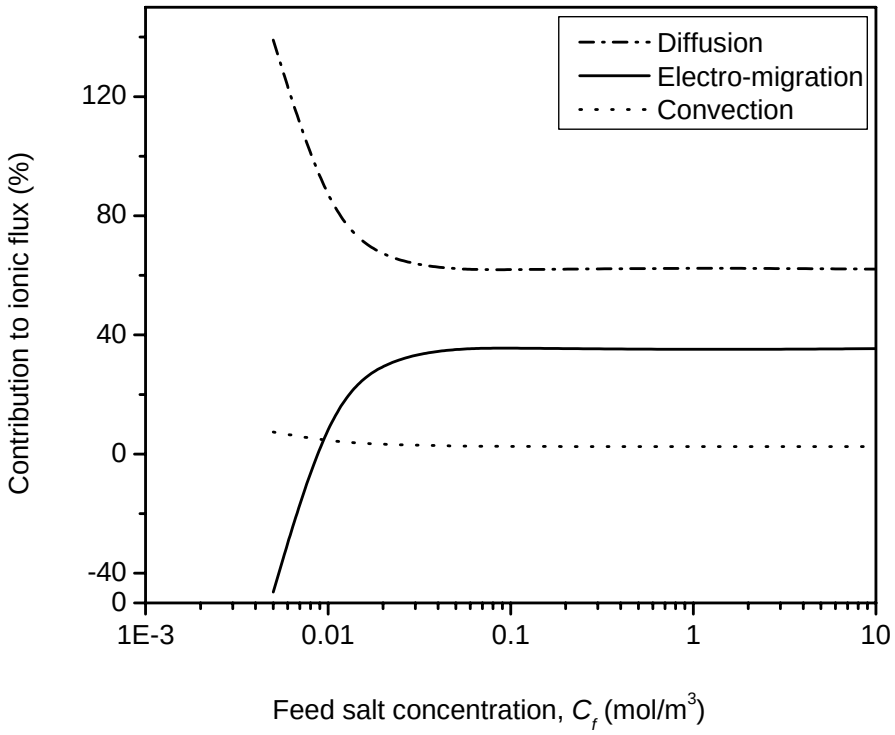

Figure 5.16 Effect of feed salt concentration on contribution of diffusion, electro-migration and convection to ion flux: X= - 0.01 mol/m^3, D_+ = 1× 10^{-12}m^2/s, D$_-$ = 5×10^{-12} m^2/s, C_f = 1.0 mol/m^3, k_c= 0.01

5.5 Summary

Transport mechanisms for ions in RO membranes have been investigated in terms of diffusion, electro-migration and convection with simulations for various situations. The model used is the unsteady-state extended Nernst-Planck equation coupled with Poisson equation with dynamic boundary conditions at both membrane-solution interfaces. The effects of membrane charge density, feed salt concentration, water flux, and diffusion coefficients on the diffusive, electromigrative, and convective components of ion flux have been presented.

It can be concluded from this study that, except for the case of symmetric electrolyte (1-1) with identical anion and cation diffusivity through non-charged membrane, the electrostatic interactions play a paramount important role in balancing the transport of different ions through membranes. The ions of low mobility or diffusivity are the limiting species in ion transport. An electric field acting as "the flux regulator" is induced due to the imbalanced transport of different ions in the transient period, which is dependent on ion diffusivity and the fixed membrane charge density. The electro-migration of the ions under the induced electric field complements the diffusive fluxes to form a balanced transport of different ions across the membrane.

For membranes without fixed charge, the electric field is induced by the difference in ion diffusivities. Diffusion is likely to be the primary mechanism in ion transport and the different transport rate of cations and anions in an initial period is the main reason for the accumulation of net charge across the membrane, which gives the rise of electrical field. The electro-migration under the induced electric field makes up the difference in diffusive fluxes. The increase in water flux increases the driving force for both diffusion and electro-migration while feed salt concentration has no effect on salt retention for the non-charged membranes.

For membrane with fixed charge, the increase in fixed membrane charge density and co-ion valence will increase the electrostatic interactions between membrane and ions. Electro-migration appears to be the more important mechanism at a high membrane charge density. Even for membrane with a small charge density, the contribution of electro-migration might contribute more than 50% of the total ion flux when co-ion diffusion coefficient is much higher than that of counter-ion.

Ion transport might be governed by convection mechanism when the coefficient factor or water flux is high enough. However, both conditions are not realistic for RO membranes. The feed salt concentration has no significant effect on convection, although it changes diffusion and electro-migration a lot.

Chapter 6

ION PERMEATION AND SELECTIVITY IN MULTI-ELECTROLYTE SOLUTION

Transport of ions in multi-electrolyte solutions across a charged membrane is of practical significance in water purification, trace metal removal and biological membrane processes. Rejection of solutes in multi-component systems by RO membranes has been addressed by several investigators using a variety of theoretical approaches (Sourirajan 1970). Several transport models of RO membranes have been proposed and the effect of feed concentration, membrane charge density and water flux on the rejection of solutes in multi-component solutions has been studied (Higa *et al.* 1990; Tsuru *et al.* 1991a; Dey *et al.* 2000; Ong *et al.* 2002). The general observation suggests a marked change in ionic rejection in the presence of a third ion: the ion with a higher permeability becomes even more permeable; while the rejection of less permeable ion increases. Ion transport against its concentration gradient is also observed. Such an uphill transport phenomenon has been investigated by many researchers (Tsuru *et al.* 1991c; Peeters *et al.* 1998; Ong *et al.* 2002).

Discussions in Chapter 5 show that the transport of two ions in membrane is coupled due to the induced electric field. It is believed that the addition of the second solute

might change the electric field induced. In this chapter, ion permeation behaviors and its selectivity were investigated theoretically by using the unsteady Nernst-Planck-Poisson model proposed in Chapter 4. Ion retention behaviors in multi-electrolyte solutions were first compared with those in single electrolyte solutions. The ionic flux in the multi-electrolyte solutions of 1-1 and 1-2 electrolytes was then investigated under different conditions. Analytical method was finally developed to estimate the effects of operating parameters on the transport behaviors. The ultimate objective of this work was to describe the ionic transport behaviors in multi-electrolyte solutions and to understand the mechanisms behind.

6.1 Method

The theory of the unsteady state Nernst-Planck-Poisson model has been presented in Chapter 4. The main equations used for this model are summarized in Table 6.1. The multi-component solutions made of two salts with same cation (CA and C_2B) were used for the model solution for the study of ion transport. Unless specifically indicated, the parameters used in the simulation take the values summarized in Table 6.2.

Table 6.1 Equations for Unsteady-state Nernst-Planck-Poisson Model

$$J_i = -D_i \frac{dc_i}{dx} - \frac{D_i F}{RT} z_i c_i \frac{d\psi}{dx} + k_{i,c} J_v c_i \tag{6.1}$$

$$\frac{dc_i}{dt} = D_i \frac{d^2 c_i}{dx^2} + \frac{D_i F}{RT} z_i \frac{d}{dx}\left(c_i \frac{d\psi}{dx} \right) - \frac{d}{dx}\left(k_{i,c} J_v c_i \right) \tag{6.2}$$

$$\varepsilon_0 \varepsilon_m \frac{d^2 \psi}{dx^2} = -F\left(\sum z_i c_i + X \right) \tag{6.3}$$

$$x = 0, \quad C_{i0} = C_{if} e^{-\frac{z_i F \Delta\psi_0}{RT}} \text{ and } x = L, \quad C_{iL} = C_{ip} e^{\frac{z_i F \Delta\psi_L}{RT}} \tag{6.4}$$

$$x = 0, \quad \psi_0 = -\frac{Q_0 \lambda_f}{\varepsilon_0 \varepsilon_a} \text{ and } x = L, \quad \left.\frac{d\psi}{dx}\right|_L = \frac{Q_L}{\varepsilon_0 \varepsilon_a} \tag{6.5}$$

$$\lambda = \sqrt{\frac{\varepsilon_a \varepsilon_0 RT}{F^2 \sum_i z_i^2 C\ (i)}} \tag{6.6}$$

$$t = 0, \quad c_i(x) = C_{if} - \frac{x}{L}\left(C_{if} - C_{ip} \right) \tag{6.7}$$

$$J_{i,x=0} = J_{i,x=L} \tag{6.8}$$

$$\sum_i z_i J_i = 0 \tag{6.9}$$

$$Q_0 + Q_m + Q_L = 0 \tag{6.10}$$

$$Q_0 = -\int_0^t \left(\sum_i z_i F J_i \right)\Bigg|_{x=0} dt \tag{6.10a}$$

$$Q_L = \int_0^t \left(\sum_i z_i F J_i \right)\Bigg|_{x=L} dt \tag{6.10b}$$

$$Q_m = \int_0^t \left(\sum_i z_i F J_i \right)\Bigg|_{x=0} dt - \int_0^t \left(\sum_i z_i F J_i \right)\Bigg|_{x=L} dt \tag{6.10c}$$

Table 6.2 Parameters used in simulation studies

Ionic type	Cation, C	Anion, A	Anion, B
Charge, z	+1	-1	-2
Diffusivity, $D_i \times 10^{12}$ (m^2s^{-1})	2.0	5.0	0.5
Coefficient for convection, k_c	0	0	0
Membrane thickness, L (m)		1×10^{-5}	
Dielectric constant of membrane, ε_m		20	
Dielectric constant of solutions, ε_a		80	

6.2 Ionic Transport Behaviors in Multi-electrolyte Solutions

The solute rejection behaviors in both single and multiple electrolyte solutions are illustrated in Figure 6.1. In single electrolyte solutions, the solute rejection increases with the water flux due to the dilution effects. As shown in Figure 6.1, the dotted lines represent the single electrolyte solutions, where C_2B has a higher rejection rate than that of CA, since A^- ion is more permeable than B^{2-} ion. However when in solutions containing both CA and C_2B, the rejection of B^{2-} increases while that of A^- decreases. The mono-valent A^- becomes more permeable than in its single solutions while the divalent B^{2-} becomes even more retainable than in its single solutions.

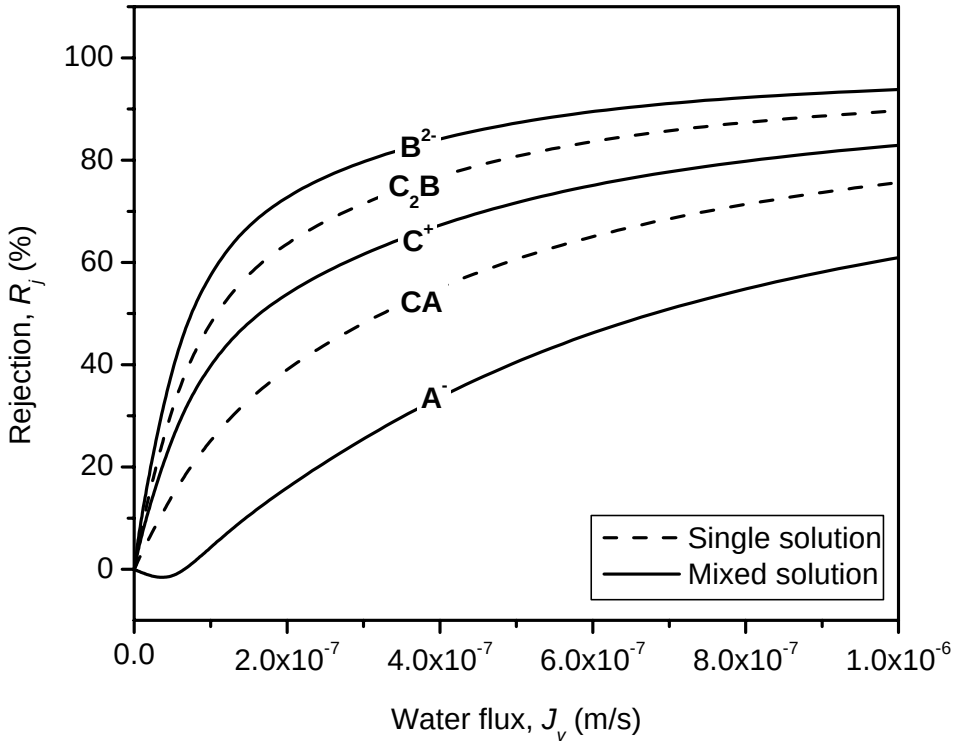

Figure 6.1 Solute rejection in single solutions: 0.3 mol/m^3 CA, 0.15 mol/m^3 C_2B and mixed solution: 0.1 mol/m^3 CA + 0.1 mol/m^3 C_2B

The more permeable ions (A^-) would become even more permeable with the addition of less permeable ions (B^{2-}); while the less permeable ions (B^{2-}) would become even less permeable with the addition of more permeable ions (A^-). The results of Figure 6.1 indicate a feasible way to increase the rejection of B^{2-} by adding a more permeable ion such as A^- into its solution. Anions with different diffusion coefficients become more selective and are ready to be separated in multi-electrolyte solutions with the same cations. It can also be seen from Figure 6.1 that negative rejection is obtained for the more permeable A^- in mixed solution under a low water flux. The negative rejection means the ion transport against its concentration gradient, resulting in a higher permeate concentration of A^- than its feed concentration.

Ion transport behaviors and mechanisms have been discussed in Chapter 5. The elevated selectivity in multi-electrolyte solution can also be explained by the electrostatic forces in induced electric field. In single CA solutions, because A^- has a higher diffusivity than C^+, A^- ions would accumulate at the membrane surface of permeate side while C^+ would accumulate at the feed side, which causes a net charge profile as illustrated in Figure 6.2 (a). The induced electric field would then accelerate the limiting species C^+ but retard the transport of A^-. Similarly, in single C_2B solutions as shown in Figure 6.2 (b), the more mobile cation C^+ accumulate at the permeate side while the less mobile anion B^{2-} accumulate at the feed side. B^{2-} becomes the limiting species, where the induced electric field would accelerate its transport.

When in a solution of both CA and C_2B, things become more complicated. In such a case, the most and least mobile ion is A^- and B^{2-}, respectively, both of which are anions. The A^- ions diffuse faster than C^+ and negative charges accumulate at the permeate side of the membrane while positive charges accumulate at the feed side. On the contrary, compared with C^+ ion, B^{2-} ion is less mobile, so negative charges will accumulate on the feed side while positive charges will accumulate at the permeate side. In the mixed CA/C_2B solutions, both accumulated charges and induced electric fields will counter-act with each other. As shown in Figure 6.3, in mixed CA/C_2B solution, the imbalanced charges profile is similar to that of C_2B, but mixed solution has a less charge density than single solutions. An electric field is then induced with the direction towards the permeate side.

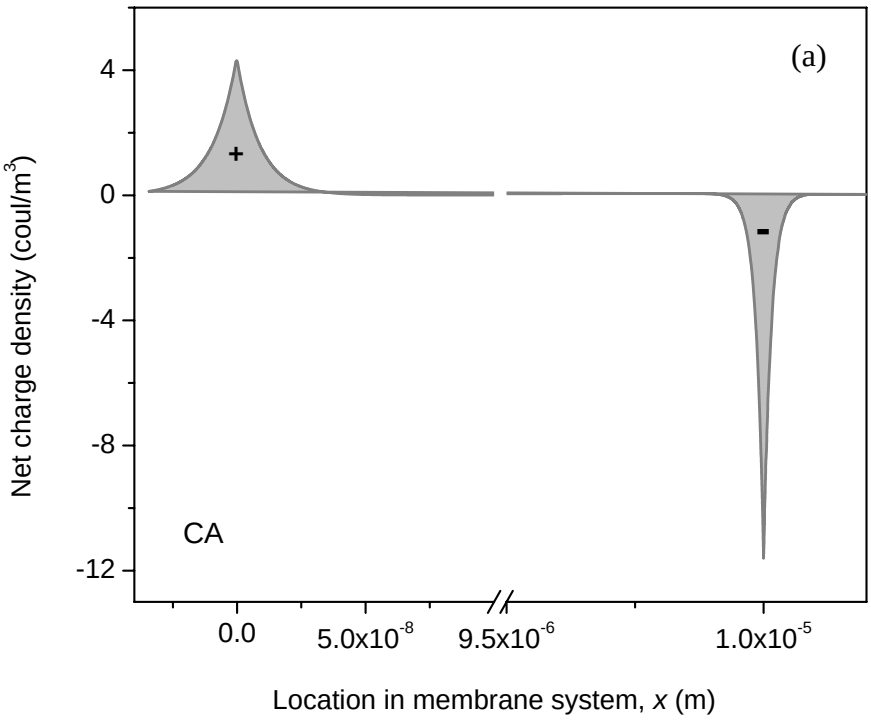

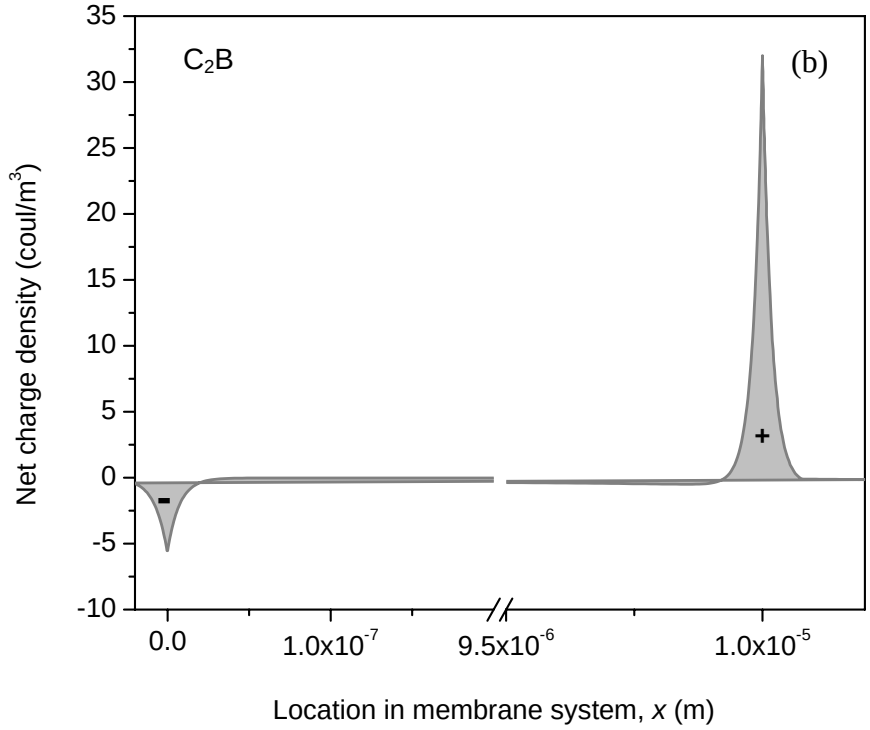

Figure 6.2 Net charge density across the membranes in (a) 0.3 mol/m^3 CA and (b) 0.15 mol/m^3 C_2B solutions: J_v= 5×10^{-7} m/s

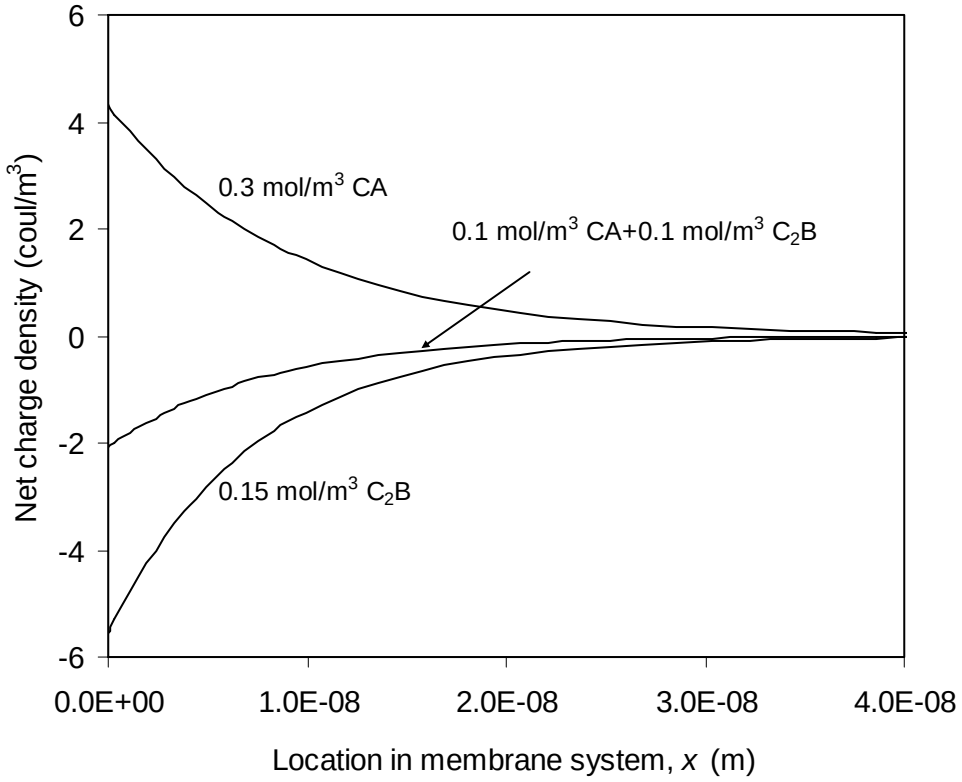

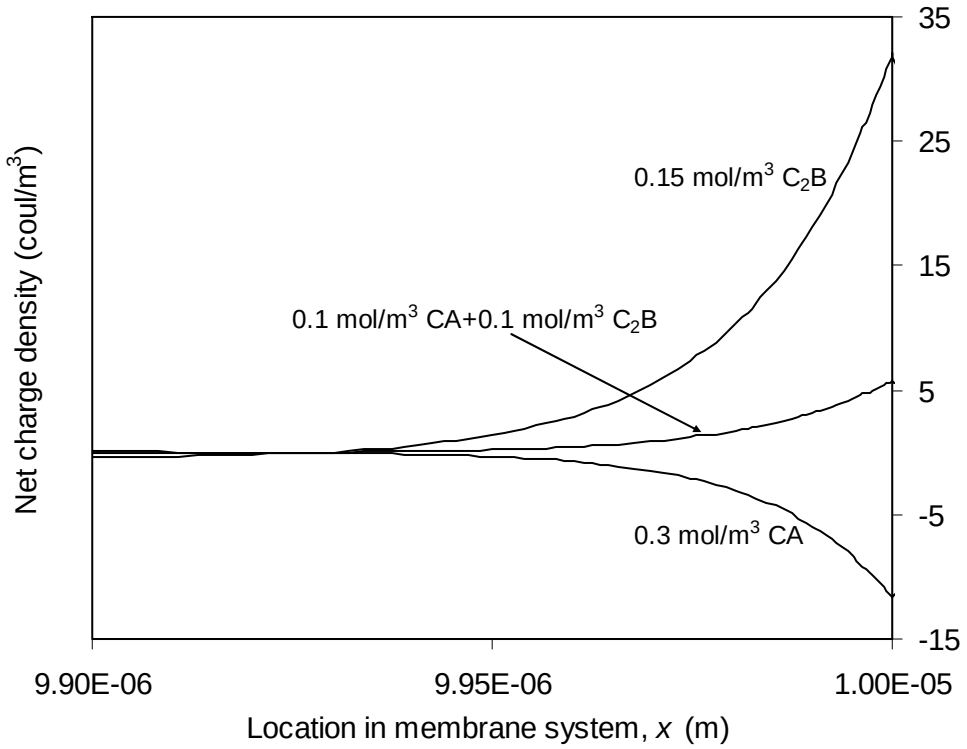

Figure 6.3 Comparison of net charge across the membrane between single and mixed solutions

The induced electric potential profiles in both single and multi-electrolyte solutions are illustrated in Figure 6.4. Owing to the imbalanced charges as shown in Figure 6.3, the corresponding electric potential decreases across the membrane for single CA solutions, but increases for both single C_2B and mixed CA/C_2B solutions. As the "flux regulator", electric field in C_2B solutions accelerates the transport of B^{2-} ions. Compared with C_2B single solution, the mixed solution has a lower electric potential. It indicates that the addition of A^- ion in C_2B solutions would reduce the electric field strength, resulting in a lower accelerating rate of transport of B^{2-}. Meanwhile, the electric field changes direction in CA solution with the addition of B^{2-} ions. Transport of A^- is thus accelerated in the mixed solutions. Hence B^{2-} is retained more while A^- is penetrated more in the mixed solutions by the membrane due to the change in the induced electric field.

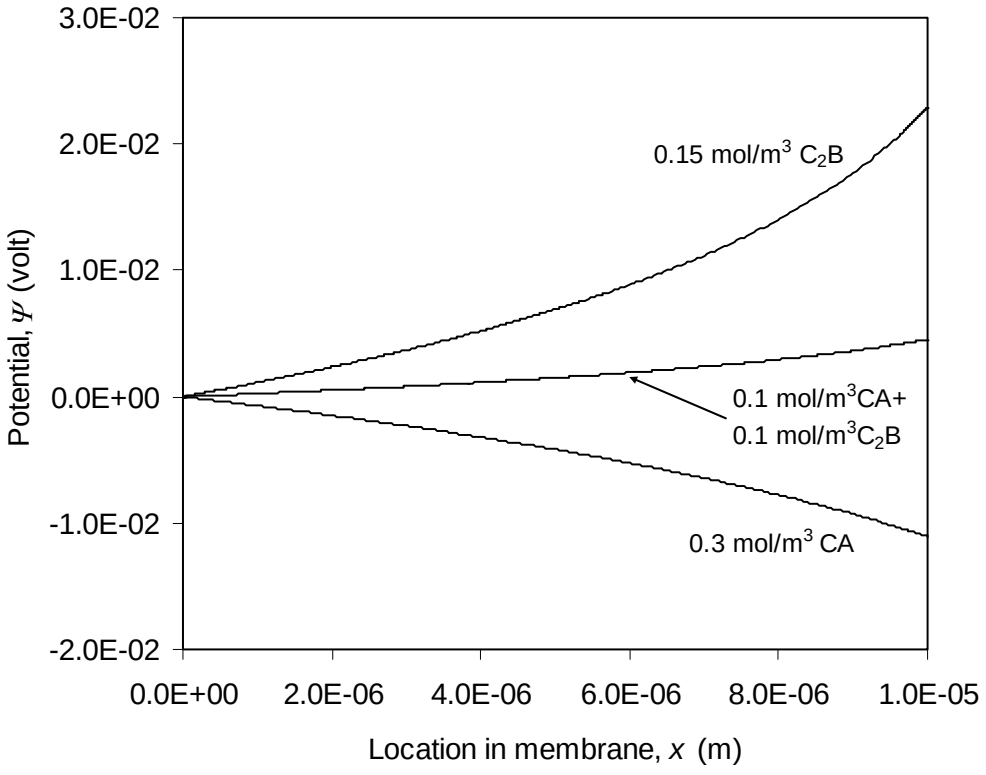

Figure 6.4 Electric potential profiles across the membrane in single and mixed electrolyte solutions

6.3 Ion Permeation and Selectivity under Different Conditions

6.3.1 Effect of Ionic Diffusion Coefficients

As shown in Figure 6.5, ionic flux increases with water flux before approaching a limiting value. The faster A^- ion has a higher flux than B^{2-} ion. The increase in ionic diffusion coefficient can also increase the ion permeation. Figure 6.6 compares the ionic flux under different diffusivities. When three ions have the same diffusion coefficients ($D_A = D_B = D_C = 1\times10^{-12}$ m^2/s), flux of A^- and B^{2-} equal to each other, which is one third of that of C^+. This is because the concentration of C^+ is three times of A^- and B^{2-} in feed solution and no imbalanced charge is accumulated across the membrane due to the identical ionic diffusivity.

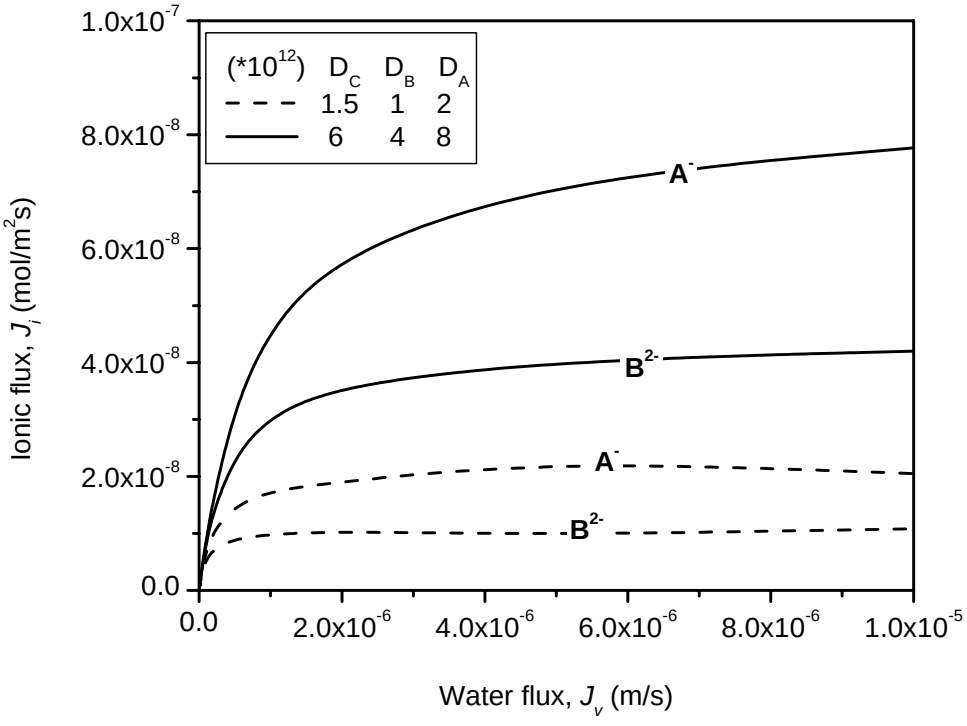

Figure 6.5 Ionic flux against water flux under different diffusion coefficients

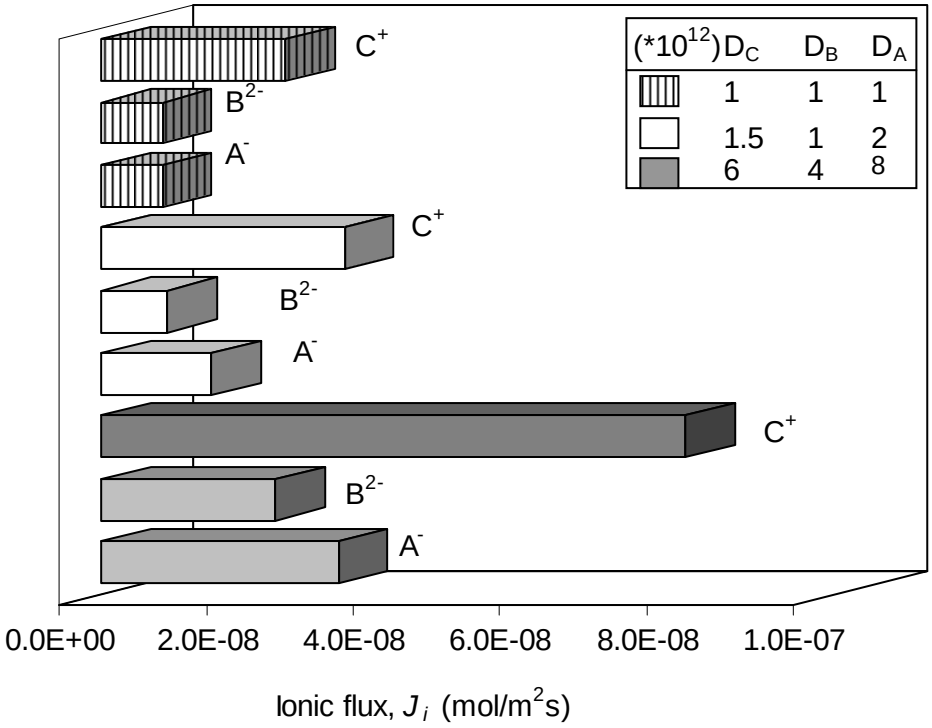

Figure 6.6 Ionic flux in mixed solutions (0.1 mol/m^3 CA + 0.1 mol/m^3 C_2B) with different ionic diffusivities at J_v=5×10^{-7} m/s

When ions in mixed solution have different diffusion coefficients, as discussed before, the imbalanced charge will cause an electric field to regulate the ionic flux. As shown in Figure 6.6, A^- has a higher flux than B^{2-}, while the flux of C^+ equal $J_{A^-} + 2J_{B^{2-}}$, following the non-electric-current criteria in the membrane system. The increase in water flux increases the electric field strength, which increases the difference in flux between two anions. When the ratio of three ion diffusion coefficients is fixed at D_A : D_B : D_C = 2: 1: 1.5 while the values of them are increased by 4 times, it can be seen from Figure 6.6 that the fluxes are not increased at the same rate but much less than 4 times. It is mostly due to the induced electric field, which regulates the flux by reducing the difference in ion diffusivities.

6.3.2 Effects of Ratio of Ion Concentrations

In this study, the ratio of ion concentrations is termed as the mole fraction of B^{2-}, f_r, which can be calculated by:

$$f_r = \frac{C_{B^{2-}}}{C_{B^{2-}} + C_{A^-}} \tag{6.11}$$

Figure 6.7 shows the rejection of A^- and B^{2-} for mixed solution comprising of CA and C_2B. The change in ionic rejection for various mole fraction of B^{2-} with change in various water fluxes is presented. The ionic rejections are highly dependent on the water flux, which is the same as for rejections in a single solution. Increasing the mole fraction of B^{2-} ions causes the rejection of both anions to decrease. As shown in Figure 6.7 (a), the A^- rejection decreases with the addition of B^{2-} in feed solution. The decline in A^- rejection is greater with increasing mole fraction of B^{2-} in the feed. When the mole fraction of B^{2-} is as high as 0.5 and 0.8, the rejection of A^- can be negative, when the water flux is below 1×10^{-7} and 2×10^{-7} m/s, respectively.

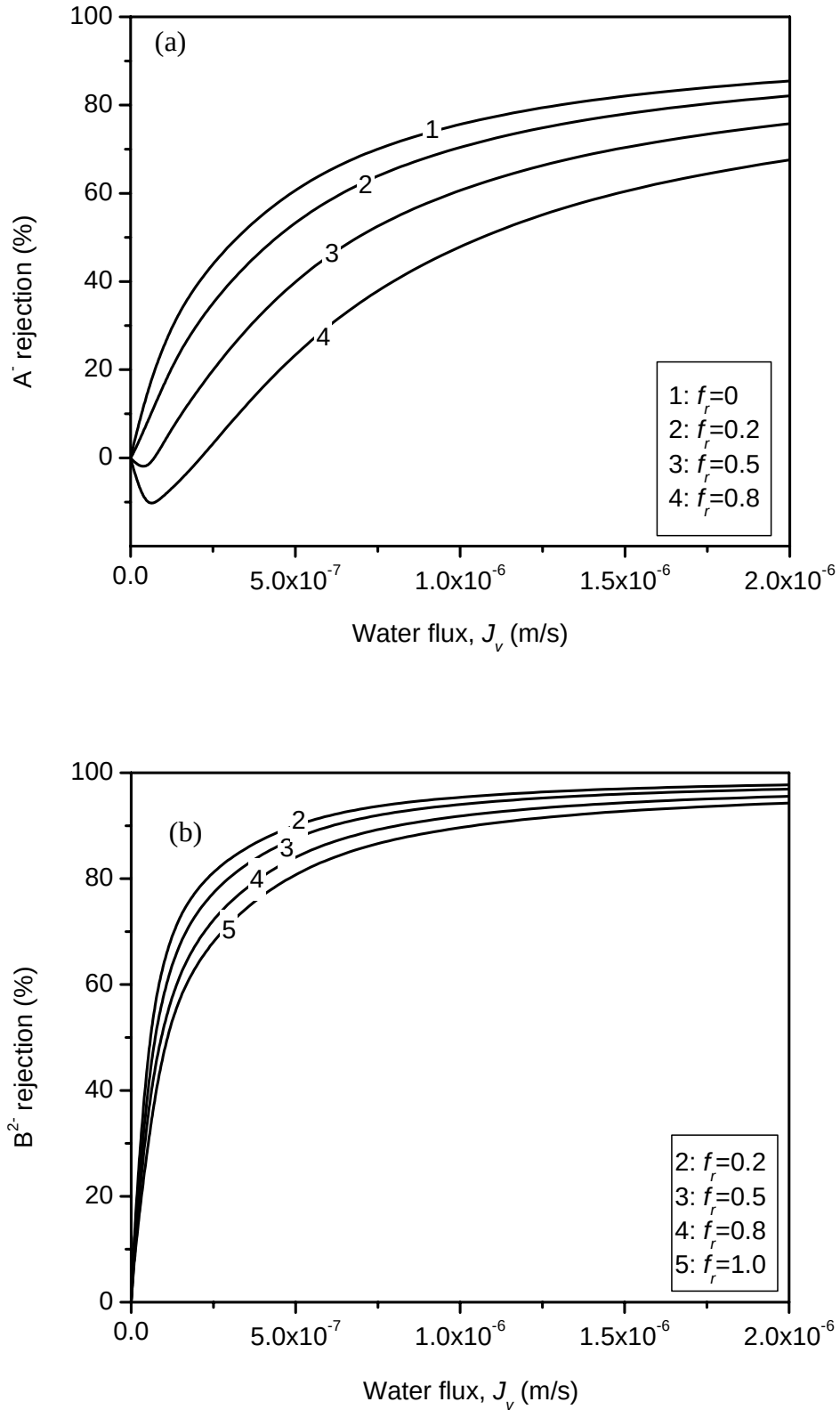

Figure 6.7 Ionic rejection in mixed solutions with different mole fraction of B^{2-}

The transition of A^- rejection from positive to negative values with an increase in mole fraction of B^{2-} in feed solution is predicted by the simulation. Such a phenomenon can also be explained by the "flux regulator" (i.e., electric field). As shown in Figure 6.8, when the mole fraction of B^{2-} increases, more net charge is accumulated at both sides of membrane, which produces an electric field with a higher strength. An increase in electric field strength accelerates the transport of both anions, resulting in an increase in both A^- and B^{2-} permeation.

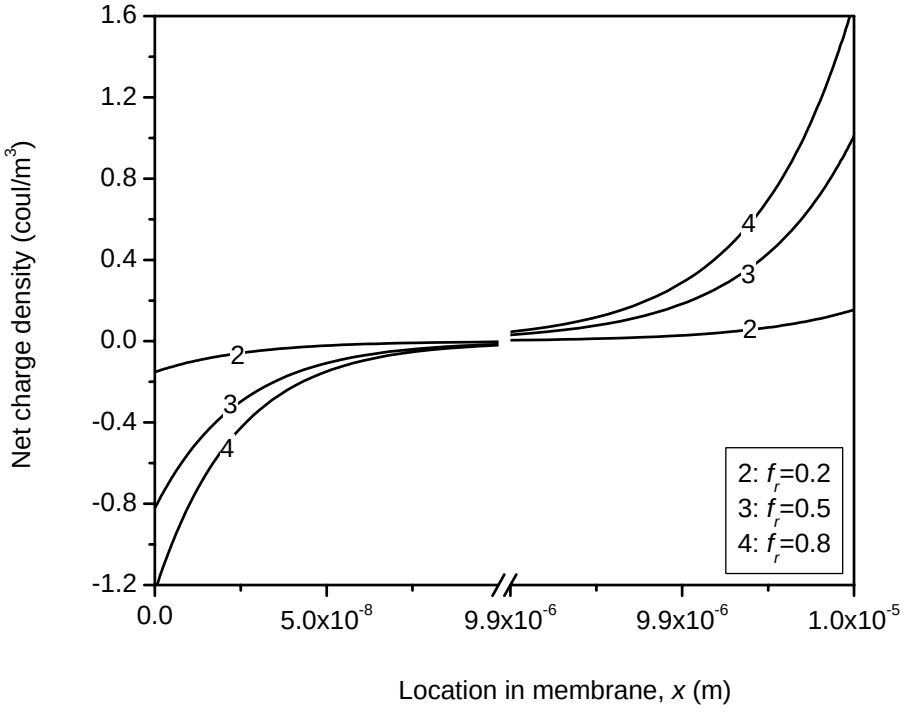

Figure 6.8 Net charge profiles under different mole fraction of B^{2-}

The ionic rejection as a function of mole fraction of B^{2-} is illustrated in Figure 6.9. Both anion rejections decrease linearly with the increase of B^{2-} molar fraction in the feed solution, while an increase in rejection of C^{+} is observed. Using the charge neutrality in bulk feed and permeate solutions, the rejections of three ions have the following relation:

$$r_{j,C^+} = \frac{1- f_r}{1+ f_r} r_{j,A^-} + \frac{2 f_r}{1+ f_r} r_{j,B^{2-}} \tag{6.12}$$

As discussed before, when mole fraction of B^{2-}, f_r increases, both r_{j,A^-} and $r_{jB^{2-}}$ decrease. But different changes occur in their coefficients: $\frac{1- f_r}{1+ f}$ will also decrease with the increase of f_r, while $\frac{2 f_r}{1+ f_r}$ will increase. Due to the large magnitude of this only-increasing term in Eq. (6.12), the rejection of C^{+} increases. That is, the permeation of C^{+} decreases with the increasing mole fraction of B^{2-}.

It is further noted from Figure 6.7 that an increase in water flux will enhance the rejection of A^{-} and its magnitude shifts from negative to a positive value. For a mixed solution with 0.1 mol/m^3 CA and 0.1 mol/m^3 C_2B, the potential difference across the membrane under different water flux is illustrated in Figure 6.10. The change in electric field has the same influence on both anionic fluxes. But the increase in water flux also dilute the permeate concentration. Thus the ionic rejection is determined by both water flux and electric field.

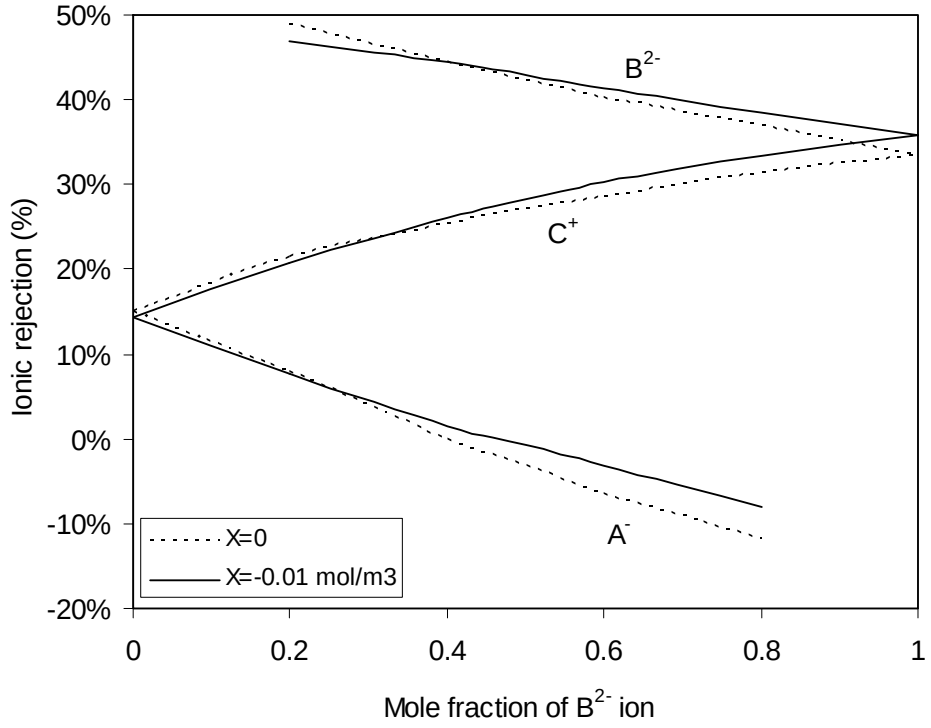

Figure 6.9 Ionic rejection as a function of mole fraction of B^{2-}

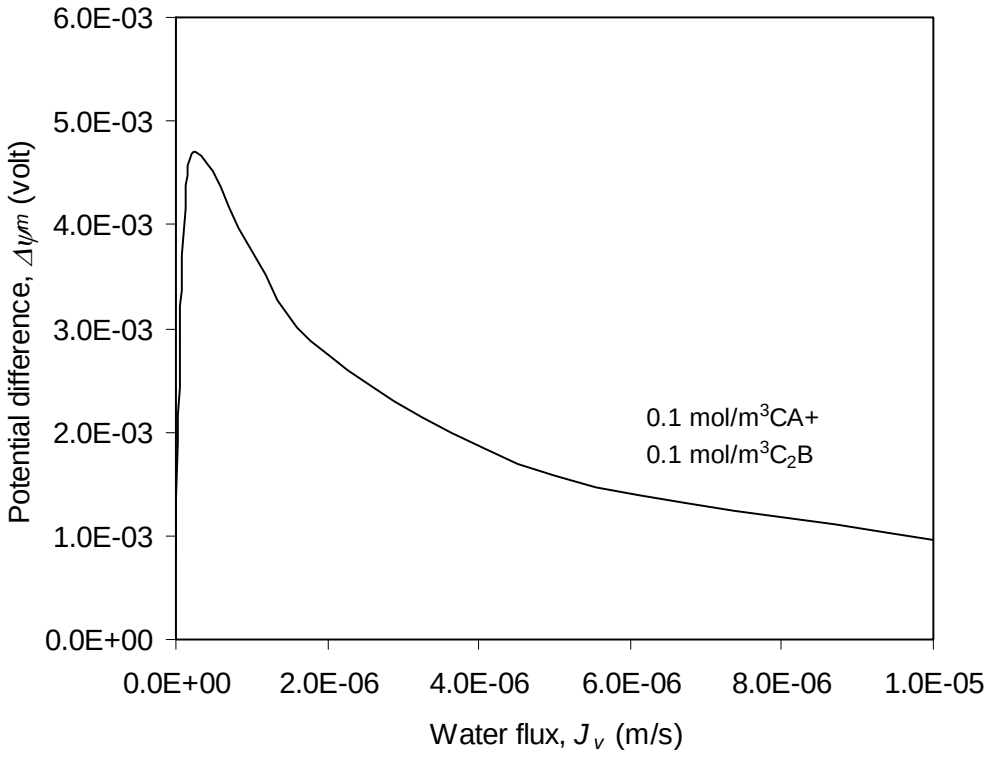

Figure 6.10 Potential difference across the membrane under different water fluxes

6.3.3 Effects of Membrane Charge Density

Membrane charge is commonly assumed to be the major reason for the high rejection of divalent ions through RO/NF membranes. Figure 6.11 shows the rejection curves for both anions in membrane with and without fixed charge density. The negative membrane charge increases the rejection of B^{2-}, but reduces that of A^- in mixed solutions. When membrane is negatively charged, the charged membrane would attract counter-ion C^+ but repel both co-ions B^{2-} and A^-. The distribution of ionic concentration on the membrane-solution interface is dependent upon the bulk concentration, the valences of ions, and the membrane charge density. Divalent co-ion B^{2-} is retained more when the value of membrane charge density increases. It can be seen from Figure 6.12 that compared with membrane with no charge, concentration of C^+ increases while concentrations of both anions decrease across the negatively charged membrane. Divalent B^{2-} experiences a higher concentration gradient across the charged membrane, resulting in a higher retention rate. As the permeation of C^+ increases under the membrane charge, by applying the electroneutrality in bulk solutions, A^- could become more permeable in charged membranes than in uncharged membranes. In other words, the fixed charges on membrane would increase the selectivity of anions in mixed solutions. It should be pointed out that for membrane with no charge, the concentration gradients for three ions are constant within the range of water flux investigated. But as shown in circle regions in Figure 6.12, when membrane is negatively charged, increase in water flux reduces the concentration gradient for C^+, and increases those for both A^- and B^{2-}, which explains the exception in circled region in Figure 6.11 when water flux is low enough, the membrane charge increases A^- rejection, but decreases B^{2-} rejection.

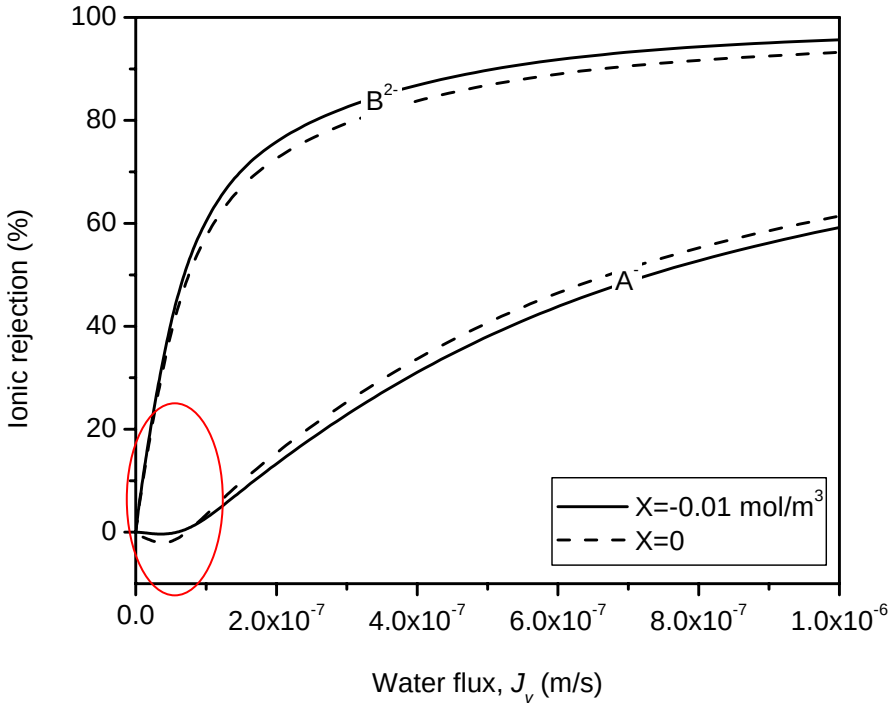

Figure 6.11 The effect of membrane charge density on ionic rejection

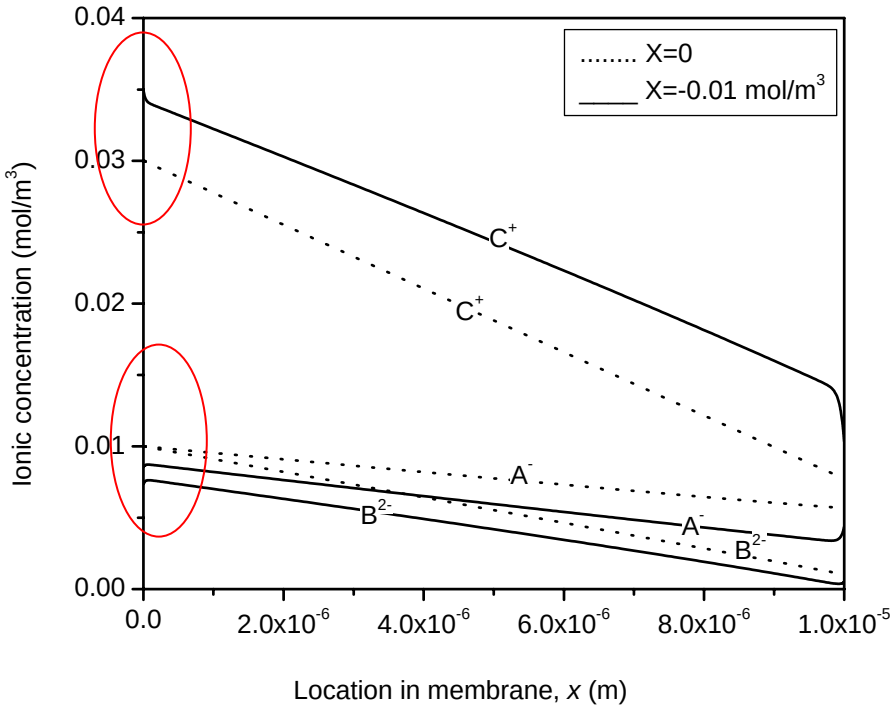

Figure 6.12 Ionic concentration profiles across the membrane

When single electrolyte solutions transport through a charged membrane, the ionic rejections normally decrease with the feed salt concentration. However in mixed solution as presented in Figure 6.13, it can be seen that the rejections of both B^{2-} and C^{+} decrease with the feed salt concentration, while that of A^{-} increases. When the feed concentration is higher than the value of fixed membrane charge density, the ionic rejection becomes constant and independent upon the feed concentration.

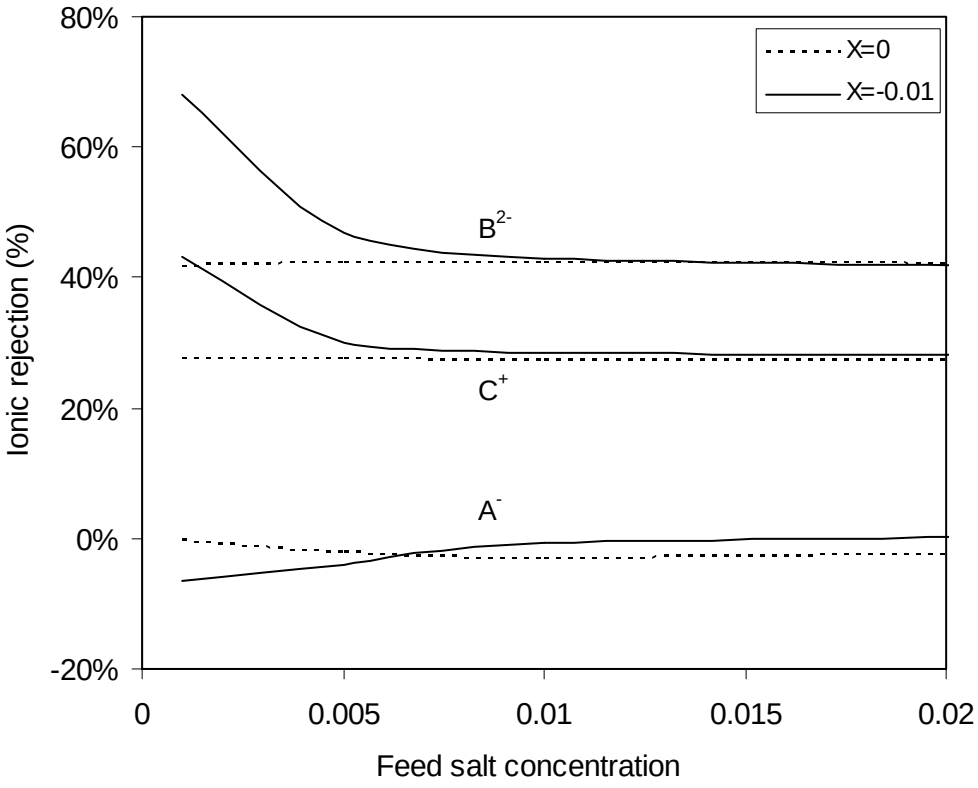

Figure 6.13 Ionic rejections against feed salt concentration

6.4 Analytical Approximation of Transport Phenomenon

As discussed before, transport of different ions in multi-electrolyte solutions through membrane is coupled and regulated by the induced electric field, which is affected by the ionic diffusion coefficients, ion valences, water flux, mole fraction, feed salt concentration, and membrane charge density. The effects of these parameters on ionic permeation and selectivity can be simulated by the unsteady-state Nernst-Planck-Poisson model. However, an analytical solution is always preferable in industry or for engineering applications. Although it is impossible to obtain the analytical solution for Nernst-Planck and Poisson's equations mathematically, an analytical method is developed in this section to estimate the transport phenomenon in mixed solutions quantitatively. The analytical equations are derived for the single solutions before being applied to the mixed solutions.

6.4.1 Calculation of Equivalent Diffusion Coefficient in Single Solutions

Consider the single electrolyte solution first. Assume the diffusion coefficient and valences for ions 1 and 2 are D_1, z_1 and D_2, z_2, respectively. Using Nernst-Planck equation, the ionic fluxes for two ions are:

$$J_1 = -D_1 \frac{dc_1}{dx} - D_1 z_1 c_1 \frac{F}{RT} \frac{d\psi}{dx} \tag{6.13a}$$

$$J_2 = -D_2 \frac{dc_2}{dx} - D_2 z_2 c_2 \frac{F}{RT} \frac{d\psi}{dx} \tag{6.13b}$$

The basic concept in analytical derivation is drawn upon the understanding that the first term of diffusion flux differs between two ions due to the different ionic diffusivity. Such a difference would be regulated by the second term of electromigrative flux, where the electric field $\frac{F}{RT}\frac{d\psi}{dx}$ for both ions is the same. If this

term can be calculated directly, then the equivalent diffusion coefficient can be obtained for both ions, which can be used to estimate the solute transport behaviors much easily. To calculate the electric field, the non-electric-current is used. Since $z_1 J_1 + z_2 J_2 = 0$, that is:

$$-z_1 D_1 \frac{dc_1}{dx} - D_1 z_1^{\,2} c_1 \frac{F}{RT}\frac{d\psi}{dx} - z_2 D_2 \frac{dc_2}{dx} - D_2 z_2^{\,2} c_2 \frac{F}{RT}\frac{d\psi}{dx} = 0 \tag{6.14}$$

So,

$$\frac{F}{RT}\frac{d\psi}{dx} = -\frac{D_1 z_1 \dfrac{dc_1}{dx} + D_2 z_2 \dfrac{dc_2}{dx}}{D_1 z_1^{\,2} c_1 + D_2 z_2^{\,2} c_2} \tag{6.15}$$

It is known that the imbalanced charge is accumulated at both membrane-solution interfaces while charge is nearly neutral within the membrane. To get the analytical approximation, it is assumed that the charge is balanced within the membrane and the concentration gradient is constant across the membrane.

$$z_1 c_1 + z_2 c_2 = 0 \tag{6.16a}$$

$$z_1 \frac{dc_1}{dx} + z_2 \frac{dc_2}{dx} = 0 \tag{6.16b}$$

Substituting Eq. (6.16) into Eq. (6.15) leads to:

$$\frac{F}{RT}\frac{d\psi}{dx} = -\frac{D_1 z_1 - D_2 z_1}{\left(D_1 z_1^{\,2} - D_2 z_1 z_2\right) c_1}\frac{dc_1}{dx} \tag{6.17}$$

Substituting Eq. (6.17) into Eq. (6.13a), the ionic flux can be written as:

$$J_1 = -\frac{D_1 D_2 z_1 - D_1 D_2 z_2}{D_1 z_1 - D_2 z_2}\frac{dc_1}{dx} = -D'\frac{dc_1}{dx} \tag{6.18}$$

where *D'* is equivalent diffusion coefficient for both ions in single solutions.

$$D' = \frac{D_1 D_2 z_1 - D_1 D_2 z_2}{D_1 z_1 - D_2 z_2} \tag{6.19}$$

Table 6.3 summarizes the equivalent diffusion coefficients in single electrolyte solutions calculated by this equation.

Table 6.3 Equivalent diffusion coefficient in single solutions

	Electrolyte 1-1	Electrolyte 2-1	Electrolyte 1-2
$D_1 = D_2$	D_1	D_1	D_1
$D_1 \neq D_2$	$\frac{2D_1D_2}{D_1+D_2}$	$\frac{3D_1D_2}{2D_1+D_2}$	$\frac{3D_1D_2}{D_1+2D_2}$
$D_1 << D_2$	$\approx 2D_1$	$\approx 3D_1$	$\approx 1.5D_1$
$D_1 >> D_2$	$\approx 2D_2$	$\approx 1.5D_2$	$\approx 3D_2$

Since $J_i = C_{p,i} J_v$, substitute it into Eq. (6.18) and assume that the concentration profile is a straight line, it gets

$$C_{p,i}\left(1+\frac{J_v}{D'}L\right) = c_{0,i} \tag{6.20}$$

Thus the solute rejection for single electrolyte can be estimated by

$$r_j = \frac{J_v L}{D' + J_v L} \tag{6.21}$$

This estimation is correlated well with the simulation data for the non-charged membranes. However, when membrane is charged, concentration profiles change a lot. As a result, the above assumption could not be applied. That is, the deviations by the approximation can not be neglected.

6.4.2 Calculation of Electric Field in Mixed Solutions

The analytical approximation can be extended and applied to three ions in a mixed solution. Consider the mixed CA/C_2B solution as discussed in previous sections. The electric field in the mixed solutions is assumed to be the sum of two electric fields induced individually from the single solutions. From Eq. (6.17), the electricmigrative flux for C^+ in both single CA and C_2B solutions can be calculated as:

$$J_{e,C,CA} = -D_C z_C c_C^{CA} \frac{F}{RT}\frac{d\psi}{dx} = D_C \frac{D_C z_C - D_A z_C}{\left(D_C z_C - D_A z_A\right)} \cdot \frac{dc_C^{CA}}{dx} \tag{6.22a}$$

$$J_{e,C,C_2B} = -D_C z_C c_C^{C_2B} \frac{F}{RT}\frac{d\psi}{dx} = D_C \frac{D_C z_C - D_B z_C}{\left(D_C z_C - D_B z_B\right)} \cdot \frac{dc_C^{C_2B}}{dx} \tag{6.22b}$$

The concentration gradient can be obtained from Eqs. (6.20) and (6.21):

$$-\frac{dc}{dx} = \frac{c_0 J_v}{D' + J_v L} \tag{6.23}$$

Substitute Eq. (6.23) into Eq. (6.22), we get:

$$J_{e,C,CA} = -D_C z_C c_C^{CA} \frac{F}{RT}\frac{d\psi}{dx} = -D_C \frac{D_C z_C - D_A z_C}{\left(D_C z_C - D_A z_A\right)} \cdot c_C^{CA} \cdot \frac{J_v}{D'_{CA} + J_v L} \tag{6.24a}$$

$$J_{e,C,C_2B} = -D_C z_C c_C^{C_2B} \frac{F}{RT}\frac{d\psi}{dx} = -D_C \frac{D_C z_C - D_B z_C}{\left(D_C z_C - D_B z_B\right)} \cdot c_C^{C_2B} \cdot \frac{J_v}{D'_{C^2B} + J_v L} \tag{6.24b}$$

D'_{CA} and D'_{C_2B} is the equivalent diffusion coefficient for single CA and C_2B solutions, respectively. When CA is mixed with C_2B with the mole fraction of B^{2-} equal f_r, the C^+ concentration in CA and C_2B can be calculated by Eq. (6.25a) and (6.25b), respectively:

$$c_C^{CA} = \frac{1 - f_r}{1 + f_r} c_T \tag{6.25a}$$

$$c_C^{C_2B} = \frac{2 f_r}{1 + f_r} c_T \tag{6.25b}$$

where c_T is the total concentration of C^+ in mixed CA/C_2B solutions. Hence the analytical approximation equation for electromigrative flux can be written as:

$$J_{e,C,CA} = -D_C z_C c_C^{CA} \frac{F}{RT}\frac{d\psi}{dx} = -D_C \frac{D_C z_C - D_A z_C}{\left(D_C z_C - D_A z_A\right)} \cdot \frac{1-f_r}{1+f_r} \cdot \frac{J_v c_T}{D'_{CA} + J_v L} \qquad (6.26a)$$

$$J_{e,C,C_2B} = -D_C z_C c_C^{C_2B} \frac{F}{RT}\frac{d\psi}{dx} = -D_C \frac{D_C z_C - D_B z_C}{\left(D_C z_C - D_B z_B\right)} \cdot \frac{2f_r}{1+f_r} \cdot \frac{J_v c_T}{D'_{C^2B} + J_v L} \qquad (6.26b)$$

These two equations quantify the electromigrative fluxes as a function of diffusion coefficients D_i, valence z_i, mole fraction f_r, water flux J_v, feed concentration c_T and membrane length L. Table 6.4 shows an example to estimate ionic transport phenomenon by using the above analytical derivations. The calculated electromigrative flux for C^+ in CA and C_2B solutions is 5.45×10^{-9} mol/m^{2}s and -1.67×10^{-8} mol/m^{2}s, respectively. The opposite signs in electromigrative fluxes show that the induced electric field in CA and C_2B solutions are directed to permeate and feed side, respectively. The electromigrative flux for C^+ in mixed CA/C_2B solution can be estimated as the sum of $J_{e,C,CA}$ and J_{e,C,C_2B} . The consequent negative value (i.e. $5.45\times10^{-9} - 1.67\times10^{-8} = -1.125\times10^{-8}$ mol/m^{2}s) indicates that the induced electric field in mixed CA/C_2B solutions is directed towards the feed side. Compared with transport in single solutions, such an electric field in mixed solutions would accelerate the permeation of A^- but retain more B^{2-}.

Table 6.4 An example of analytical approximation of transport phenomenon

Given:	$J_v = 5\times10^{-7}$ m/s;	$L = 1\times10^{-5}$ m;	$c_T = 0.3$ mol/m^3;	$f_r = 0.5$
	$D_C = 2\times10^{-12}$ m^2/s;	$D_A = 5\times10^{-12}$ m^2/s;	$D_B = 5\times10^{-13}$ m^2/s	
	$z_c = +1$;	$z_A = -1$;	$z_B = -2$	

Calculated:

$$D'_{CA} = \frac{D_C D_A z_C - D_C D_A z_A}{D_C z_C - D_A z_A} = 2.86\times10^{-12}\, m^2/s$$

$$D'_{C_2B} = \frac{D_C D_B z_C - D_C D_B z_B}{D_C z_C - D_B z_B} = 1\times10^{-12}\, m^2/s$$

$$c_C^{CA} = \frac{1-f_r}{1+f_r} c_T = \frac{1-0.5}{1+0.5}\cdot 0.3 = 0.1 mol/m^3$$

$$c_C^{C_2B} = \frac{2f_r}{1+f_r} c_T = \frac{2\cdot 0.5}{1+0.5}\cdot 0.3 = 0.2 mol/m^3$$

$$J_{e,C,CA} = -D_C \frac{D_C z_C - D_A z_C}{\left(D_C z_C - D_A z_A\right)} \cdot c_C^{CA} \cdot \frac{J_v}{D'_{CA} + J_v L}$$

$$= -2\times10^{-12} \cdot \frac{2\times10^{-12} - 5\times10^{-12}}{2\times10^{-12} + 5\times10^{-12}} \cdot 0.1 \cdot \frac{5\times10^{-7}}{2.86\times10^{-12} + 5\times10^{-7}\cdot10^{-5}}$$

$$= 5.45\times10^{-9} mol/m^2 s$$

$$J_{e,C,C_2B} = -D_C \frac{D_C z_C - D_B z_C}{\left(D_C z_C - D_B z_B\right)} \cdot c_C^{C_2B} \cdot \frac{J_v}{D'_{C^2B} + J_v L}$$

$$= -2\times10^{-12} \cdot \frac{2\times10^{-12} - 0.5\times10^{-12}}{2\times10^{-12} + 2\cdot0.5\times10^{-12}} \cdot 0.2 \cdot \frac{5\times10^{-7}}{10^{-12} + 5\times10^{-7}\cdot10^{-5}}$$

$$= -1.67\times10^{-8} mol/m^2 s$$

The analytical method derived above can also be used to estimate the effects of different parameters on ion transport in mixed solutions. For instance, the increase in mole fraction f_r reduces $\frac{1-f_r}{1+f_r}$, but increases $\frac{2f_r}{1+f_r}$. According to Eq. (6.26), $J_{e,C,CA}$ has a lower value with the increase in f_r, while J_{e,C,C_2B} has a higher absolute value, resulting in a stronger electric field, which accelerate both permeation of A^- and B^{2-}.

The effects of feed concentration, diffusion coefficients, valences and water flux can also be calculated and discussed by this method.

6.5 Summary

In this chapter, ion transport behaviors across membrane in mixed feed solutions under different conditions have been investigated by the unsteady-state Nernst-Planck-Poisson model. In a mixed solution, the addition of a second ion can increase the permeability of more permeable ion and increase the rejection of less permeable ion. The higher selectivity is obtained in mixed solutions due to the change in induced electric field, which is dependent on ionic diffusion coefficients, feed salt concentration, mole fraction, membrane charge density and water flux. The effects of these parameters on ion transport can also be quantified by the analytical method derived in this study, which provide a much easier and more direct way to estimate the transport phenomenon in both single and mixed solutions.

Chapter 7

CONCLUSIONS AND RECOMMENDATIONS

7.1 Conclusions

The following conclusions can be drawn from this research work:

1. The Nernst-Planck-Donnan model considers the electrostatic interaction on ion transport in an oversimplified manner. It is noted that:
   i. Although the Donna exclusion effect of the charged membrane on ion transport can be reasonably dealt with Nernst-Planck-Donnan model, it generally fails in explaining the fundamental phenomena associated with electrostatic interactions on ion transport across RO/NF membranes, such as the acquirement of charge, coupled transport, etc.
   ii. The limitation mainly arises from the employment of the local electroneutrality assumption, which virtually eliminates the electrostatic interaction between membrane and ions as ions transport through the membranes.
   iii. In the Nerst-Planck-Donnan model, salt/ion rejection by the membranes can be explained with the membrane charge density when it is assumed to have an empirical Freudlich type relationship with the feed salt concentration.

2. Electrostatic interactions on ion transport through RO/NF membranes can be well described with an unsteady-state Nernst-Planck-Poisson equation with dynamic boundary conditions developed in this study. The following conclusions can be drawn on the new formulation:

   i. The main obstacle to use the Nernst-Planck-Poisson equation is the determination of appropriate boundary conditions. This is also one important reason for the popular use of Nernst-Planck-Poisson equation, in which the boundary conditions are readily available with the local electroneutrality assumption.

   ii. The boundary conditions of the unsteady state Nernst-Planck-Poisson equation can be properly described with the linearized Boltzmann equation, which relates the ion concentration distribution in the solution adjunct to the membrane surface to the (fixed or induced) membrane charge density. Ion transport through the membrane at steady state can be simulated with the numerical solution of the unsteady state transport equation for a sufficiently long time.

   iii. The model (unsteady state Nernst-Planck-Poisson equation + appropriate boundary condition) can clearly show or explain the phenomena of fundamental importance associated with ion transport, such as the charge acquiring process of the membrane due to unbalanced ion transport, charge distribution along the membrane thickness and the induced potential, and the effect of fixed charge of membrane on ion transport.

   iv. Numerical simulations with the new model demonstrate that electroneutrality is maintained in the bulk solutions in both sides of the membrane, i.e., there is no net electrical current across the membrane at steady state no matter how different the diffusivities (mobilities) of the cations and anions are. The membrane charge or potential is shown to provide the needed self-regulation mechanism for ions of

different mobilities to transport through the membranes without net charge flow at steady state.

3. Ion transport behaviors under various conditions have been investigated with the newly developed model. It is demonstrated that the electrostatic interactions plays a paramount important role in ion transport. The following conclusions are drawn with this respect:
   i. For membranes without fixed charge, the electric field can be induced as a result of imbalanced transport of ions in a transient period due to different ion diffusivities. The induced electric field then will cause electro-migration of cations and anions to opposite directions to make up the difference between the diffusive fluxes. However, diffusive fluxes are always greater than the electromigrative ones.
   ii. For membranes with fixed charge, the electrostatic interaction between membrane and ions is strongly affected by fixed membrane charge density and co-ion valence. Electro-migration may contribute more than the diffusion to the total fluxes of ions under certain circumstances, e.g., high membrane charge density.
   iii. Transport of ions in a multi-electrolyte solution through membrane is a very complicated process, which involves not only electrostatic interactions between membrane and various ions but also competitions between co-ions. Preliminary simulations show that the existence of a third ion can either increases or reduces the permeation of ions of the same charge according to their relative mobility. It is interesting to observe that negative rejection of very mobile ions

(concentration in the permeate is higher than that in the feed) can occur with the existence of co-ions with much smaller mobility.

7.2 Recommendations for Future Studies

Based on the results obtained from this research work, the following are recommended for future studies:

1. Develop a steady-state model based on results from this study.

   The boundary conditions for the steady-state Nernst-Planck-Poisson model for RO/NF membranes are more difficult to define. In this study much effort has been made to obtain the appropriate boundary conditions for unsteady-state model with the non-electric-current as the steady-state constraint. However, time-dependent unsteady-state model is always more complicated and consumes more time than the steady state model. With the understanding of physical process and based on the findings from this work, the steady-state model might be developed.

2. Modeling of virus and microbes transport through membranes.

   Most virus and bacteria are negatively charged and microbe removal by membranes is of practical significance to pharmacy and water industry. However, biological concerns have to be involved in such a research. The model developed in this work might be modified to accommodate additional requirements relating to virus and microbes transport.

3. Experimental study of membrane material properties on ion transport.

As concluded before, the electrostatic interaction between membrane and ions is critical in ion transport. Such an interaction is dependent on the membrane surface properties, e.g., membrane surface charge, permittivity as well as the ion transport properties like diffusion coefficients in the membrane. If new experimental methods are available to determine these properties, it is feasible to find or invent new materials for better membrane transport performance.

REFERENCES

Aguilella, V.M., Mafe, S. And Pellicer, J. (1987) On the nature of the diffusion potential derived from Nernst-Planck flux equations by using the electroneutrality assumption. *Electrochimica Acta,* 32 (3) 483-488.

Aitkuliev, K., Sobolev, V. D., and Churaev, N. V. (1984) Influence of the flow rate and concentration of the electrolyte on the selectivity of reverse osmosis membranes. *Colliod J*. 46, 179-190.

Anderson, J.D. (1995) *Computational fluid dynamics: the basics with applications,* McGraw-Hill, New York.

Ariza, M. J. and Benavente, J. (2001) Streaming potential along the surface of polysulfone membranes: a comparative study between two different experimental systems and determination of electrokinetic and adsorption parameters. *J. Membr. Sci*. 190, 119-132.

Banks, W., and Sharples, A. (1966) Studies on desalination by reverse osmosis: III. Mechanism of solute rejections, *J. Applied Chem*. 16, 153-158.

Bekefi, G. and Barrett, A. H. (1977) Electromagnetic vibrations, waves, and radiation. Cambridge, Mass. MIT Press.

Bhattacharjee, S., Chen, J. C., and Elimelech, M. (2001). Coupled model of concentration polarization and pore transport in crossflow nanofiltration of multi-component electrolytes. *AIChE J.* 47, 2733-2745.

Bockris, J.O'M., and Reddy, A.K.N. (1970) *Modern electrochemistry*, Plenum. NY.

Boltzmann, L. (1868) Studien über das Gleichgewicht der lebendigen Kraft zwischen bewegten materiellen Punkten. *Akad Wiss Berlin, Güttingen, Leipzig, München Wien* 58, 517.

Bowen, W. R. and Mukhtar, H. (1996) Characterisation and prediction of separation performance of nanofiltration membranes. *J. Membr. Sci.*, 112, 263-274.

Bowen, W. R. Mohammad, A. W., and Hilal, N. (1997) Characterization of nanofiltration membranes for predictive purposes—use of salts, uncharged solutes and atomic force microscopy. *J. Membr. Sci.* 126, 91-105.

Bowen, W. R and Cao, X. (1998) Electrokinetic effects in membrane pores and the determination of zeta-potential. *J. Membr. Sci*. 140, 267-273.

Bowen, W. R. and Mohammad, A. W. (1998a) Diafiltration by nanofiltration: prediction and optimization, *AIChE J*. 44, 1799-1812.

Bowen, W. R. and Mohammad, A. W. (1998b) Characterization and prediction of nanofiltration membrane performance—a general assessment. *Trans Ichem*. 76, 885-893.

Buck, R.P. (1984) Kinetics of bulk and interfacial ionic motion: microscopic bases and limits for the Nernst-Planck equation applied to membrane systems, *J. Membr. Sci.* 17, 1-62.

Chaudry, M.A. (1995) Water and ions transport mechanism in hyperfiltration with symmetric cellulose acetate membranes. *J. Membr. Sci.* 206, 319-332.

Cheney, W., and Kincaid, D. (1999) *Numerical mathematics and computing*, 4th Ed. Brooks/Cole Publishing Co. Monterey, CA.

Childress, A. E. and Elimelech, M. (1996) Effect of solution chemistry on the surface charge of polymeric reverse osmosis and nanofiltration membranes. *J. Membr. Sci.* 119, 253-268.

Childress, A. E. and Elimelech, M. (2000) Relating nanofiltration membrane performance to membrane charge (electrokinetic) characteristics. *Environ. Sci. & Technol.* 34, 3710-3716.

Clark, M.M. (1996) *Transport modeling for environmental engineers and scientists*, John Wiley & Sons.

Debye, P., and Hückel, E. (1923) Zur theorie der electrolyte. *Physik. Zeitschr*. 24, 185.

Deen, W. M. (1987) Hindered transport of large molecules in liquid-filled pores. *AIChE J*. 33, 1409-1425.

DeGroot, J. M. and Masur, P. (1962) Non-equilibrium thermodynamics, North Holland, Amsterdam, Wiley, New York.

Dey, T.K., Ramachandran, V. and Misra, B.M. (2000) Selectivity of anionic species in binary mixed electrolyte systems for nanofiltration membranes. *Desalination* 127, 165-175.

Donnan, F.G. (1924) The theory of membrane equilibrium. *Chemical Reviews* 1, 73-90.

Donnan, F. G. (1995) Theory of membrane equilibria and membrane potentials in the presence of non-dialyzing electrolytes, a contribution to physical-chemical physiology. *J. Membr. Sci.* 100, 45-55.

Dresner, L. (1972) Some remarks on the intergration of the extended Nernst-Planck equations in the hyperfiltration of multicomponent solutions. *Desalination* 10, 27-46.

Elimelech, M. and Childress, A. E. (1996) Zeta potential of reverse osmosis membranes: implications for membrane performance. Water Treatment Technology Repaort No. 10, US Department of the Interior, Bureau of Reclamation, Denver Office.

Epperson, J.F. (2002) *An introduction to numerical methods and analysis*, John Wiley & Sons, New York Singapore.

Eriksson, P. (1988a) Nanofiltration extends the range of membrane ultrafiltration. *Environ. Prog.* 7, 58-62.

Eriksson, P. (1988b) Water and salt transport through two types of polyamide composite membranes. *J. Membr. Sci.* 36, 297-313.

Fievet, P., Labbez, C., Szymczyk, A., Vidonne, A., Foissy, A. and Pagetti, J. (2002) Electrolyte transport through amphoteric nanofiltration membranes. *Chem. Eng. Sci.* 57, 2921-2931.

Glueckauf, E. (1976) The distribution of electrolytes between CA membranes and aqueous solutions. *Desalination* 18, 155-172.

Griffiths, D.J. (1999) Introduction to electrodynamics, 3rd Ed. Prentice Hall, New Jersey, USA.

Gummel, H.K. (1964) A self-consistent interative scheme for one-dimensional steady state transistor calculation. *IEEE Transactions on Electron Devices* ED-11, 455-465.

Hafiane, A., Lemordant, D. and Dhahbi, M. (2000) Removal of hexavalent chromium by nanofiltration. *Desalination* 130, 305-312.

Hajeeh, M., and Chaudhuri, D. (2000) Reliability and availability assessment of reverse osmosis. *Desalination* 130, 185-192.

Hall, M. S., Starov, V. M., and Lloyd, D. R. (1997) Reverse osmosis of multicomponent electrolyte solutions. 1. Theoretical development. *J. Membr. Sci*. 128 23-37.

Harnwell, P. G. (1949) Principles of electricity and electromagnetism, McGraw-hill book company, Inc.

Hickman, H.J. (1970) The liquid junction potential – the free diffusion junction. *Chem. Eng. Sci.* 25, 381-398.

Higa, M., Tanioka, A. and Miyasaka, K. (1990) A study of ion permeation across a charged membrane in multicomponent ion systems as a function of membrane charge density. *J. Membr. Sci.* 49, 145-169.

Higa, M., Tanioka, A., and Kira, A. (1998) A novel measurement method of Donnan potential at an interface between a charged membrane and mixed salt solution. *J. Membr. Sci.* 140, 213-220.

Hoffer, E. and Kedem, O. (1967) Hyperfiltration in charged membranes: the fixed charge model. *Desalination* 2 25-39.

Hodgson, T. D. (1970) Properties of cellulose membranes towards ions in aqueous solutions. *Desalination* 8 99-138.

Honig, B., and Nicholls, A. (1995) Classical electrostatics in biology and chemistry. *Science* 268, 1144-1149.

IUPAC (1996) Terminology for membranes and membrane processes. *J. Membr. Sci.* 120, 149-159.

Jackson, J.L. (1974) Charge neutrality in electrolytic solutions and the liquid junction potential. *J. Phys. Chem.* 78, 2060-2064.

Jacobasch, H. J. and Schurz. J (1988) Characterization of polymer surfaces by means of electrokinetic measurements. *Progr. Colloid Polym. Sci*. 77, 40.

Jitsuhara, I. and Kimura, S. (1983) Rejection of inorganic slats by charged ultrafiltration membranes made of sulfonated polysulfone. *J. Chem. Eng. Jpn.* 16 394-399.

Johnson, J. S., Dresner, L., and Kraus, K. A. (1966) Hyperfiltration (reverse osmosis) in Principles of desalination, K. S. Spiegler, Ed., Chapter 8, Academic Press, New York.

Jonsson, G. (1980) Overview of theories for water and solute transport in UF/RO membranes. *Desalination* 35, 21-38.

Kargol A. (2000) Modified Kedem-Katchalsky equations and their applications. *J. Membr. Sci.* 174, 43-53.

Kastelan-Kunst, L., Kosutic, K., Dananic, V., and Kunst, B. (1997) FT30 membranes of characterized porosities in the reverse osmosis organics removal from aqueous solutions. *Wat. Res.* 31 (11), 2878-2884.

Katchalsky, A., and Curran, P. E. (1975) Nonequlibrium thermodynamics in biophysics. Harvard University Press, 4th printing.

Kato, M. (1995) Numerical analysis of the Nernst-Planck-Poisson system. *J. theor. Biol.* 177, 299-304.

Kedem, O. and Katchalsky, A. (1958) Thermodynamic analysis of the permeability of biological membranes to non-electrolytes. *Biochimica Et Biophysica Acta.* 27, 229-246.

Kedem, O. and Katchalsky, A. (1963) Permeability of composite membranes: Part 1. Electric current, volume flow and flow of solute through membranes. *Trans. Faraday Soc.*, 59, 1918-1933.

Kiso, Y., Sugiura, Y., Kitao, T., and Nishimura, K. (2001) Effects of hydrophobicity and molecular size on rejection of aromatic pesticides with nanofiltration membranes. *J. Membr. Sci.* 119, 1-10.

Kondepudi, D. and Prigogine, I. (1999) Modern thermodynamics, from heat engines to dissipative structures. John Wiley & Sons.

Lee, D.J., Choi, Y.K., Lee, S.B., Ahn, K.H., and Min, B.R. (1998) The analysis of electric properties of thin film composite reverse osmosis membrane with wet impedance method. *J. Membr. Sci.* 150, 9-21.

Levenstein, R., Hasson, D., and Semiat, R. (1996) Utilization of the Donnan effect for improving electrolyte separation with nanofiltration membranes, *J. Membr. Sci.* 116, 77-92.

Lipp, P., Gimbel, R., and Frimmel, F.H. (1994) Parameters influencing the rejection properties of FT30 membranes. *J. Membr. Sci.* 95, 185-197.

Lonsdale, H.K., Merten, U., and Riley, R. L. (1965) Transport properties of cellulose acetate osmotic membranes. *J. Appl. Pol. Sci*. 9, 1341-1362.

Lonsdale, H.K., Pusch, W., and Walch, A. (1975) Donnan-membrane effects in hyperfiltration of ternary system. *J. Chem. Soc. Faraday Trans. I.* 71 501-514.

MacGillivray, A. D. (1968) Nernst-Planck equations and the electroneutrality and Donnan equilibrium assumptions. *J. Chem. Phys.* 48(7) 2903-2907.

Mahan, G. D. (2002) *Applied mathematics*, Kluwer/Plenum Publishers, New York.

Martuzans, B., and Skryl, Y. (1998) Ambipolar diffusion and electroneutrality problem. *Latvian Journal of Physics and Technical Sciences* N4, 52-59.

Mason, E. A. and Lonsdale, H. K (1990) Statistical-mechanical theory of membrane transport. *J. Membr. Sci*. 51, 1-81.

Meares, P. (1976) Membrane Separation Processes, Elsevier.

Metern, U. (1966) Transport Properties of Osmonic Membranes, in *Desalination by reverse osmosis*. The MIT Press, Cambridge, Mass.

Michaels, A. S., Bixler, H. J., Hodges, R. M. (1965) *J. Colloid Sci*. 20, 1034.

Min, B.R. and Im, K.B. (1992) The energy of an ion in a cylindrical pore of a low dielectric membranes. *J. Membr. Sci.* 52, 89-95.

Moy, G., Corry, B., Kuyucak, S., and Chung, S.-H. (2000) “Tests of continuum theories as models of ion channel. I. Poisson-Boltzmann theory versus Brownian dynamics,” *Biophysical J.* 78, 2349.

Mulder, M. (1996) *Basic Principles of Membrane Technology*. Kluwer Acedemic Publishers, 2nd ed., Dordrecht.

Nernst, W. (1888) *Z. Phys. Chem.* 2, 613.

Ong, S. L., Zhou, W.W., Song, L., and Ng, W. J. (2002) Evaluation of feed concentration effects on salt/ion transport through RO/NF membranes with Nernst-Planck-Donnan model. *Environ. Eng. Sci.* 19 (6), 429-439.

Orofino, T. A., Hopfenberg, H. B., Stannett, V. (1969) Characterization of penetrant clustering in polymers. *J. Macromol. Sci. Phys.* B3, 777-788.

Page, L. and Adams, I. N. (1949) Principles of electricity, an intermediate text in electricity and magnetism, 2nd Ed., D. Van Nostrand Company.

Palmeri, J., Blanc, P., Larbot, A., and David, P. (1999) Theory of pressure driven transport of neutral solutes and ions in porous ceramic nanofiltration membranes. *J. Membr. Sci.* 160, 141-170.

Paul, D. R. (1965) The solution-diffusion model for highly swollen membranes, *Separation and purification Methods* 5(1), 33-50.

Peeters, J. M. M., Boom, J. P., Mulder, M. H. V., and Strathmann, H.(1998) Retention measurements of nanofiltration membranes with electrolyte solutions. *J. Membr. Sci.* 145, 199-209.

Planck, M. (1890) Über die Erregung von Elektrizität und Electrolyten. *Ann. Phys. Chem.* 39, 161.

Purcell, E.M.(1985) *Electricity and magnetism*, McGraw-Hill. NY.

Pusch, W. (1977a) Determination of transport parameters of synthetic membranes by hyperfiltration experiments Part I: derivation of transport relationship from the linear relations of thermodynamics of irreversible processes. *Ber. Bunsenges. Phys. Chem.* 81 (3) 269-276.

Pusch, W. (1977b) Determination of transport parameters of synthetic membranes by hyperfiltration experiments; Part II: membrane transport parameters independent of pressure and/or pressure difference. *Ber. Bunsenges. Phys. Chem.* 81, 854-864.

Raman, L. P., Cheryan, M., and Rajagopalan, N. (1994) Consider nanofiltration for membrane separation. *Chem. Eng. Progr*., 3, 68-80.

Rautenbach, R. and Gröschl, A. (1993) Fractionation of aqueous organic mixtures by reverse osmosis. *Desalination* 90, 93-106.

Reid, C. E., and Breton, E. J. (1959) Water and ion flow across cellulosic membranes. *J. Appl. Poly. Sci.* 1, 133-143.

Rosenbaum, S. and Skeins, W.E. (1968) Concentration and pressure dependence of rate of membrane permeation. *J. Applied Polym. Sci.* 122, 169-2181.

Rubinstein, I. (1990) Electro-diffusion of ions. Society for Industrial and Applied Mathematics, SIAM, Philadelphia.

Schaep, J., and Vandecasteele, C. (2001) Evaluating the charge of nanofiltration membranes. *J. Membr. Sci*. 188, 129-136.

Schaep, J., Vandecasteele, C., Mohammad, A. W., and Bowen, W. R. (2001) Modelling the retention of ionic components for different nanofiltration membranes. *Separation and Purification Technology* 22-23, 169-179.

Schirg, P. and Widmer, F. (1992) Characterisation of nanofiltration membranes for the separation of aqueous dye-salt solutions. *Desalination* 89, 89-107.

Schlögl, R. (1964) Stofftransport durch Membranen, Dr. Dietrich Steinkoff Verlag, Darmstadt.

Schlögl, R. (1966) *Berichte der Bunsengeselschaft*, 70, 400.

Seidel, A., Waypa, J. J. and Elimelech, M. (2001) Role of charge (Donnan) exclusion in removal of Arsenic from water by a negatively charged porous nanofiltration membrane. *Environ. Eng. Sci*. 18(2), 105-113.

Selberherr, S. (1984) *Analysis and simulation of semiconductor devices*, Springer-Verlag.

Shaw, D. J. (1969) Electrophoresis, Academic Press, London.

Sherwood, T. K., Brian, P. L. T., and Fisher, R. E. (1967) Desalination by reverse osmosis. *I & EC Fund.* 6, 2-12.

Slater, C. S. and Brooks, C.A. (1992) Development of a simulation model predicting performance of reverse osmosis batch systems. *Separation Science and Technology*, 27, 1361-1388.

Soltanieh, M. and Gill, W. N. (1981) Review of reverse osmosis membranes and transport models. *Chem. Eng. Commun*. 12, 279-363.

Song, L. F. (2000) Thermodynamic modeling of solute transport through reverse osmosis membrane. *Chem. Eng. Comm*. 180, 145-167.

Sourirajan, S. (1970) Reverse osmosis, Academic Press.

Spiegler, K. S. and Kedem, O. (1966) Thermodynamics of hyperfiltration (reverse osmosis): Criteria for efficient membranes. *Desalination* 1, 311-326.

Szymczyk, A., Labbez, C., Fievet, P., Vidonne, A., and Foissy, A. (2003) Contribution of convection, diffusion and migration to electrolyte transport through nanofiltration membranes. *Adv. Colloid Interface Sci.* 103, 77-94.

Tannehill, J.C., Anderson, D.A., and Pletcher, R.H. (1997) *Computational fluid mechanics and heat transfer* 2nd Ed. Taylor & Francis, Washington DC.

Tsuru, T. Nakao, S. I., and Kimura, S. (1991a) Calculation of ion rejection by extended Nernst-Planck equation with charged reverse osmosis membrane for single and mixed electrolyte. *J. Chem. Eng. Jpn.* 24, 511-517.

Tsuru, T., Urairi, M., Nakao, S. I., and Kimura, S. (1991b) Reverse osmosis of single and mixed electrolytes with charged membranes: experiment and analysis. *J. Chem. Eng.Jpn.* 24, 518-524.

Tsuru, T., Urairi, M., Nakao, S. I., and Kimura, S. (1991c) Negative rejection of anions in the loose reverse osmosis separation of mono- and divalent ion mixtures. *Desalination* 81, 219-227.

Van der Bruggen, B., Braeken, L., and Vandecasteele, C. (2002) Evaluation of parameters describing flux decline in nanofiltration of aqueous solutions containing organic compounds. *Desalination* 147, 281-288.

Van Gauwbergen, D., Baeyens, J., and Creemers, C. (1997) Modeling osmotic pressures for aqueous solutions for 2-1 and 2-2 electrolytes. *Desalination* 109, 57-65.

Van Gauwbergen, D. and Baeyens, J. (1998) Modeling reverse osmosis by irreversible thermodynamics. *Separation and Purification Technology* 13, 117-128.

Van Gauwbergen, D. and Baeyens, J. (1999) Assessment of the design parameters for wastewater treatment by reverse osmosis. *Wat. Sci. Tech*. 40 (4-5), 269-276.

Wijmans, J.G. and Baker, R.W. (1995) The solution-diffusion model: a review. *J. Membr. Sci.* 107, 1-21.

Wilf, M. and Klinko, K. (1999) "Improved performance and cost reduction of RO seawater systems using pretreatment." *Membrane Technology* 113, 5-8.

Williams, M. E., Hestekin, J. A., Smothers, C. N., and Bhattacharyya, D. (1999) Separation of organic pollutants by reverse osmosis and nanofiltration membranes: mathematical models and experimental verification. *Industrial and Engineering Chemistry Research* 38 (10), 3683-3695.

Yaroshchuk, A.E. (1995) Solution-diffusion-imperfection model revised. *J. Membr. Sci.* 101, 83-87.

Yaroshchuk, A.E. (2001) Non-steric mechanisms of nanofiltration: superposition of Donnan and dielectric exclusion. *Separation and Purification Technology* 22-23, 143-158.

APPENDIX

Appendix A: Publications from This Research Work

A.1 Journal Paper

1. Ong, S. L., Wenwen Zhou, Lianfa Song, and Ng, W. J. (2002) "Evaluation of Concentration Effects on Salt/Ion Transport through RO/NF Membranes with the Nernst-Planck-Donnan Model", *Environmental Engineering Science*, 19 (6), 429-439.

2. Zhou, W.W., Song, L.F., Ong, S.L., and Ng, W.J. (2003) "A Method for Predicting Salt Rejection through RO Membranes", *Advances in Asian Environmental Engineering*, 3 (1), 12-21.

3. Song, L., Zhou, W.W**.,** Ong, S. L., and Ng, W. J. (under review) "Ion Transport through Reverse Osmosis Membranes: an Unsteady State Model", *Chemical Engineering Science.*

4. Zhou, W.W., Song, L. Ong, S. L., and Ng, W. J. "Transport Mechanisms for Ions in Reverse Osmosis Membranes: the Contribution of Diffusion, Electro-migration and Convection", Submitted to *Advances in Colloid and Interface Science*.

5. Zhou, W.W., Song, L. Ong, S. L., and Ng, W. J. "Experimental Study of Water and Solute Flux through Reverse Osmosis Membranes", Submitted to *Environmental Science & Technology*.

A.2 Conference Paper

1. Zhou, W.W., Song, L. F., Ong, S. L., and Ng, W. J. (2002) "Study on Ion Transport through RO/NF Membranes with the Extended Nernst-Planck Equation and Donnan-Steric Exclusion", Presented at North American Membrane Society (NAMS) 13th Annual Meeting, May 11-15, Long Beach, California.

2. Zhou, W.W., Song, L.F., Ong, S.L., and Ng, W.J. (2002) "A Method for Predicting Salt Rejection through RO Membranes", Presented at 12th KAIST-KU-NTU-NUS Symposium on Environmental Engineering, June 26-29, Taipei, Taiwan.

3. Song, L.F., Zhou, W.W., Ong, S.L., and Ng, W.J. (2003) "Study on membrane potential and ion transport through reverse osmosis membranes', Presented at North American Membrane Society (NAMS) 14th Annual Meeting, May 17-21, Jackson Hole, WY.

4. Song, L. F., Zhou, W. W., Ong, S. L. and Ng, W. J. (2003) "A new formulation for ion transport through reverse osmosis membranes", Presented at 8th IUMRS (International Union of Materials Research Society) Internation Conference on Advanced Materials, IUMRS-ICAM2003: session-D-4: Materials for Membrane Separation, October 12-13,Yokohama, Japan.

5. Zhou, W., Song, L., Ong, S.L., and Ng, W.J. (2004) "The role of electrostatic interaction in salt rejection during reverse osmosis process", accepted by Water Environmental Membrane Technology (WEMT) 2004, June 7-10, Seoul, Korea.